On the diffusion in inhomogeneous systems

von der Fakultät für Naturwissenschaften der Technischen Universität Chemnitz

genehmigte Dissertation zur Erlangung des akademischen Grades

doctor rerum naturalium

(Dr. rer. nat.)

vorgelegt von Mario Heidernätsch, M. Sc.

geboren am 6. Juni 1983 in Karl-Marx-Stadt, jetzt Chemnitz

eingereicht am 29.07.2014

Gutachter: Prof. Dr. Günter Radons
Prof. Dr. Christian von Borczyskowski

Tag der Verteidigung: 29.05.2015

Bibliographische Beschreibung

Dokumentenart	Dissertation (in englischer Sprache), 2014 91 Seiten, 24 Abbildungen, 148 Literaturzitate
Titel	On the diffusion in inhomogeneous systems
Autor	Mario Heidernätsch
Ort	Fakultät für Naturwissenschaften, Technische Universität Chemnitz

Referat

Ziel dieser Arbeit ist die Untersuchung des Einflusses der stochastischen Interpretation der Langevin Gleichung mit zustandsabhängigen Diffusionskoeffizienten auf den Propagator des zugehörigen stochastischen Prozesses bzw. dessen Mittelwerte. Dies dient dem besseren Verständnis und der Interpretation von Messdaten von Diffusion in inhomogenen Systemen und geht einher mit der Frage der Form der Diffusionsgleichung in solchen Systemen. Zur Vereinfachung der Fragestellung werden in dieser Arbeit nur Systeme untersucht die vollständig durch einen ortsabhängigen Diffusionskoeffizienten und Angabe der stochastischen Interpretation beschrieben werden können.

Dazu wird zunächst für mehrere experimentell relevante eindimensionale Systeme der jeweilige allgemeine Propagator bestimmt, der für jede denkbare stochastische Interpretation gültig ist. Der analytisch bestimmte Propagator wird dann für zwei exemplarisch ausgewählte stochastische Interpretationen, hier für die Itô und Klimontovich-Hänggi Interpretation, gegenübergestellt und die Unterschiede identifiziert. Für Mittelwert und Varianz der Prozesse werden die drei wesentlichen stochastischen Interpretationen verglichen, also Itô, Stratonovich und Klimontovich-Hänggi Interpretation. Diese systematische Untersuchung von inhomogenen Diffusionsprozessen kann zukünftig helfen diese Art von, in genau einer stochastischen Interpretation, driftfreien Systemen einfacher zu identifizieren.

Ein weiterer wesentlicher Teil der Arbeit erweitert die Frage auf mehrdimensionale inhomogene anisotrope Systeme. Dies wird z.B. bei der Untersuchung von Diffusion in Flüssigkristallen mit inhomogenem Direktorfeld relevant. Obwohl hier, im Gegensatz zu eindimensionalen Systemen, der Propagator nicht allgemein berechnet werden kann, wird dennoch der Einfluss der Inhomogenität auf Messgrößen, wie die mittlere quadratische Verschiebung oder die Verteilung der Diffusivitäten, bestimmt. Anhand eines Beispiels wird auch der Einfluss der stochastischen Interpretation auf diese Messgrößen demonstriert.

Schlagworte

Diffusion, Inhomogenität, Langevin Gleichung, multiplikatives Rauschen, Fokker-Planck Gleichung, Anisotropie, Flüssigkristalle, Statistische Analyse, Verteilung von Diffusivitäten

Abstract

The aim of this thesis is to investigate the influence of the stochastic interpretation of the Langevin equation with state-dependent diffusion coefficient on the propagator of the related stochastic process, or its averages, respectively. This helps to obtain a deeper understanding and to interpret measurement data of diffusion in inhomogeneous systems and is accompanied with the question of the proper form of the diffusion equation in such systems. To simplify the question, in this thesis only systems are considered which can be fully described by a spatially dependent diffusion coefficient and a given stochastic interpretation.

Therefore, for several experimentally relevant one-dimensional systems, the respective general propagator is determined, which is valid for any possible stochastic interpretation. Then, the propagator for two exemplary stochastic interpretations, here the Itô and Klimontovich-Hänggi interpretation, are compared and the differences are identified. For mean and variance of the processes three major interpretations are compared, namely the Itô, the Stratonovich and the Klimontovich-Hänggi interpretation. This systematic research on inhomogeneous diffusion process may help in future to identify these kind of, in exactly one stochastic interpretation, drift-free systems more easily.

Another important part of this thesis extends this question to multidimensional inhomogeneous anisotropic systems. This is of high relevance, for instance, for the research of diffusion in liquid crystalline systems with an inhomogeneous director field. Although, in contrast to one-dimensional systems, the propagator may not be calculated generally, the influence of the inhomogeneity on measurement data like the mean squared displacement or the distribution of diffusivities is determined. Based on one example, also the influence of the stochastic interpretation on these quantities is demonstrated.

Keywords

diffusion, inhomogeneity, Langevin equation, multiplicative noise, Fokker-Planck equation, anisotropy, liquid crystals, statistical analysis, distribution of diffusivities

Contents

1. Introduction

1.1. Diffusion in inhomogeneous systems

Diffusion or the thermally driven random motion of single particles or of single molecules in a fluid is the dominant transport process on very small length scales. This jittery motion of individual particles on microscopical scale was, at first, well documented by Brown [1] and, thus, named Brownian motion. On the macroscopic level, if no active transport processes like flow or turbulence are present, the Brownian motion leads to a net particle flux from regions of high particle concentration to regions of low particle concentrations. The first who put this into a phenomenological law was Fick [2]. He stated that the particle flux $\mathbf{J}(\mathbf{x}, t)$ is proportional to the gradient of the concentration

$$\mathbf{J}(\mathbf{x}, t) = -D_c \frac{\partial c(\mathbf{x}, t)}{\partial \mathbf{x}}, \tag{1.1}$$

with the proportionality factor D_c, the diffusion constant. Furthermore, he connected the change of the concentration in time with the divergence of this particle flux $\mathbf{J}(\mathbf{x}, t)$, which results in the diffusion equation

$$\frac{\partial c(\mathbf{x}, t)}{\partial t} = -\frac{\partial}{\partial \mathbf{x}} \cdot \mathbf{J}(\mathbf{x}, t) = D_c \frac{\partial^2 c(\mathbf{x}, t)}{\partial \mathbf{x}^2}. \tag{1.2}$$

Nevertheless, it took some time until Einstein [3] and von Smoluchowski [4], independently from each other, derived this law from thermodynamic principles and, thus, gave it a solid theoretical background.

Furthermore, the diffusion pathway of individual molecules can be interpreted as a stochastic trajectory and described via statistical means. Hence, Einstein [3] was able to connect the mean squared displacement (MSD) of the individual particles with the diffusion constant D_c via

$$\left\langle r^2(\tau) \right\rangle = \left\langle [\mathbf{x}(t+\tau) - \mathbf{x}(t)]^2 \right\rangle = 2dD_c\tau, \tag{1.3}$$

where d is the dimensionality of the process, e.g. $d = 3$ for a three-dimensional trajectory, and $\langle \dots \rangle$ denotes an average over an ensemble of many particles. Furthermore, he showed the relation between diffusion coefficient D_c, the Stokes-friction of a spherical particle and the temperature of a system, known as Stokes-Einstein relation

$$D_c = \frac{k_B T}{6\pi\eta R}. \tag{1.4}$$

Here, k_B is the Boltzmann constant, T the temperature, η the viscosity of the surrounding liquid and R the particle radius. Although, these laws apply in many real systems, there are some severe restrictions on these systems in order that these laws are valid. Thus, the diffusing particles or molecules should be well approximated by a sphere as well as the surrounding liquid molecules. Hence, the particles diffuse in an isotropic liquid. Furthermore, the viscosity, the temperature and the molecular size of the liquid molecules have to be homogeneous and, thus, independent of the position. And finally, the system must not driven by external forces. If any of these restrictions does not apply, theses laws may not be valid anymore.

A huge class of such systems, where the classical diffusion laws are questioned, are inhomogeneous systems [5–7]. Thereby, the source of the inhomogeneity may be manifold and ranges from an inhomogeneous temperature field [8–10] to locally varying viscosity due to the vicinity of a boundary [11–14], due to confinement of the liquid [15, 16], or due to immiscible liquids with different viscosities [17, 18]. In those systems, the diffusion coefficient D_c is not a simple constant anymore, but depends on the position of the diffusing particle. Thus, it is a state-dependent diffusion coefficient [19]. Such a spatially varying diffusion coefficient may also be used to describe the Brownian motion in other complex systems like heterogeneous porous media [20–22] or biological tissue, e.g. protein diffusion in bacterial [23] and eukaryotic cells [24].

With the progressing development of experimental methods, it is nowadays also possible to obtain the paths of individual particles or of single fluorescent dye molecules using video-microscopy on very small time and length scales. For instance, the observation and the analysis of two-dimensional trajectories obtained by single particle tracking (SPT) methods are already successfully applied to biological systems [25–27] or to understand the microrheological properties of complex liquids [28, 29]. Furthermore, recently also the observation of three-dimensional paths becomes feasible [30–33]. In such experiments, usually, the mean squared displacement is measured in order to obtain the diffusion coefficient, although, already advanced methods like the distribution of diffusivities [34–36] exist, which allow to quantify the diffusion coefficients in heterogeneous systems, involving more than one diffusion coefficient.

Regardless of the method, which is used to measure the local diffusion coefficients, the exact form of the diffusion equation is not a priory known in inhomogeneous systems. The same holds for the stochastic differential equation (SDE), i.e. the Langevin equation, which describes the stochastic motion of the particles, since the state-dependence of the diffusion coefficient automatically leads to multiplicative noise and, thus, to the question of the stochastic interpretation of the Langevin equation. In order to obtain a deeper understanding of the influence of the stochastic interpretation of the Langevin equation and, related, of the influence of the different possible forms of the diffusion equation with state-dependent diffusion coefficient, one main part of this thesis focuses on the calculation of the propagator and the averages of several example processes and this for the very first time simultaneously for any possible interpretation of the Langevin equation. The regarded model processes are drift-free and differ only in their stochastic interpretation, this allows to identify the influence of the stochastic interpretation on the propagator and on the averages of the process. And furthermore, it allows prospectively to distinguish the form of the diffusion equation in inhomogeneous systems with help of these quantities. Additionally, many of the presented methods to calculate the general propagator for Langevin equations with state-dependent diffusion coefficient may also be applied to other systems which are not considered in this thesis and, thus, this thesis may also be used as a guide.

1.2. Diffusion in inhomogeneous anisotropic systems

A single diffusion constant D_c is also not sufficient to describe the temporal behavior of the concentration in systems where the diffusion is direction dependent. This may be caused, for instance, by an ellipsoidal shape of the diffusing particle or molecule [37] or by a direction dependent viscosity of the surrounding liquid, i.e. an anisotropic medium [38]. Hence, such anisotropic diffusion processes may be observed in many different systems such as liquid crystals [39–41], porous media [20, 21, 42, 43], or in biological tissue [44–46], where the anisotropy originates, e.g. from aligned filaments in cells [47, 48].

If the anisotropy is homogeneous, i.e. independent of the position, the system may still be

described by a simple diffusion equation

$$\frac{\partial c(\mathbf{x},t)}{\partial t} = \frac{\partial}{\partial \mathbf{x}} \cdot \mathbf{D} \cdot \frac{\partial c(\mathbf{x},t)}{\partial \mathbf{x}} \tag{1.5}$$

and, thus, with help of a constant diffusion tensor $\mathbf{D}$. The diffusion tensor includes information about the diffusion coefficients along the principal axes of the system and their orientation.

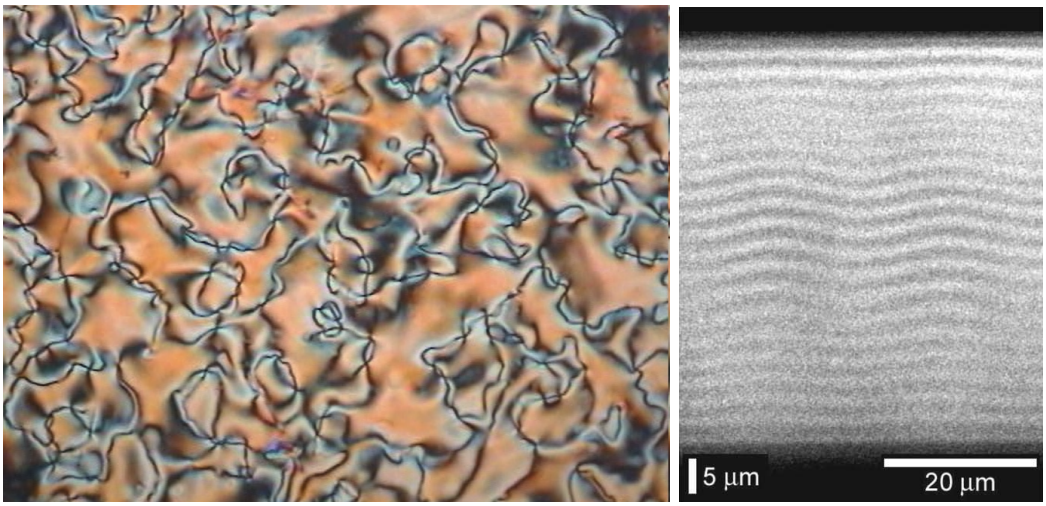

Figure 1.1.: Schlieren texture of a nematic liquid crystal recorded with polarized light microscopy (left, image from [49]) and undulation texture of a cholesteric liquid crystal recorded with fluorescence confocal polarizing microscopy (right, image from [50])

Of course, in many real world systems the anisotropy is not homogeneous, especially the orientation of the principal axes of diffusion are not constant in real systems. This inhomogeneity in the orientation is easily observed in liquid crystalline systems, where the local orientation of the liquid crystal molecule is also reflected by the inhomogeneous textures observed via polarized light microscopy [49]. Here the birefringence property of the liquid crystal molecules is used, which is also found for other aspheric molecules like polymers. Two examples of such inhomogeneous orientations are found in Fig. 1.1 where the local orientation of the liquid crystal molecules is visualized with help of polarized light microscopy. Using fluorescent dyes [34, 40, 41] or colloidal particles [51, 52], it is nowadays possible to measure spatially resolved diffusion in such inhomogeneous anisotropic systems.

Like in inhomogeneous isotropic systems, the form of the diffusion equation with state-dependent diffusion tensor is not a priory clear. This is aggravated by the fact that also the analytical computation of the propagator in such higher dimensional partial differential equations (PDEs) is often not possible. Nevertheless, in this thesis three experimentally relevant systems with a state-dependent diffusion tensor are investigated. And for one out of the different possible stochastic interpretations of the corresponding Langevin equation, namely the Itô interpretation, also analytical predictions for the behavior of the mean squared displacement and the distribution of diffusivities are presented. Furthermore, it is established that the distribution of diffusivities in such inhomogeneous anisotropic systems may be used to determine the eigenvalues of the diffusion tensor independently of the stochastic interpretation. Finally, for one example also a second stochastic interpretation is examined, namely the Stratonovich interpretation, and its influence on the MSD and other averages is presented.

1.3. Outline of this thesis

This thesis is organized as follows. In Chap. 2, Sec. 2.1 and 2.2, a brief recall is given about the stochastic description of diffusion processes. This is followed in Sec. 2.3 and 2.4 with an overview over the problems and questions which arise with a state-dependent diffusion coefficient and which approaches already exist and may be used to answer the questions. After that, in Sec. 2.5 a brief excursion to anisotropic systems with state-dependent diffusion tensor is given. The chapter ends with a short recapitulation of experimental methods to measure diffusion processes.

In Chap. 3 several examples of one-dimensional systems with state-dependent diffusion coefficient are presented. Here for the very first time a general propagator is calculated, which is valid for any possible stochastic interpretation and compared with the respective measured propagator from simulations. The chapter ends with an example where an explicit propagator is only found for the Stratonovich interpretation of the respective Langevin equation. However, in this Sec. 3.4 is demonstrated how averages for other stochastic interpretations can still be predicted.

In Chap. 4 inhomogeneous anisotropic systems with state-dependent diffusion tensor are considered. Here the influence of the stochastic interpretation is only investigated for one example, presented in Sec. 4.2. But for all examples, interpreted in Itôs sense, the temporal behavior of the mean squared displacement and of the distribution of diffusivities is predicted by analytical means and compared with results from simulations.

Finally in Chap. 5, the main results of this thesis are summarized and open questions and suggestions for future research on this topic are given.

2. Theory

The diffusion pathway of individual molecules can be interpreted as a stochastic trajectory and described via statistical means. Under certain conditions it is possible to give the related probability density function of such trajectories and, thus, predict averages of this stochastic process. In this chapter the theoretical bases are introduced, which are used in Chap. 3 and Chap. 4 to derive analytical predictions for certain heterogeneous diffusion systems. In Sec. 2.1 the used nomenclature for the stochastic description is introduced very briefly. In Sec. 2.2 the connection between the path description and the probability density function (PDF) for homogeneous diffusion processes is drawn. This is followed by Sec. 2.3 showing the difficulties which are introduced by making the diffusion coefficient state-dependent and Sec. 2.4 which provides methods to overcome these difficulties. In Sec. 2.5 the problem is extended to heterogeneous anisotropic systems and some well chosen restrictions are explained, which help to derive analytical predictions. Finally, in Sec. 2.6 some experimentally valuable methods are explained, which are used to determine the coefficients which characterize the diffusion process, e.g. the diffusion constant in homogeneous isotropic systems.

2.1. Nomenclature

If $X \in \mathbb{R}$ is a real random variable, $p(x)$ defines its probability density function and the PDF is normalized such that $\int \mathrm{d}x\, p(x) = 1$, the expectation values of an observable of the random variable can be calculated via

$$\langle O(X) \rangle = \int \mathrm{d}x\, O(x) p(x). \tag{2.1}$$

Furthermore, the distribution of X may be characterized by the moments of the distribution

$$M^m = \langle X^m \rangle = \int \mathrm{d}x\, x^m p(x) \tag{2.2}$$

with $m \in \mathbb{N}_0$ and $M^0 = 1$ the normalization. These moments may also be computed from the characteristic function $G(k) = E\left[\exp(\mathrm{i}kX)\right]$ via

$$M^m = \mathrm{i}^{-m} \left. \frac{\partial^m G(k)}{\partial k^m} \right|_{k=0}, \tag{2.3}$$

here $k \in \mathbb{R}$ and $\mathrm{i} = \sqrt{-1}$ is the imaginary unit. Thus, $G(k)$ is the Fourier transform of the probability density function. Also the cumulants can be obtained from the characteristic function via

$$\kappa^m = \mathrm{i}^{-m} \left. \frac{\partial^m \ln G(k)}{\partial k^m} \right|_{k=0}, \tag{2.4}$$

with $m \in \mathbb{N}$ and the moments are recursively related to the cumulants by

$$M^m = \sum_{k=0}^{m-1} \binom{m-1}{k} \kappa^{m-k} M^k \tag{2.5}$$

with initial value $M^0 = 1$ [53]. Furthermore, in case of one-sided PDFs and if all cumulants are known, the PDF can be expressed in terms of the cumulants via [54]

$$p(x) = \frac{2}{\pi}\int_0^\infty \mathrm{d}k\, \exp\left(\sum_{m=1}^{\infty}(-1)^m \frac{\kappa^{2m}}{2m!}k^{2m}\right)\cos\left(-\sum_{m=1}^{\infty}(-1)^m \frac{\kappa^{2m-1}}{(2m-1)!}k^{2m-1}\right)\cos\left(xk\right). \tag{2.6}$$

Recently, Cottone and Paola [55] showed that also fractional moments can be computed from the characteristic function via fractional derivatives. They obtained the fundamental relation

$$\langle(\pm \mathrm{i}X)^\gamma\rangle = \int \mathrm{d}x\,(\pm \mathrm{i}x)^\gamma p(x) = \left(\mathcal{D}_\pm^\gamma G\right)(0) \tag{2.7}$$

for $\gamma \in \mathbb{R}$ and $\gamma > 0$. $\left(\mathcal{D}_\pm^\gamma f\right)(x)$ denotes the Riemann-Liouville fractional derivative, defined as

$$\left(\mathcal{D}_\pm^{n+\nu} f\right)(x) \stackrel{\text{def}}{=} \frac{(\pm 1)^{n+1}}{\Gamma(1-\nu)}\frac{\mathrm{d}^{n+1}}{\mathrm{d}x^{n+1}}\int_0^\infty \mathrm{d}\xi\, \xi^{-\nu} f(x \mp \xi) \tag{2.8}$$

with $\gamma = n + \nu$, $\nu \in \mathbb{R}$, $1 > \nu > 0$ and $n \in \mathbb{N}_0$. Here $\Gamma(x)$ denotes the gamma function. The signs at both equations have to be treated carefully, in the original paper [55] the signs at Eq. (2.7) are reversed. A simple test with an exponential distribution $p(x) = \theta(x)\frac{1}{\lambda}\exp\left(-\frac{x}{\lambda}\right)$, which has the fractional moments $\langle(\pm \mathrm{i}X)^\gamma\rangle = (\pm \mathrm{i}\lambda)^\gamma\Gamma(1+\gamma)$ and the characteristic function $G(k) = \frac{\mathrm{i}}{\mathrm{i}+\lambda k}$, shows that the relations should take the form of Eq. (2.7). Here $\theta(x)$ denotes the Heaviside unit step function. For the calculation of real-valued fractional moments the relation $\langle X^\gamma\rangle = \mathrm{i}^\gamma\langle(-\mathrm{i}X)^\gamma\rangle$ can be used, also given in [55].

In case of probability density functions for $X \in \mathbb{R}^+$, the relation [56]

$$E\left[X^\gamma\right] = (-1)^{\lfloor\gamma\rfloor}\left(\mathfrak{D}^\gamma L\right)(0), \tag{2.9}$$

may be used, with $L(k) = \int_0^\infty \mathrm{d}x \exp(-kx)p(x)$ the Laplace transform of $p(x)$, $\gamma > 0$ and $\lfloor\gamma\rfloor$ giving the integer part of γ. Here $\left(\mathfrak{D}^\gamma f\right)(x)$ denotes the Marchaud fractional derivative [57] given by

$$\left(\mathfrak{D}^{n+\nu} f\right)(x) \stackrel{\text{def}}{=} \frac{\nu}{\Gamma(1-\nu)}\int_0^\infty \mathrm{d}\xi\, \frac{f^{(n)}(x) - f^{(n)}(x+\xi)}{\xi^{1+\nu}} \tag{2.10}$$

with $\gamma = n + \nu$, $\nu \in \mathbb{R}$, $1 > \nu > 0$ and $n \in \mathbb{N}_0$. Here, $f^{(n)}(x)$ denotes the derivative of order n. It should be noted that the Marchaud fractional derivative also exists for functions growing algebraically at infinity.

In this thesis, $x(t)$ denotes the state of a stochastic process and $p(x,t)$ its PDF. Hence, $x(t)$ behaves like a random variable and averages are calculated in the same fashion as the expectation values before. Thus,

$$\langle O(x(t))\rangle = \int \mathrm{d}x\, O(x)p(x,t) \tag{2.11}$$

denotes the average of an observable of the states given by an ensemble of trajectories at time t. Furthermore, here only Markov processes are considered, i.e. memoryless processes, which fulfill the Markov property and therefore the Chapman-Kolmogorov equation [58]. Thus, these stochastic processes are completely defined by the transition probability density $p(x,t|x',t')$. Knowing the probability density $p(x_0,t_0)$ of the process at time t_0, it allows to compute the probability density at any later times $t > t_0$ via the propagator

$$p(x,t) = \int \mathrm{d}x_0\, p(x,t|x_0,t_0)p(x_0,t_0). \tag{2.12}$$

Hence, $p(x,t|x',t')$ acts as an integral kernel to the propagator. Nevertheless, in this thesis if the propagator is referenced, the transition probability density $p(x,t|x',t')$ is meant.

The moments of these stochastic processes can be computed according to Eq. (2.2) using the PDF $p(x,t)$. In case that only the propagator of a process is known, the conditional moments can be calculated via

$$M^m_{x_0(t_0)}(t) = \langle x^m(t)\rangle_{x_0(t_0)} = \int \mathrm{d}x\, x^m p(x,t|x_0,t_0), \tag{2.13}$$

which describe the averages over an ensemble of processes which are all at $t = t_0$ in the same state x_0. If the complete PDF at $t = t_0$ is known, the conditional moments can be used to calculate the general moments of the density $p(x,t)$ via

$$M^m(t) = \langle x^m(t)\rangle = \int \mathrm{d}x\, x^m p(x,t) = \int \mathrm{d}x_0\, \langle x^m(t)\rangle_{x_0(t_0)}\, p(x_0,t_0). \tag{2.14}$$

2.2. Theoretical description of homogeneous diffusion processes

The stochastic path of a d-dimensional homogeneous anisotropic Brownian motion can be described by its propagator, which is a multivariate Gaussian distribution [19]

$$p(\mathbf{x},t|\mathbf{x}',t') = \frac{(2\pi)^{-\frac{d}{2}}}{\sqrt{[2(t-t')]^d \det \mathbf{D}}} \exp\left[-\frac{1}{2}\frac{1}{2(t-t')}(\mathbf{x}-\mathbf{x}')^{\mathsf{T}}\mathbf{D}^{-1}(\mathbf{x}-\mathbf{x}')\right]. \tag{2.15}$$

Here $\mathbf{D} = \mathbf{O}^{\mathsf{T}}\hat{\mathbf{D}}\mathbf{O}$ is the positive definite and symmetric diffusion tensor, $\hat{\mathbf{D}} = \mathrm{diag}(D_1, D_2, \ldots, D_d)$ denotes its diagonalized form with the diffusion coefficients D_i belonging to the principal axes, and $\mathbf{O}$ is an orthogonal matrix, which describes the orientation of the principal axes relative to the frame of reference. In case of isotropic diffusion $D_1 = D_2 = \ldots = D_d = D_c$ and, thus, the propagator reduces to an univariate Gaussian distribution

$$p(\mathbf{x},t|\mathbf{x}',t') = \frac{(2\pi)^{-\frac{d}{2}}}{\sqrt{[2(t-t')D_c]^d}} \exp\left[-\frac{1}{2}\frac{(\mathbf{x}-\mathbf{x}')^2}{2D_c(t-t')}\right]. \tag{2.16}$$

Introducing for positional displacement $\mathbf{r} = \mathbf{x} - \mathbf{x}'$ and for temporal displacement $\tau = t - t'$, both propagators of Eqs. (2.15) and (2.16) reduce to a Gaussian displacement distribution

$$p(\mathbf{x}'+\mathbf{r}, t'+\tau|\mathbf{x}',t') = p(\mathbf{r},\tau) = \frac{(2\pi)^{-\frac{d}{2}}}{\sqrt{\det \boldsymbol{\Sigma}}} \exp\left(-\frac{1}{2}\mathbf{r}^{\mathsf{T}}\boldsymbol{\Sigma}^{-1}\mathbf{r}\right), \tag{2.17}$$

which is homogeneous in space and time. These Gaussian displacement distributions are completely determined by their zero mean and their covariance $\boldsymbol{\Sigma}$. Thereby, the covariance in the first case is $\boldsymbol{\Sigma} = \left\langle \mathbf{r}(\tau)\mathbf{r}(\tau)^{\mathsf{T}}\right\rangle = 2\mathbf{D}\tau$ and in the second case it is $\boldsymbol{\Sigma} = \left\langle \mathbf{r}(\tau)\mathbf{r}(\tau)^{\mathsf{T}}\right\rangle = 2D_c\tau\mathbf{I}$, where $\mathbf{I}$ denotes the unit tensor. If the process possesses a spatial heterogeneity, the displacement distribution still depends on $\mathbf{x}'$ and is not necessarily a Gaussian distribution. In general, the process is also not time-translation invariant and, thus, depends additionally on t'.

If either the propagator or the displacement distribution is known, such a process can be simulated by

$$\mathbf{x}(t+\Delta t) = \mathbf{x}(t) + \mathbf{r}(\mathbf{x}(t), t, \Delta t) \tag{2.18}$$

using discrete time steps Δt and drawing $\mathbf{r}(\mathbf{x}(t), t, \Delta t)$, e.g. from the displacement distribution $p(\mathbf{r}, \Delta t|\mathbf{x}(t), t)$. For homogeneous Brownian motion $p(\mathbf{r}, \Delta t|\mathbf{x}(t), t) = p(\mathbf{r}, \Delta t)$. Alternatively, the trajectories of the process are evolved by the Langevin equation

$$\frac{\mathrm{d}\mathbf{x}}{\mathrm{d}t} = \sqrt{2\mathbf{D}}\boldsymbol{\xi}(t) \tag{2.19}$$

with $\sqrt{\mathbf{D}} = \mathbf{O}^\mathsf{T}\sqrt{\hat{\mathbf{D}}}\mathbf{O}$ and $\sqrt{\hat{\mathbf{D}}} = \mathrm{diag}(\sqrt{D_1}, \sqrt{D_2}, \ldots, \sqrt{D_d})$. The vector $\boldsymbol{\xi}(t) = [\xi_1(t), \ldots, \xi_d(t)]^\mathsf{T}$ denotes Gaussian white noise in d dimensions with $\langle\boldsymbol{\xi}(t)\rangle = \mathbf{0}$ and $\langle\xi_i(t)\xi_j(t')\rangle = \delta_{ij}\delta(t-t')\,\forall\, i, j \in \{1, 2, \ldots, d\}$. This Langevin equation is an example of a stochastic differential equation, which means that the outcome of an integration differs in each sample process. Despite of this, averaging over different realizations of the process leads to well defined mean values and, thus, the probability density $p(\mathbf{x}, t)$ of such processes can be found.

The probability density $p(\mathbf{x}, t)$ of the process given by the Langevin equation Eq. (2.19) evolves via the Fokker-Planck equation

$$\frac{\partial}{\partial t}p(\mathbf{x}, t) = \sum_{i=1}^{d}\sum_{j=1}^{d} D_{ij}\frac{\partial}{\partial x_i}\frac{\partial}{\partial x_j}p(\mathbf{x}, t) \tag{2.20}$$

where D_{ij} are the elements of the diffusion tensor $\mathbf{D}$. In the isotropic case the equation reduces to the well known diffusion equation

$$\frac{\partial}{\partial t}p(\mathbf{x}, t) = D_c\frac{\partial^2}{\partial \mathbf{x}^2}p(\mathbf{x}, t). \tag{2.21}$$

Using $p(\mathbf{x}, t = t') = \delta(\mathbf{x} - \mathbf{x}')$ as initial condition, the Fokker-Planck equation can be used to determine the propagator. In the case of Eq. (2.20), it gives the propagator of the homogeneous anisotropic process Eq. (2.15) as solution and in the case of Eq. (2.21) it results in the propagator of the homogeneous isotropic process Eq. (2.16), respectively. Furthermore, any of the three descriptions, Langevin equation, Fokker-Planck equation, or propagator, is sufficient to describe a Markovian diffusion process completely.

2.3. Isotropic systems with state-dependent diffusion coefficient

In case of a spatial dependent diffusion coefficient the situation is not that simple. Although there exists a propagator and a Fokker-Planck equation which describes the system completely, their mathematical form can not be determined from knowing of spatial dependency of the diffusion coefficient and assuming that there exist no external drift. This problem is easily identified when the nonlinear Langevin equation

$$\frac{\mathrm{d}\mathbf{x}}{\mathrm{d}t} = \sqrt{2D(\mathbf{x})}\boldsymbol{\xi}(t) = g(\mathbf{x})\boldsymbol{\xi}(t) \tag{2.22}$$

is considered with the position dependent diffusion coefficient $D(\mathbf{x}) = 1/2\, g^2(\mathbf{x})$, which characterizes the noise amplitude. Thus, the process is driven by multiplicative noise. In contrast to homogeneous systems, where the Langevin equation Eq. (2.19) completely defines the propagator and the corresponding Fokker-Planck equation, in this case the information is incomplete and the stochastic integration cannot be carried out without further information [59]. In order to solve this stochastic integration the SDE can be discretized

$$\Delta\mathbf{x} = g(\mathbf{x}^*)\Delta\mathbf{W}(t), \tag{2.23}$$

where $\Delta\mathbf{x} = \mathbf{x}(t+\Delta t) - \mathbf{x}(t)$ and Δt is the time increment. Here $\Delta\mathbf{W}(t)$ denotes the increment of a d-dimensional Wiener process, given by

$$\Delta\mathbf{W}(t) = \int_t^{t+\Delta t} \mathrm{d}s\, \boldsymbol{\xi}(s), \tag{2.24}$$

which satisfies $\langle \Delta\mathbf{W}(t)\rangle = \mathbf{0}$ and $\left\langle \Delta\mathbf{W}(t)\Delta\mathbf{W}(t)^{\mathsf{T}}\right\rangle = \Delta t\, \mathbf{I}$. The position $\mathbf{x}^*$ for $\mathbf{g}(\mathbf{x}^*)$ can be any value between $\mathbf{x}(t)$ and $\mathbf{x}(t+\Delta t)$, i.e.

$$\mathbf{x}^* = \alpha\mathbf{x}(t+\Delta t) + (1-\alpha)\mathbf{x}(t) \tag{2.25}$$

with $0 \leq \alpha \leq 1$. In contrast to ordinary differential equations (ODEs) and SDEs with additive noise, here different alpha lead to a different behavior of the process. Thus, only if α is defined, the Langevin equation Eq. (2.22) is also defined properly. If the increments of the Wiener process $\Delta\mathbf{W}(t)$ are interpreted as small random pulses, the value α defines when the standard deviation of amplitude of these pulses is determined. If $\alpha = 0$, the amplitude is determined just before the pulse, which corresponds to the Itô interpretation of Eq. (2.22) [60]. Another well known interpretation is the Stratonovich interpretation ($\alpha = 1/2$) [61]. It occurs naturally, if a nonlinear system is not driven by white noise $\boldsymbol{\xi}(t)$, but instead by some physical noise $\boldsymbol{\eta}(t)$, which has zero mean and is correlated in time, i.e $\langle\boldsymbol{\eta}\rangle = \mathbf{0}$ and $\langle\eta_i(t+\tau)\eta_j(t)\rangle = \delta_{ij}f_i(\tau)$. Here $f_i(\tau)$ are arbitrary correlation functions which have finite correlation times τ_i^c, such that $\left\langle\boldsymbol{\eta}(t+\tau)\boldsymbol{\eta}(t)^{\mathsf{T}}\right\rangle = 0$ for $|\tau| \gg \max(\tau_1^c, \tau_2^c, \ldots, \tau_d^c)$. For large times, such processes can be well described by the Langevin equation Eq. (2.22) interpreted in the Stratonovich sense ($\alpha = 1/2$) and using white noise (c.f. [59]).

The differences in the various possible interpretations of the nonlinear SDE from Eq. (2.22) are also reflected in their corresponding Fokker-Planck equations. When using the parameter α as identifier for the stochastic interpretation, the Fokker-Planck equation for the drift-free Langevin equation

$$\frac{\mathrm{d}\mathbf{x}}{\mathrm{d}t} = \sqrt{2D(\mathbf{x})}\boldsymbol{\xi}(t) = g(\mathbf{x})\boldsymbol{\xi}(t) \quad (\alpha\text{-Interpretation}) \tag{2.26}$$

takes the general form

$$\frac{\partial}{\partial t}p(\mathbf{x},t) = \sum_{i=1}^{d} -\frac{\partial}{\partial x_i}\left(\alpha\frac{\partial g(\mathbf{x})}{\partial x_i}g(\mathbf{x})p(\mathbf{x},t)\right) + \frac{1}{2}\frac{\partial^2}{\partial x_i^2}\left(g^2(\mathbf{x})p(\mathbf{x},t)\right). \tag{2.27}$$

In $d = 1$ dimensions it simplifies to

$$\frac{\partial}{\partial t}p(x,t) = -\frac{\partial}{\partial x}\left(\alpha g'(x)g(x)p(x,t)\right) + \frac{1}{2}\frac{\partial^2}{\partial x^2}g^2(x)p(x,t), \tag{2.28}$$

where $g'(x)$ is the derivative of $g(x)$. From the form of the Fokker-Planck equation the term $\alpha\frac{\partial g(\mathbf{x})}{\partial x_i}g(\mathbf{x}) = f_i^{\alpha}(\mathbf{x})$ is identified as a force or drift term. In literature this is known as noise induced drift or "spurious" drift [19, 62, 63]. Although for each nonlinear Langevin equation a corresponding Fokker-Planck equation is found, provided the stochastic interpretation is given, the reverse is ambiguous. For example, the Fokker-Planck equation given by

$$\frac{\partial}{\partial t}p(x,t) = \frac{1}{2}\frac{\partial^2}{\partial x^2}g(x)^2p(x,t) \tag{2.29}$$

could either be the corresponding PDE for the density of the process

$$\frac{\mathrm{d}x}{\mathrm{d}t} = g(x)\xi(t) \quad \text{(Itô)} \tag{2.30}$$

interpreted in the Itô sense or PDE for the density of the process

$$\frac{\mathrm{d}x}{\mathrm{d}t} = -\frac{1}{2}g'(x)g(x) + g(x)\xi(t) \quad \text{(Stratonovich)} \tag{2.31}$$

interpreted in the Stratonovich sense. Thus, for a given nonlinear physical process the corresponding Langevin equation is also ambiguous, despite some cases where the noise source is properly characterized and has some finite correlation time which leads to Stratonovich interpretation.

Although the question which value of α or which kind of interpretation is the proper one is still part of current research [17, 18, 64–66], the scientific consensus [59, 67] is that

- The value of α is part of the model, or should be chosen on physical grounds.
- In experiments its more useful to measure the probability density, but this knowledge is insufficient to infer the value of α, but the form of the Fokker-Planck equation can be determined.
- The Stratonovich calculus usually applies in typical, continuous, physical systems, whereas the Itô calculus usually applies in systems which are intrinsically discontinuous, e.g. stock exchange [68, 69] or the evolution of biological populations [70, 71].

Hence, one part of this thesis is to infer the form of the Fokker-Planck equation based on the statistical analysis of typical trajectories under the assumption that no other drift than the noise induced drift exists. Consequently, for the trajectories of the considered systems there exists always a Langevin description without a drift-term, but with a specific stochastic interpretation which is quantified by the value of α. Thus, in Chap. 3 some examples of one-dimensional systems with state-dependent diffusion coefficient are examined and the impact of the stochastic interpretation of the given drift-free Langevin equation on the propagator and on moments of the process are shown. This may help in future to identify the proper Fokker-Planck equation describing experimentally measured systems.

Although it is possible to identify the proper form of the Fokker-Planck equation by measuring the temporal evolution of the probability density or the stationary density in the long-term limit, only a few experiments try to tackle the question of the proper form of the Fokker-Planck equation. Up to now, neither general research is done on this field nor several systems with state-dependent diffusion coefficient are compared. Nevertheless, there are some experiments which seem to favor

$$\frac{\partial}{\partial t}p(\mathbf{x},t) = \frac{1}{2}\frac{\partial^2}{\partial \mathbf{x}^2}\left(g^2(\mathbf{x})p(\mathbf{x},t)\right) = \frac{\partial^2}{\partial \mathbf{x}^2}\left(D(\mathbf{x})p(\mathbf{x},t)\right) \tag{2.32}$$

as form of the Fokker-Planck equation [17, 18]. This form is hence denoted as Itô form of the Fokker-Planck equation, since it is the corresponding equation for the density of Eq. (2.22) interpreted in the Itô sense ($\alpha = 0$). Here the right part of the equation uses the diffusion coefficient $D(\mathbf{x}) = 1/2\, g^2(\mathbf{x})$ as abbreviation. These experiments were performed in a system with a sharp interface between a low viscosity liquid and a high viscosity liquid, so that the system is not continuous and the Itô form is the natural consequence.

There are also theoretical considerations [72, 73], experimental measurements [16, 64, 65, 74], as well as computer simulations [66] which favor the form

$$\frac{\partial}{\partial t}p(\mathbf{x},t) = \frac{1}{2}\frac{\partial}{\partial \mathbf{x}} \cdot \left(g^2(\mathbf{x}) \frac{\partial}{\partial \mathbf{x}} p(\mathbf{x},t) \right) = \frac{\partial}{\partial \mathbf{x}} \cdot \left(D(\mathbf{x}) \frac{\partial}{\partial \mathbf{x}} p(\mathbf{x},t) \right). \tag{2.33}$$

Hence, this form is called Fickian form [2] or Klimontovich-Hänggi [75, 76] form, since it is the corresponding equation for the density of Eq. (2.22) interpreted with $\alpha = 1$. Here, either a viscosity gradient $\gamma(\mathbf{x})$ or a temperature gradient $T(\mathbf{x})$ is used to create the position-dependent diffusion coefficient.

For the sake of completeness, also the Stratonovich form has to be mentioned

$$\frac{\partial}{\partial t}p(\mathbf{x},t) = \frac{1}{2}\frac{\partial}{\partial \mathbf{x}} \cdot \left(g(\mathbf{x}) \frac{\partial}{\partial \mathbf{x}} g(\mathbf{x}) p(\mathbf{x},t) \right), \tag{2.34}$$

but it is rarely used to describe inhomogeneous diffusion systems in experiments. In the literature the Itô form and the Klimontovich form are more present. Nevertheless, Smythe *et al.* [77] and McClintock and Moss [78] showed the applicability of the Stratonovich calculus and Stratonovich form of the Fokker-Planck equation to real nonlinear systems driven by physical noise in an analog simulator.

2.4. One-dimensional systems with state-dependent diffusion coefficient

2.4.1. Stratonovich case

Given a general one-dimensional Langevin equation with state-dependent drift and diffusion coefficient interpreted in Stratonovich sense

$$\frac{\mathrm{d}x}{\mathrm{d}t} = f(x) + g(x)\xi(t), \quad \text{(Stratonovich)} \tag{2.35}$$

the usual differential calculus can be applied to transform the equation to a different variable. For instance, if a new variable $\tilde{x} = \Phi(x)$ is introduced, the Langevin equation for $\tilde{x}$ is

$$\frac{\mathrm{d}\tilde{x}}{\mathrm{d}t} = \tilde{f}(\tilde{x}) + \tilde{g}(\tilde{x})\xi(t) \quad \text{(Stratonovich)} \tag{2.36}$$

with the new drift term $\tilde{f}(\tilde{x}) = f(\Phi^{-1}(\tilde{x}))\ \frac{\partial \Phi}{\partial x}\big|_{x=\Phi^{-1}(\tilde{x})}$ and the new diffusion coefficient $\tilde{g}(\tilde{x}) = g(\Phi^{-1}(\tilde{x}))\ \frac{\partial \Phi}{\partial x}\big|_{x=\Phi^{-1}(\tilde{x})}$ and Φ^{-1} is the inverse function of Φ. If a propagator of the transformed variable is found, the propagator of the original Langevin equation can be found via back-transformation $\tilde{x} \to x$.

2.4.2. Itô case and calculation of moments

Given again a general one-dimensional Langevin equation with state-dependent drift and diffusion coefficient but now interpreted in Itô sense

$$\frac{\mathrm{d}x}{\mathrm{d}t} = \hat{f}(x) + \hat{g}(x)\xi(t), \quad \text{(Itô)} \tag{2.37}$$

the usual differential calculus cannot be applied. Here Itôs-Lemma [60] has to be applied, which means that for a variable transformation $\tilde{x} = \Phi(x,t)$, the Langvin equation for $\tilde{x}$ has the form

$$\frac{\mathrm{d}\tilde{x}}{\mathrm{d}t} = \left(\frac{\partial\Phi(x,t)}{\partial t} + \hat{f}(x)\frac{\partial\Phi(x,t)}{\partial x} + \frac{\hat{g}^2(x)}{2}\frac{\partial^2\Phi(x,t)}{\partial x^2}\right)\Bigg|_{x=\Phi^{-1}(\tilde{x})} + \left(\hat{g}(x)\frac{\partial\Phi(x,t)}{\partial x}\right)\Bigg|_{x=\Phi^{-1}(\tilde{x})}\xi(t). \quad \text{(Itô)} \tag{2.38}$$

In can be seen that for a transformation function $\tilde{x} = \Phi(x) = \int^x \mathrm{d}x' \frac{1}{\hat{g}(x')}$ and $\hat{g}(x) = g(x)$ the transformed equations of the Itô and Stratonovich cases coincide if $\hat{f}(x) = f(x) + \frac{1}{2}g'(x)g(x)$. Thus, also the original processes behave equally. The term $\frac{1}{2}g'(x)g(x)$ is the noise induced drift term (c.f. Sec. 2.3). Although a Stratonovich process provides the much simpler differential calculus, the Itô process also has a huge advantage, namely the independence of the stochastic driving $\xi(t)$ and the process itself $x(t)$. This allows to give dynamical equations for the moments directly from the form of the Langevin equation. Hence, considering the process from Eq. (2.37) in discretized time

$$x(t+\mathrm{d}t) = x(t) + \hat{f}(x(t))\mathrm{d}t + \hat{g}(x(t))\sqrt{\mathrm{d}t}\xi, \tag{2.39}$$

both sides of the equation can be averaged with knowledge of distribution functions. Thereby the density $p(x,t|x_0,t_0)$ can be used and, additionally, that ξ is a standard normally distributed variable and independent from the first. And the first can formally be written as

$$\begin{aligned} p(x_n,t_n|x_0,t_0) = &\int \mathrm{d}x_{n-1}\int \mathrm{d}x_{n-2}\ldots\int \mathrm{d}x_1 \\ &\times p(x_n,t_n|x_{n-1},t_{n-1})p(x_{n-1},t_{n-1}|x_{n-2},t_{n-2})\ldots p(x_1,t_1|x_0,t_0) \end{aligned} \tag{2.40}$$

with $t_i = t_0 + i\mathrm{d}t$, $\mathrm{d}t = \frac{t-t_0}{n}$ and, thus, $t = t_0 + n\mathrm{d}t$. It should be noted that in the limit $n\to\infty$, i.e. $\mathrm{d}t\to 0$, the transition probability densities $p(x_i,t_i|x_{i-1},t_{i-1}) = p(x,t+\mathrm{d}t|x',t)$ are Gaussian distributed with mean $x(t)+\hat{f}(x(t))\mathrm{d}t$ and variance $\hat{g}(x(t))^2\mathrm{d}t$. Now by averaging the left-hand side (lhs) of the Eq. (2.39) with $p(x,t+\mathrm{d}t|x_0,t_0)$ and the right-hand side (rhs) with $p(x,t|x_0,t_0)p(\xi)$ and using $\langle\xi\rangle = 0$, the equation becomes

$$\langle x(t+\mathrm{d}t)\rangle = \langle x(t)\rangle + \left\langle \hat{f}(x(t))\right\rangle \mathrm{d}t. \tag{2.41}$$

By subtracting $\langle x(t)\rangle$ and dividing by $\mathrm{d}t$, an ordinary differential equation for the mean is obtained

$$\frac{\mathrm{d}}{\mathrm{d}t}\langle x(t)\rangle = \left\langle \hat{f}(x(t))\right\rangle. \tag{2.42}$$

If $\left\langle \hat{f}(x(t))\right\rangle$ is constant or $\hat{f}(x)$ is only a linear function of x, then a solution can be found and is the same as the deterministic solution. For instance, if $\frac{\mathrm{d}}{\mathrm{d}t}\langle x(t)\rangle = a + b\langle x(t)\rangle$, then $\langle x(t)\rangle = x_0\exp(bt) + \frac{a}{b}(\exp(bt)-1)$ using $\langle x(t_0=0)\rangle = x_0$. It should be noted that the first moment of the unbounded drift-free Itô process, i.e. $\hat{f}=0$, is constant.

Higher order moments can be treated as the average of an arbitrary function $\langle\Phi(x)\rangle$ and, thus by applying Itôs lemma

$$\frac{\mathrm{d}}{\mathrm{d}t}\langle\Phi(x)\rangle = \left\langle \hat{f}(x(t))\frac{\partial\Phi(x)}{\partial x} + \frac{\hat{g}^2(x(t))}{2}\frac{\partial^2\Phi(x)}{\partial x^2}\right\rangle. \tag{2.43}$$

For instance, for the second moment $\left\langle x^2(t)\right\rangle$ the equation reads

$$\frac{\mathrm{d}}{\mathrm{d}t}\left\langle x^2(t)\right\rangle = \left\langle 2x(t)\hat{f}(x(t)) + \hat{g}^2(x(t))\right\rangle. \tag{2.44}$$

2.4.3. Drift-free, Stratonovich case

For a drift-free system with state-dependent diffusion coefficient interpreted in Stratonovich sense

$$\frac{\mathrm{d}x}{\mathrm{d}t} = g(x)\xi(t) \quad \text{(Stratonovich)} \tag{2.45}$$

the transformation $\tilde{x} = \Phi(x) = \int^x \mathrm{d}x' \frac{1}{g(x')}$ can be applied. Thus, $\tilde{g} = 1$ and the transformed Langevin equation belongs to the well known Wiener process

$$\frac{\mathrm{d}\tilde{x}}{\mathrm{d}t} = \xi(t), \tag{2.46}$$

which has the propagator

$$\tilde{p}(\tilde{x}, t|\tilde{x}', t') = \frac{1}{\sqrt{2\pi(t-t')}} \exp\left[-\frac{1}{2}\frac{(\tilde{x}-\tilde{x}')^2}{(t-t')}\right]. \tag{2.47}$$

In consequence, the propagator of the original process is found via the back-transformation of $\tilde{x}$ to x

$$\begin{aligned} p(x, t|x', t') &= \tilde{p}(\Phi(x), t|\Phi(x'), t') \left|\frac{\partial\Phi(x)}{\partial x}\right| \\ &= \frac{1}{\sqrt{2\pi(t-t')}g(x)} \exp\left[-\frac{1}{2}\frac{(\int_{x'}^{x} \mathrm{d}x'' \frac{1}{g(x'')})^2}{(t-t')}\right]. \end{aligned} \tag{2.48}$$

Any moments of the process can now be computed. Either, as usual, with the propagator $p(x, t|x', t')$ and knowledge of some initial distribution $p(x', t')$ utilizing Eq. (2.12)

$$M^m(t) = \langle x(t)^m \rangle = \int \mathrm{d}x \int \mathrm{d}x' x^m p(x, t|x', t') p(x', t'), \tag{2.49}$$

or by using the inverse of the transformation function $\Phi^{-1}(\tilde{x})$ and the Gaussian propagator from the Wiener process Eq. (2.47)

$$M^m(t) = \langle x(t)^m \rangle = \int \mathrm{d}\tilde{x} \int \mathrm{d}\tilde{x}' \left(\Phi^{-1}(\tilde{x})\right)^m \tilde{p}(\tilde{x}, t|\tilde{x}', t') \tilde{p}(\tilde{x}', t'). \tag{2.50}$$

In both cases, by applying the transformation $\tau = t - t'$ the propagator becomes independent of t' and for $\tau \gg \Phi(x')^2$ also independent of x'.

If $g(x)$ is an even function, i.e. $g(x) = g(-x)$, then all odd moments are equal zero. The proof is simple, because if $g(x)$ is an even function, then $\frac{1}{g(x)}$ is also even and, thus, $\Phi(x) = \int^x \mathrm{d}x' \frac{1}{g(x')}$ is an odd function, i.e. $\Phi(x) = -\Phi(-x)$. Consequently, its inverse $\Phi^{-1}(\tilde{x})$ is odd as well and thus $(\Phi^{-1}(\tilde{x}))^m$ is odd, if m is an odd number. As consequence, the integration of Eq. (2.50) is zero in these cases.

2.4.4. General, drift-free case

A drift-free system with state-dependent diffusion coefficient interpreted in a general α interpretation (c.f. Sec. 2.3) is given by the Langevin equation

$$\frac{\mathrm{d}x}{\mathrm{d}t} = g(x)\xi(t) \quad (\alpha\text{-Interpretation}). \tag{2.51}$$

The same process may as well be described by a Langevin equation

$$\frac{\mathrm{d}x}{\mathrm{d}t} = (\alpha - \frac{1}{2})g'(x)g(x) + g(x)\xi(t) \quad \text{(Stratonovich)} \tag{2.52}$$

interpreted in the Stratonovich sense. Thus, by applying the transformation $\tilde{x} = \Phi(x) = \int^x \mathrm{d}x' \frac{1}{g(x')}$, the Langevin equation for $\tilde{x}$ is

$$\frac{\mathrm{d}\tilde{x}}{\mathrm{d}t} = (\alpha - \frac{1}{2})g'(\Phi^{-1}(\tilde{x})) + \xi(t). \tag{2.53}$$

Here, $g'(\Phi^{-1}(\tilde{x}))$ can be written as $g'(\Phi^{-1}(\tilde{x})) = \frac{\partial^2\Phi^{-1}(\tilde{x})}{\partial\tilde{x}^2} / \frac{\partial\Phi^{-1}(\tilde{x})}{\partial\tilde{x}}$, utilizing $g(x) = \frac{1}{\Phi'(x)}$ and $g(\Phi^{-1}(\tilde{x})) = \frac{\partial\Phi^{-1}(\tilde{x})}{\partial\tilde{x}}$. Thus, by introducing the potential $V(\tilde{x}) = (\frac{1}{2} - \alpha)\log\left(g(\Phi^{-1}(\tilde{x}))\right) = (\frac{1}{2} - \alpha)\log\left(\frac{\partial\Phi^{-1}(\tilde{x})}{\partial\tilde{x}}\right)$ the Langevin equation can be expressed as

$$\frac{\mathrm{d}\tilde{x}}{\mathrm{d}t} = -\frac{\partial V(\tilde{x})}{\partial\tilde{x}} + \xi(t). \tag{2.54}$$

Consequently, the transformed equation corresponds to the diffusion in a potential landscape. The corresponding Fokker-Planck equation of Eq. (2.54) is

$$\frac{\partial}{\partial t}\tilde{p}(\tilde{x},t) = -\frac{\partial}{\partial\tilde{x}}\left(-\frac{\partial V(\tilde{x})}{\partial\tilde{x}}\tilde{p}(\tilde{x},t)\right) + \frac{1}{2}\frac{\partial^2}{\partial\tilde{x}^2}\tilde{p}(\tilde{x},t) = -\hat{L}_{\mathrm{FP}}\tilde{p}(\tilde{x},t), \tag{2.55}$$

with the Fokker-Planck Operator

$$\hat{L}_{\mathrm{FP}} = \left[\frac{\partial}{\partial\tilde{x}}f(\tilde{x}) - \frac{1}{2}\frac{\partial^2}{\partial\tilde{x}^2}\right] \tag{2.56}$$

and the force $f(\tilde{x}) = -\frac{\partial V(\tilde{x})}{\partial\tilde{x}}$. The normalized steady state solution of this density is found by setting $\frac{\partial}{\partial t}\tilde{p}(\tilde{x},t) = 0$ and zero probability current and solving Eq. (2.55) resulting in the Boltzmann distribution

$$\tilde{p}_{eq}(\tilde{x}) = \frac{1}{Z}\exp(-2V(\tilde{x})); \;\; Z = \int \mathrm{d}\tilde{x}\exp(-2V(\tilde{x})). \tag{2.57}$$

The steady state exists if it is normalizable, i.e. $Z = \int \mathrm{d}\tilde{x}\exp(-2V(\tilde{x}))$ is finite. For the logarithmical potential $V(\tilde{x}) = (\frac{1}{2} - \alpha)\log\left(\frac{\partial\Phi^{-1}(\tilde{x})}{\partial\tilde{x}}\right)$ an equilibrium distribution $\tilde{p}_{\mathrm{eq}}(\tilde{x}) = \frac{1}{Z}g(\Phi^{-1}(\tilde{x}))^{2\alpha-1} = \frac{1}{Z}\left(\frac{\partial\Phi^{-1}(\tilde{x})}{\partial\tilde{x}}\right)^{2\alpha-1}$ is obtained. This corresponds well to the known equilibrium distributions of the original system $p_{\mathrm{eq}}(x) = \tilde{p}_{\mathrm{eq}}(\Phi(x))\frac{1}{g(x)} \propto g(x)^{2\alpha-2}$ [19].

By writing $\tilde{p}(\tilde{x},t) = \mathcal{N}\exp(-V(\tilde{x}))\Psi(\tilde{x},t)$, with $\mathcal{N}$ a normalization constant, and substitute this into the Fokker-Planck equation Eq. (2.55), the imaginary-time Schrödinger equation

$$\frac{\partial\Psi(\tilde{x},t)}{\partial t} = \frac{1}{2}\left[\frac{\partial^2 V(\tilde{x})}{\partial\tilde{x}^2} - \left(\frac{\partial V(\tilde{x})}{\partial\tilde{x}}\right)^2\right]\Psi(\tilde{x},t) + \frac{1}{2}\frac{\partial^2}{\partial\tilde{x}^2}\Psi(\tilde{x},t) = -\hat{H}_{\mathrm{S}}\Psi(\tilde{x},t) \tag{2.58}$$

is obtained, with the Hermitian operator

$$\hat{H}_{\mathrm{S}} = \exp(V(\tilde{x}))\hat{L}_{\mathrm{FP}}\exp(-V(\tilde{x})) = \frac{1}{2}\left[(f(\tilde{x})^2 + f'(\tilde{x})) - \frac{\partial^2}{\partial\tilde{x}^2}\right]. \tag{2.59}$$

Hence, $\Psi(\tilde{x},t)$ describes a time-dependent wave function in a Schrödinger potential $V_{\mathrm{S}}(\tilde{x}) = f'(\tilde{x}) + f(\tilde{x})^2 = V'(\tilde{x})^2 - V''(\tilde{x})$. Consequently, by introducing $h(\tilde{x}) = \Phi^{-1}(\tilde{x})$ and using the potential $V(\tilde{x}) = (\frac{1}{2} - \alpha)\log\left(h'(\tilde{x})\right)$ the Schrödinger potential becomes

$$V_{\mathrm{S}}(\tilde{x}) = (\alpha - \frac{1}{2})\frac{\left[(\alpha - \frac{3}{2})h''(\tilde{x})^2 + h'(\tilde{x})h^{(3)}(\tilde{x})\right]}{h'(\tilde{x})^2}. \tag{2.60}$$

With $\hat{H}_{\mathrm{S}}$ as a Hermitian operator, a general solution for $\Psi(\tilde{x},t)$ can be found in terms of an eigenfunction expansion [19, 58]

$$\Psi(\tilde{x},t) = \sum_{k=0}^{\infty} a_k \psi_k(\tilde{x}) \exp(-\lambda_k t) \tag{2.61}$$

with real eigenvalues $\lambda_k \geq 0$ and real eigenfunctions $\psi_k(\tilde{x})$ satisfying the time-independent Schrödinger equation $\hat{H}_{\mathrm{S}}\psi_k(\tilde{x}) = \lambda_k \psi_k(\tilde{x})$. Furthermore, these eigenfunctions $\psi_k(\tilde{x})$ are orthonormal, i.e.

$$\int \mathrm{d}\tilde{x}\ \psi_k(\tilde{x})\psi_l(\tilde{x}) = \delta_{kl} \tag{2.62}$$

and satisfy the completeness relation

$$\sum_k \psi_k(\tilde{x})\psi_k(\tilde{x}') = \delta(\tilde{x} - \tilde{x}'). \tag{2.63}$$

For eigenvalue $\lambda_0 = 0$ the equation $\hat{H}_{\mathrm{S}}\psi_0(\tilde{x}) = 0$ has the solution

$$\psi_0(\tilde{x}) = C\exp(-V(\tilde{x})) = C\check{\psi}_0(\tilde{x}) \tag{2.64}$$

with C a normalization constant and $\check{\psi}_0(\tilde{x})$ the unnormalized eigenfunction. Thus, by setting $\mathcal{N} = C$ and combining the transformation to the probability $\tilde{p}(\tilde{x},t) = \mathcal{N}\exp(-V(\tilde{x}))\Psi(\tilde{x},t) = \psi_0(\tilde{x})\Psi(\tilde{x},t)$ and the eigenfunction expansion of $\Psi(\tilde{x},t)$ Eq. (2.61) the probability reads

$$\tilde{p}(\tilde{x},t) = a_0\psi_0^2(\tilde{x}) + \sum_{k=1}^{\infty} a_k\psi_0(\tilde{x})\psi_k(\tilde{x})\exp(-\lambda_k t). \tag{2.65}$$

Hence, if $\psi_0(\tilde{x})$ is normalizable, i.e. $C = \left(\int \mathrm{d}\tilde{x}\check{\psi}_0^2(\tilde{x})\right)^{-\frac{1}{2}}$ is finite, then from the orthonormality of the eigenfunctions follows

$$\int \mathrm{d}x\ \tilde{p}(\tilde{x},t) = \int \mathrm{d}x\ \psi_0^2(\tilde{x}) = a_0 \tag{2.66}$$

and, hence, $a_0 = 1$. In the limit $t \to \infty$ only the ground state $\psi_0^2(\tilde{x})$ remains, which corresponds to the equilibrium distribution $\tilde{p}_{\mathrm{eq}}(\tilde{x}) = Z^{-1}\exp(-2V(\tilde{x}))$, i.e. $Z^{-1} = C^2$. In the limit $t \to 0$, the relation between the coefficients a_k and the initial distribution $\tilde{p}_0(\tilde{x})$ can be obtained from

$$\tilde{p}(\tilde{x}, t=0) = \tilde{p}_0(\tilde{x}) = \sum_{k=0}^{\infty} a_k\psi_0(\tilde{x})\psi_k(\tilde{x}) \tag{2.67}$$

via multiplying by $\frac{\psi_l(\tilde{x})}{\psi_0(\tilde{x})}$ and integrating over $\tilde{x}$. Thus, with use of orthonormality of the eigenfunctions, the coefficients read

$$\int \mathrm{d}\tilde{x}\frac{\psi_l(\tilde{x})}{\psi_0(\tilde{x})}\tilde{p}_0(\tilde{x}) = \sum_{k=0}^{\infty} a_k\delta_{kl} = a_l. \tag{2.68}$$

Hence, if the initial condition is given as a delta peak $\tilde{p}_0(\tilde{x}) = \delta(\tilde{x} - \tilde{x}_0)$, then $a_k = \frac{\psi_k(\tilde{x}_0)}{\psi_0(\tilde{x}_0)}$. Consequently $\tilde{p}(\tilde{x}, t|\tilde{x}_0, t = 0)$ is given by

$$\tilde{p}(\tilde{x}, t|\tilde{x}_0, t = 0) = C^2 \exp\left(-2V(\tilde{x})\right) + \frac{\exp\left(V(\tilde{x}_0)\right)}{\exp\left(V(\tilde{x})\right)} \sum_{k=1}^{\infty} \psi_k(\tilde{x}_0)\psi_k(\tilde{x}) \exp(-\lambda_k t). \tag{2.69}$$

The formal solution to the original problem is found by the variable transformation $\tilde{x} \to x$, which gives

$$p(x, t) = \tilde{p}(\Phi(x), t)\frac{1}{g(x)} = Cg(x)^{\alpha-\frac{3}{2}} \sum_{k=0}^{\infty} a_k \psi_k(\Phi(x)) \exp(-\lambda_k t). \tag{2.70}$$

And with initial condition $p(x, t = 0) = \delta(x - x_0)$

$$\begin{aligned} p(x, t|x_0, t = 0) &= \tilde{p}(\Phi(x), t|\Phi(x_0), t = 0)\frac{1}{g(x)} \\ &= C^2 g(x)^{2\alpha-2} + \frac{g(x)^{\alpha-\frac{3}{2}}}{g(x_0)^{\alpha-\frac{1}{2}}} \sum_{k=1}^{\infty} \psi_k(\Phi(x_0))\psi_k(\Phi(x)) \exp(-\lambda_k t). \end{aligned} \tag{2.71}$$

Due to the time-independence of $g(x)$, this solution is time-translation invariant, i.e. also the propagator solution $p(x, t' + \tau|x', t') = p(x, \tau|x')$.

Without further knowledge of $g(x)$ no additional information of $p(x, t)$ can be given. However, in chapter 3 some examples of one-dimensional systems with state dependent diffusion coefficient are given using the method from above for solution.

2.5. Anisotropic systems with state-dependent diffusion tensor

If a d-dimensional diffusion process is given by the Langevin equation

$$\frac{\mathrm{d}\mathbf{x}}{\mathrm{d}t} = \sqrt{2\mathbf{D}(\mathbf{x})}\boldsymbol{\xi}(t) = \mathbf{g}(\mathbf{x})\boldsymbol{\xi}(t), \quad (\alpha\text{-Interpretation}) \tag{2.72}$$

with the position dependent diffusion tensor $\mathbf{D}(\mathbf{x}) = \frac{1}{2}\mathbf{g}(\mathbf{x})\mathbf{g}(\mathbf{x})^{\mathsf{T}}$, the same rules as in the one-dimensional case (c.f. Sec. 2.3) apply regarding the stochastic interpretation of the equation. Using the α-interpretation as before, the different interpretations can be distinguished with help of their corresponding Fokker-Planck equation

$$\frac{\partial p(\mathbf{x}, t)}{\partial t} = \sum_{i=1}^{d}\sum_{j=1}^{d}\sum_{k=1}^{d} -\frac{\partial}{\partial x_i}\left(\alpha \frac{\partial g_{ij}(\mathbf{x})}{\partial x_k} g_{kj}(\mathbf{x}) p(\mathbf{x}, t)\right) + \frac{1}{2}\frac{\partial}{\partial x_i}\frac{\partial}{\partial x_j}\left(g_{ik}(\mathbf{x})g_{jk}(\mathbf{x})p(\mathbf{x}, t)\right). \tag{2.73}$$

Here $\alpha \sum_{j=1}^{d}\sum_{k=1}^{d} \frac{\partial g_{ij}(\mathbf{x})}{\partial x_k} g_{kj}(\mathbf{x}) = f_i^{\alpha}(\mathbf{x})$ act as the noise-induced drift term. For $\alpha = 0$ the equation reduces to

$$\frac{\partial p(\mathbf{x}, t)}{\partial t} = \sum_{i=1}^{d}\sum_{j=1}^{d}\sum_{k=1}^{d} \frac{1}{2}\frac{\partial}{\partial x_i}\frac{\partial}{\partial x_j}\left(g_{ik}(\mathbf{x})g_{jk}(\mathbf{x})p(\mathbf{x}, t)\right) = \sum_{i=1}^{d}\sum_{j=1}^{d} \frac{\partial}{\partial x_i}\frac{\partial}{\partial x_j} D_{ij}(\mathbf{x}) p(\mathbf{x}, t) \tag{2.74}$$

and for $\alpha = \frac{1}{2}$ to

$$\frac{\partial p(\mathbf{x}, t)}{\partial t} = \sum_{i=1}^{d}\sum_{j=1}^{d}\sum_{k=1}^{d} \frac{1}{2}\frac{\partial}{\partial x_i} g_{ik}(\mathbf{x}) \frac{\partial}{\partial x_j} g_{jk}(\mathbf{x}) p(\mathbf{x}, t). \tag{2.75}$$

The Fickian form of Fokker-Planck equation

$$\frac{\partial p(\mathbf{x},t)}{\partial t} = \operatorname{div}\left(\mathbf{D}\operatorname{grad} p(\mathbf{x},t)\right) \tag{2.76}$$

$$= \sum_{i=1}^{d}\sum_{j=1}^{d}\sum_{k=1}^{d}\frac{1}{2}\frac{\partial}{\partial x_i}g_{ik}(\mathbf{x})g_{jk}(\mathbf{x})\frac{\partial p(\mathbf{x},t)}{\partial x_j} = \sum_{i=1}^{d}\sum_{j=1}^{d}\frac{\partial}{\partial x_i}D_{ij}(\mathbf{x})\frac{\partial p(\mathbf{x},t)}{\partial x_j} \tag{2.77}$$

is also often used, especially for liquid crystalline systems [38, 79, 80]. This equation cannot be gained by setting $\alpha = 1$ and, thus, by interpreting the Langevin equation Eq. (2.72) in the Klimontovich-Hänggi sense, in contrast to the isotropic systems. For this purpose another drift term $\tilde{f}_i^{\beta}(\mathbf{x}) = \beta\sum_{j=1}^{d}\sum_{k=1}^{d} g_{ik}(\mathbf{x})\frac{\partial g_{jk}}{\partial x_j}(\mathbf{x})$ has to be introduced. Consequently, the density of the Langevin equation

$$\frac{\mathrm{d}\mathbf{x}}{\mathrm{d}t} = \mathbf{f}^{\frac{1}{2}}(\mathbf{x}) + \tilde{\mathbf{f}}^{\frac{1}{2}}(\mathbf{x}) + \sqrt{2\mathbf{D}(\mathbf{x})}\boldsymbol{\xi}(t), \quad \text{(Itô)} \tag{2.78}$$

follows this Fokker-Planck equation Eq. (2.76) and $f_i^{\frac{1}{2}}(\mathbf{x}) + \tilde{f}_i^{\frac{1}{2}}(\mathbf{x}) = \sum_{j=1}^{d}\frac{\partial D_{ij}(\mathbf{x})}{\partial x_j}$.

2.5.1. Restrictions to the considered systems and resulting simplifications

In this thesis some restrictions are imposed to the considered diffusion tensors in order to simplify the equations and allow analytical predictions. The first simplification is that the diffusion tensor has constant eigenvalues. Thus, it can be written as $\mathbf{D}(\mathbf{x}) = \mathbf{O}^{\mathsf{T}}(\mathbf{x})\hat{\mathbf{D}}\mathbf{O}(\mathbf{x})$, with $\mathbf{O}(\mathbf{x})$ a position-dependent orthogonal matrix and $\hat{\mathbf{D}} = \operatorname{diag}(D_1, D_2, \ldots, D_d)$ a constant diagonal tensor with the diffusion coefficients D_i belonging to the local principal axes. This is easily motivated with the background of tracer diffusion in liquid crystals [40, 51], where the direction dependent viscosity is locally constant, but the orientation of the local principal axis changes with the orientation of the liquid crystal, i.e. with its director. For a function $F(\mathbf{x},t)$ of the process the multidimensional Itô calculus can be applied, which is given by [81]

$$\frac{\mathrm{d}F(\mathbf{x},t)}{\mathrm{d}t} = \frac{\partial F(\mathbf{x},t)}{\partial t} + \sum_{i=1}^{d}\frac{\partial F(\mathbf{x},t)}{\partial x_i}f_i + \frac{1}{2}\sum_{i,j,k=1}^{d}\frac{\partial^2 F(\mathbf{x},t)}{\partial x_i \partial x_j}g_{ik}g_{jk} + \sum_{i,k=1}^{d}\frac{\partial F(\mathbf{x},t)}{\partial x_i}g_{ik}\xi_k(t). \quad \text{(Itô)} \tag{2.79}$$

Thus, for the general process Eq. (2.72) with force-term $f_i = f_i^{\alpha}(\mathbf{x})$ and volatility term $g_{ij} = g_{ij}(\mathbf{x}) = \sqrt{2}\sum_{k=1}^{d} O_{ki}(\mathbf{x})\sqrt{D_k}O_{kj}(\mathbf{x})$, the Langevin equation for the absolute square of the process yields

$$\frac{\mathrm{d}\sum_{i=1}^{d} x_i^2}{\mathrm{d}t} = \frac{\mathrm{d}r^2(t)}{\mathrm{d}t} = 2\sum_{i=1}^{d} x_i f_i^{\alpha}(\mathbf{x}) + \sum_{i,j,k=1}^{d}\delta_{ij}g_{ik}(\mathbf{x})g_{jk}(\mathbf{x}) + 2\sum_{i,k=1}^{d} x_i g_{ik}\xi_k(t) \quad \text{(Itô)}$$

$$= 2\mathbf{x}^{\mathsf{T}}\mathbf{f}^{\alpha}(\mathbf{x}) + 2\operatorname{tr}(\mathbf{D}) + 2\mathbf{x}^{\mathsf{T}}\mathbf{g}(\mathbf{x})\boldsymbol{\xi}(t) \tag{2.80}$$

with $\operatorname{tr}(\mathbf{D}) = \sum_i D_i$ the constant trace of the diffusion tensor and utilizing $\frac{\partial\sum_{i=1}^{d} x_i^2}{\partial x_i} = 2x_i$ and $\frac{\partial^2\sum_{i=1}^{d} x_i^2}{\partial x_i \partial x_j} = 2\delta_{ij}$. The same can be done for the projection of a component of the vector $\mathbf{x}$, which then reads

$$\frac{\mathrm{d}x_i(t)}{\mathrm{d}t} = f_i^{\alpha}(\mathbf{x}) + \sum_{k=1}^{d} g_{ik}(\mathbf{x})\xi_k(t) \quad \text{(Itô)} \tag{2.81}$$

and its square

$$\frac{\mathrm{d}x_i^2(t)}{\mathrm{d}t} = 2x_i f_i^\alpha(\mathbf{x}) + 2D_{ii}(\mathbf{x}) + \sum_{k=1}^{d} 2x_i g_{ik}(\mathbf{x})\xi_k(t). \quad \text{(Itô)} \tag{2.82}$$

If now each of these equations is averaged over all possible realizations, the equations simplify a bit, which means that averages of type $\left\langle \mathbf{h}^\mathsf{T}(\mathbf{x}(t))\boldsymbol{\xi}(t)\right\rangle$ for some arbitrary vector function $\mathbf{h}(\mathbf{x}(t))$ vanish since $\boldsymbol{\xi}(t)$ and $\mathbf{x}(t)$ are non-anticipating [81]. Thus, the equations for the mean of the absolute square yields

$$\frac{\mathrm{d}\left\langle r^2(t)\right\rangle}{\mathrm{d}t} = \left\langle 2\mathbf{x}(t)^\mathsf{T}\mathbf{f}^\alpha(\mathbf{x}(t))\right\rangle + 2\,\mathrm{tr}(\mathbf{D}). \tag{2.83}$$

Averages like $\left\langle \mathbf{x}^\mathsf{T}\mathbf{f}^\alpha(\mathbf{x})\right\rangle$ can not be given without knowledge of the propagator of the process $\mathbf{x}(t)$. But in the Itô interpretation of the original Langevin equation Eq. (2.72), i.e. $\alpha = 0$, the force term vanishes and the equation for the mean absolute square is a simple ODE, which can be solved and, thus $\left\langle r^2(t)\right\rangle = \left\langle r^2(0)\right\rangle + 2\,\mathrm{tr}(\mathbf{D})t$. The same can be done for the projection $x_i(t)$ and its square $x_i^2(t)$, which yields the equations for the averages

$$\frac{\mathrm{d}\left\langle x_i(t)\right\rangle}{\mathrm{d}t} = \left\langle f_i^\alpha(\mathbf{x})\right\rangle \tag{2.84}$$

and

$$\frac{\mathrm{d}\left\langle x_i^2(t)\right\rangle}{\mathrm{d}t} = 2\left\langle x_i(t) f_i^\alpha(\mathbf{x}(t))\right\rangle + 2\left\langle D_{ii}(\mathbf{x}(t))\right\rangle. \tag{2.85}$$

In consequence, for the Itô interpretation of the Langevin equation Eq. (2.72) the mean of each component is constant.

A further simplification can be done by assuming that the orientation change of the principal axes of the diffusion tensor only happens along a single direction, i.e. $\mathbf{D}(\mathbf{x}) = \mathbf{D}(x_i)$. This means that the Langevin equation for this component reads

$$\frac{\mathrm{d}x_i(t)}{\mathrm{d}t} = f_i^\alpha(x_i) + \sum_{k=1}^{d} g_{ik}(x_i)\xi_k(t), \quad \text{(Itô)} \tag{2.86}$$

which can be expressed also by another Langevin equation

$$\frac{\mathrm{d}x_i(t)}{\mathrm{d}t} = f_i^\alpha(x_i) + \hat{g}(x_i)\hat{\xi}(t) \quad \text{(Itô)} \tag{2.87}$$

with $\hat{g}(x_i) = \sqrt{\sum_{k=1}^{d} g_{ik}^2(x_i)} = \sqrt{2D_{ii}(x_i)}$. Here the fact that the sum of Gaussian variables with different variances itself is a Gaussian variable with variance given by the sum of the variances of the individual variables is used. Thus, the Langevin equation for this component can be treated like the one-dimensional Langevin equations with state-dependent diffusion constant before (see Sec. 2.4). Furthermore, with knowledge of the propagator of x_i also the averages needed for the Eqs. (2.83) to (2.85) can be computed and, thus, the temporal behavior of $\left\langle r^2(t)\right\rangle$, $\left\langle x_i(t)\right\rangle$ and $\left\langle x_i^2(t)\right\rangle$ can be predicted.

2.6. Measuring diffusion processes

The methods available to determine the coefficients characterizing a diffusion process are as diversified as the experimental setups which provide the necessary data. It is usually distinguished between ensemble methods and methods which measure on single particle/molecule level.

One example for ensemble methods is fluorescence recovery after photobleaching (FRAP) [82–85], where a small volume of a liquid which contains fluorescent dyes is bleached with help of a strong laser pulse. Afterwards, the intensity of this volume is measured over time and recovers slowly to the unbleached value due to invasion of dyes from the surrounding liquid. Here the recovery time is connected to the diffusion constant of the surrounding liquid [83]. One last example for ensemble methods is the pulsed field gradient nuclear magnetic resonance (PFG NMR) [86, 87], which measures the molecular motion with help of the echo signal of a Hahn spin echo pulse sequence [88]. Here the attenuation of the spin echo signal, which results from the dephasing of the nuclear spins due to translational motion and from the superposition of localized gradient pulses, is used to measure the diffusive motion. The measured signal attenuation in these experiments is the Fourier transform of the ensemble averaged propagator [89–91].

In contrast to these ensemble measurements, methods which observe single particles or molecules are of high relevance as well. Here one example is fluorescence correlation spectroscopy (FCS) [34, 41, 92, 93], which measures the temporal correlation of fluorescence burst signal from single dye molecules which diffuse through the small observation volume given by the laser focus. Here the correlation time is connected to the diffusion constant of the surrounding liquid [94]. Another examples for single molecule observation are the methods of single particle tracking (SPT) or single molecule tracking (SMT). In case of SPT it is usually referred to the optical tracking of colloidal particles [13, 28, 95], in case of SMT it is referred to the tracking of individual fluorescent dye molecules [12, 14, 40] or in biological systems to the tracking of larger macromolecules [25, 26, 96, 97] which are labeled via fluorescent dyes or quantum dots. In all cases, the stochastic motion of the individual tracer is recorded and the statistical analysis of these trajectories reveals the rheological properties of the surrounding liquid [28, 29]. Since these recorded trajectories are representations of the underlying diffusion process, averages and distributions of ensembles of the recorded paths (ensemble averages) or along a single path (time averages) are measured in order to obtain all necessary quantities to describe the propagator of the process completely. Hence, in many cases the knowledge of the diffusion constant is sufficient. Furthermore, the statements about the propagator from single molecule/particle methods can be compared with that from the ensemble methods in order to complete the picture of the observed process.

In this thesis, the focus is laid on the examination of an ensemble of trajectories and the relation of measurable averages and distributions to the underlying propagator. Thus, in the next sections some of the methods are explained which are able to obtain information of the propagator.

2.6.1. Mean squared displacement

The most used and best known quantity for diffusion processes is the mean squared displacement (MSD). It is obtained from an ensemble of N trajectories via

$$\left\langle r^2(\tau, t_0)\right\rangle_N = \frac{1}{N}\sum_{i=1}^{N}\left[(\mathbf{x}_i(t_0+\tau) - \mathbf{x}_i(t_0))^2\right] \tag{2.88}$$

using the displacement variable $\mathbf{r}(\tau, t_0) = \mathbf{x}(t_0+\tau) - \mathbf{x}(t_0)$ and its absolute value $r(\tau, t_0) = |\mathbf{r}(\tau, t_0)|$. It may also be obtained from a single trajectory via the time average

$$\overline{r^2(\tau, t_0)}_T = \frac{1}{T-\tau}\int_{t_0}^{t_0+T-\tau} \mathrm{d}t\left[(\mathbf{x}(t+\tau) - \mathbf{x}(t))^2\right]. \tag{2.89}$$

In case of ergodic processes both quantities, in the limit of a large ensemble or a large integration time, respectively, should be independent of the start time t_0 and of the initial state x_0. Thus, they should yield the same value, i.e.

$$\lim_{N\to\infty} \left\langle r^2(\tau)\right\rangle_N = \lim_{T\to\infty} \overline{r^2(\tau)}_T. \tag{2.90}$$

If this is not the case the processes are non-ergodic.

In this thesis the ensemble averages are of interest and they can be computed directly from the propagator $p(\mathbf{x}, t|\mathbf{x}', t')$. By introducing the positional displacement $\mathbf{r} = \mathbf{x} - \mathbf{x}'$ and the temporal displacement $\tau = t - t'$, the propagator can be written $p(\mathbf{x}' + \mathbf{r}, t' + \tau|\mathbf{x}', t')$. Since in this thesis state-dependent processes are relevant, the propagators of these processes are time-translation invariant and, thus, the propagator simplifies even more to $p(\mathbf{x}' + \mathbf{r}, \tau|\mathbf{x}')$. In case of homogeneous systems, e.g. the d-dimensional anisotropic motion Eq. (2.15), the propagator is also translation invariant with respect to the position $\mathbf{x}'$. Hence, it simplifies to $p(\mathbf{r}, \tau)$. From this simple displacement distribution, the expressions for the homogeneous anisotropic system Eq. (2.17) is already computed, now the MSD can be calculated via

$$\left\langle r^2(\tau)\right\rangle = \int \mathrm{d}^d r\ \mathbf{r}^2 p(\mathbf{r}, \tau). \tag{2.91}$$

For homogeneous d-dimensional anisotropic Brownian motion the MSD gives $\left\langle r^2(\tau)\right\rangle = 2\,\mathrm{tr}(\mathbf{D})\tau = 2\tau\sum_{i=1}^{d} D_i$ and for the d-dimensional isotropic process this simplifies to $\left\langle r^2(\tau)\right\rangle = 2dD_c\tau$. Of course, for such processes the ensemble quantity Eq. (2.88) should converge quickly to the theoretical values as the number N of recorded trajectories increases. In case of state-dependent processes, the MSD may also be computed via

$$\left\langle r^2(\tau)\right\rangle = \int \mathrm{d}^d r \int \mathrm{d}^d x'\ \mathbf{r}^2 p(\mathbf{x}' + \mathbf{r}, \tau|\mathbf{x}') p_{\mathrm{eq}}(\mathbf{x}'), \tag{2.92}$$

utilizing $p_{\mathrm{eq}}(\mathbf{x}')$ the equilibrium distribution or Boltzmann distribution. In experiments on isotropic systems usually the slope MSD-τ diagram is determined and, thus, the diffusion constant D_c. It follows immediately that in anisotropic systems, the information about the slope of the MSD is not enough to determine all the involved diffusion coefficients.

2.6.2. Distribution of diffusivities

In systems where more than one diffusion coefficient is relevant, e.g. heterogeneous and anisotropic systems, the MSD is insufficient to detect the heterogeneity or the anisotropy and unable to quantify the underlying diffusion coefficients [98–100]. For such reasons Bauer *et al.* [101] introduced the distribution of single-particle diffusivities as an advanced method to analyze stochastic motion in heterogeneous systems (see also [35]). Hence, it is distinguished between diffusivities as fluctuating quantities and diffusion coefficients as mean values. Furthermore, it was shown by Heidernätsch *et al.* [36] that the distribution of diffusivities can also be applied to homogeneous anisotropic systems in order to identify all the eigenvalues of the diffusion tensor. Moreover, Albers and Radons [102] extended this method to the distribution of generalized diffusivities to characterize also data from anomalous diffusion processes. This offers, as example, a deeper understanding of weak ergodicity breaking. Finally, in several experiments like for diffusion in inhomogeneous media [13, 14], for spectral diffusion [103, 104], for rotational diffusion [105] and also for diffusion in anisotropic media [34, 39, 41] this distribution is already successfully applied to analyze the trajectories. Furthermore, in Chap. 4 the distribution of diffusivities is applied to inhomogeneous anisotropic systems.

With knowledge of a trajectory of a stochastic process $\mathbf{x}(t)$ in d dimensions an individual displacement during a time lag τ is simply measured. Moreover, since the MSD for normal diffusion processes scales linear in time, it is natural to relate the measured displacements to a diffusivity

$$D_t(\tau) = \frac{[\mathbf{x}(t+\tau) - \mathbf{x}(t)]^2}{2d\tau}. \tag{2.93}$$

This simple transformation of displacements to diffusivities now allows to compare these quantities for different experimental setups and different τ. The diffusivity for a given time-lag τ is a fluctuating quantity along a trajectory as well as from trajectory to trajectory, analogously to the displacements. Thus, an important quantity is given by its probability density function $p(D, \tau)$ and is defined as

$$p(D, \tau) = \langle \delta \left[D - D_t(\tau) \right] \rangle , \tag{2.94}$$

where $\langle \dots \rangle$ either denotes a time average $\langle \dots \rangle = \lim_{T\to\infty} 1/T \int_0^T \dots \mathrm{d}t$ or an ensemble average. Furthermore, this distribution obtained from processes observed on different time scales τ can be compared. It should be noted that other definitions of diffusivity distributions exist in the literature [106].

For time-homogeneous systems, i.e. when the distribution of displacements is independent of t' and is obtained from the propagator via

$$p(\mathbf{r}, \tau) = \int \mathrm{d}^d x' \; p(\mathbf{x}' + \mathbf{r}, \tau | \mathbf{x}') p_{\mathrm{eq}}(\mathbf{x}'), \tag{2.95}$$

the distribution of diffusivities can be computed via

$$p(D, \tau) = \int \mathrm{d}^d r \; \delta \left(D - \frac{\mathbf{r}^2}{2d\tau} \right) p(\mathbf{r}, \tau). \tag{2.96}$$

Furthermore, it can be shown that the moments of the distribution of diffusivities may also be expressed in terms of the even moments of the displacement distribution, i.e.

$$M^m(\tau) = \int_0^\infty \mathrm{d}D \; D^m p(D, \tau) = \frac{1}{(2d\tau)^m} \int \mathrm{d}^d r \; \mathbf{r}^{2m} p(\mathbf{r}, \tau) = \frac{\left\langle \mathbf{r}^{2m} \right\rangle}{(2d\tau)^m}. \tag{2.97}$$

Thus, the first moment of the distribution or the mean diffusivity $M^1(\tau) = \langle D(\tau) \rangle$ is related to the mean squared displacement via

$$\left\langle r^2(\tau) \right\rangle = 2d \left\langle D(\tau) \right\rangle \tau, \tag{2.98}$$

thus, it gives the slope of the MSD.

For experimental data, e.g. from single particle tracking experiments, the recorded displacements are transformed via Eq. (2.93) to diffusivities and then collected in a normalized histogram according to Eq. (2.94). Since in experiments the number of samples may be small, there could be fluctuations in the distribution which are related to insufficient statistics of rare displacements. Nevertheless, by adapting the bin width it is possible to reduce these fluctuations.

Distribution of diffusivities in homogeneous systems

For homogeneous diffusion processes Heidernätsch *et al.* [36] give analytical expressions for the distribution of diffusivities. Here, $p(D, \tau)$ simplifies to $p(D)$. For d-dimensional homogeneous

anisotropic processes, with $\mathbf{D} = \mathbf{O}^\mathsf{T}\hat{\mathbf{D}}\mathbf{O}$ the positive definite and symmetric diffusion tensor and $\hat{\mathbf{D}} = \mathrm{diag}(D_1, D_2, \ldots, D_d)$ its diagonalized form, the distribution is computed via

$$p^d_{\hat{\mathbf{D}}}(D) = \int \mathrm{d}q_1 \cdots \int \mathrm{d}q_d \; \delta\left(D - \frac{1}{d}\sum_{i=1}^{d} D_i q_i^2\right) \prod_{j=1}^{d} p_{(0,1)}(q_j), \tag{2.99}$$

where $p_{(0,1)}(q_j) = \frac{1}{\sqrt{2\pi}} \exp(-\frac{1}{2}q_j^2)$ or as convolution via

$$p^d_{\hat{\mathbf{D}}}(D) = \{p^1_{D_1/d} * p^1_{D_2/d} * \cdots * p^1_{D_d/d}\}(D) = \int_0^\infty \mathrm{d}\Delta_1 \cdots \int_0^\infty \mathrm{d}\Delta_d \; \delta\left(D - \sum_{i=1}^{d}\Delta_i\right) \prod_{j=1}^{d} p^1_{D_j/d}(\Delta_j), \tag{2.100}$$

utilizing $p^1_{D_i/d}(D) = \sqrt{2\pi D D_i/d}^{-1} \exp\left(-\frac{dD}{2D_i}\right)$ the distribution of the homogeneous one-dimensional system with diffusion coefficient D_i/d. Furthermore, the characteristic function of the distribution of diffusivities can be computed explicitly and yields

$$\begin{aligned} G^d_{\hat{\mathbf{D}}}(k) = \int_0^\infty \mathrm{d}D \; \exp(\mathrm{i}kD)p(D) &= \prod_{j=1}^{d} \int \mathrm{d}q_j \; \exp\left(\mathrm{i}k\frac{D_j q_j^2}{d}\right) p_{(0,1)}(q_j) \\ &= \prod_{j=1}^{d} \left(1 - \mathrm{i}k\frac{2D_j}{d}\right)^{-\frac{1}{2}}. \end{aligned} \tag{2.101}$$

From this characteristic function the moments and cumulants can be computed using Eqs. (2.3) and (2.4). The cumulants yield

$$\kappa^m = \frac{1}{\mathrm{i}^m}\frac{\partial^m \ln G^d_{\hat{\mathbf{D}}}(k)}{\partial k^m}\bigg|_{k=0} = \frac{2^{m-1}(m-1)!}{d^m}\sum_{i=1}^{d} D_i^m \tag{2.102}$$

for $m > 0$. The first moment of the distribution of diffusivities is given by

$$M^1 = \frac{1}{d}\sum_{i=1}^{d} D_i = \langle D(\tau)\rangle\,, \tag{2.103}$$

which is simply the arithmetic mean of all diffusion coefficients D_i. With help of the relation Eq. (2.5) between cumulants and moments, the moments of the distribution can be predicted easily. Since the moments only depend on the eigenvalues of the diffusion tensor, the moments can be used to determine these eigenvalues [36].

Finally, for a d-dimensional homogeneous isotropic process with diffusion constant D_c, i.e. if all diffusion coefficients $D_i = D_c$ are the same, the distribution of diffusivities simplifies to

$$p^d_{D_c}(D) = \left(\frac{d}{2D_c}\right)^{\frac{d}{2}} \frac{D^{\frac{d}{2}-1}}{\Gamma(\frac{d}{2})} \exp\left(-\frac{d}{2D_c}D\right) \tag{2.104}$$

with the first moment $\langle D(\tau)\rangle = D_c$ and, thus, the distribution of $\frac{D}{D_C}$ is a χ^2 distribution with d degrees of freedom.

Distribution of diffusivities in a two-dimensional homogeneous anisotropic system

Since in this thesis mainly two-dimensional systems are considered, the respective diffusivity distribution for two-dimensional systems is needed. It can be given explicitly

$$\begin{aligned} p^2_{\hat{\mathbf{D}}}(D) =& \int_0^\infty \mathrm{d}\Delta_1 \int_0^\infty \mathrm{d}\Delta_2 \, \delta\left[D - (\Delta_1 + \Delta_2)\right] p^1_{D_1/2}(\Delta_1) p^1_{D_2/2}(\Delta_2) \\ =& \frac{\exp\left[-\frac{1}{2}\left(\frac{1}{D_1} + \frac{1}{D_2}\right) D\right]}{\sqrt{D_1 D_2}} I_0\left[\frac{1}{2}\left(\frac{1}{D_1} - \frac{1}{D_2}\right) D\right] \end{aligned} \tag{2.105}$$

where $I_0(x)$ denotes the modified Bessel function of the first kind. The first two moments of this distribution can be calculated with help of the cumulants Eq. (2.102) and read

$$\langle D \rangle = M^1 = \frac{1}{2}(D_1 + D_2) \tag{2.106}$$

and

$$\left\langle D^2 \right\rangle = M^2 = \frac{1}{4}(3D_1^2 + 2D_1 D_2 + 3D_2^2). \tag{2.107}$$

Hence, the mean diffusion coefficient coincides with the arithmetic mean of the diffusion coefficients belonging to the two directions of the anisotropic system as expected from Eq. (2.103). Solving the simultaneous Eqs. (2.106) and (2.107) for the eigenvalues, the relation

$$D_{1,2} = M^1 \pm \sqrt{M^2 - 2(M^1)^2} \tag{2.108}$$

is obtained and, thus, an equation for the diffusion coefficients D_1 and D_2 given in terms of the moments of the diffusivities.

The anisotropy of such processes is usually measured in terms of the eigenvalues of the diffusion tensor [107] and, thus it can be expressed also in terms of the moments of the distribution of diffusivities

$$\eta = \frac{|D_1 - D_2|}{D_1 + D_2} = \frac{\sqrt{M^2 - 2(M^1)^2}}{M^1}. \tag{2.109}$$

Furthermore, since the diffusion tensor $\mathbf{D}(\mathbf{x})$ of the state-dependent processes considered in this thesis has constant eigenvalues (see Sec. 2.5.1) and in the Itô interpretation of these drift-free processes also the mean absolute square of the position vector Eq. (2.83) is constant, the first moment of the distribution of diffusivities is constant as well. Thus, any dependence on τ in these systems caused by the heterogeneity are reflected in a τ dependence of the second moment and, thus in a τ dependence of the anisotropy measure

$$\eta(\tau) = \frac{\sqrt{M^2(\tau) - 2(M^1)^2}}{M^1}. \tag{2.110}$$

Of course, if the respective Langevin equation Eq. (2.72) is not interpreted in the Itô sense or the eigenvalues of the diffusion tensor $\mathbf{D}(\mathbf{x})$ are not constant, this assumption does not hold and both mean and second moment of the distribution of diffusivities may become dependent on τ.

2.6.3. Asymptotic invariant density

The idea of a proper scaling with the time of a process, like for the diffusivities, can also be applied to the process itself. Hence, assuming all moments of a process $x(t)$ show an asymptotical scaling behavior for large t in the form

$$\lim_{t\to\infty} M_{x_0}^m(t) \lim_{t\to\infty} \int \mathrm{d}x\, x^m p(x,t|x_0) = \hat{M}^m h(t)^m = . \tag{2.111}$$

Thus, the asymptotic growth of a moment $M_{x_0}^m(t)$ of a process is independent of the initial condition of the process and scales like $h(t)^m$. Consequently, the prefactor $\hat{M}^m$ can be calculated directly with help of the propagator via

$$\hat{M}^m = \lim_{t\to\infty} \int \mathrm{d}x \left(\frac{x}{h(t)}\right)^m p(x,t|x_0). \tag{2.112}$$

Hence, by introducing a new variable $\hat{x} = \frac{x}{h(t)}$

$$\hat{M}^m = \lim_{t\to\infty} \int \mathrm{d}\hat{x}\, \hat{x}^m p(\hat{x}h(t),t|x_0)h(t) \tag{2.113}$$

$$= \int \mathrm{d}\hat{x}\, \hat{x}^m p_{\mathrm{AID}}(\hat{x}) \tag{2.114}$$

the prefactor $\hat{M}^m$ is identified as the m-th moment of the density $p_{\mathrm{AID}}(\hat{x})$, which henceforth is called asymptotic invariant density. This probability density may be obtained from the propagator via

$$p_{\mathrm{AID}}(\hat{x}) = \lim_{t\to\infty} p(\hat{x}h(t),t|x_0)h(t) = \lim_{t\to\infty} \left\langle \delta\left(\hat{x} - \frac{x}{h(t)}\right)\right\rangle . \tag{2.115}$$

This concept can also be extended to higher dimensions, but then all multivariate moments must obey the same asymptotic scaling relation Eq. (2.111). Furthermore, since this is a simple coordinate transformation from $x(t)$ to $\hat{x}$, the PDF of the process for large times, i.e. $p(x,t) = p_{\mathrm{AID}}(x/h(t))/h(t)$ can be computed from the asymptotic invariant density. This means that $p_{\mathrm{AID}}(x/h(t))/h(t)$ has to fulfill the Fokker-Planck equation of the process $x(t)$.

As example, for a homogeneous one-dimensional diffusion process $h(t) = \sqrt{t}$, thus, the asymptotic invariant density yields

$$p_{\mathrm{AID}}(\hat{x}) = \lim_{t\to\infty} \frac{1}{\sqrt{4\pi D_c t}} \exp\left[-\frac{(\hat{x}\sqrt{t} - x')^2}{4D_c t}\right] \sqrt{t} \tag{2.116}$$

$$= \frac{1}{\sqrt{4\pi D_c}} \exp\left[-\frac{\hat{x}^2}{4D_c}\right], \tag{2.117}$$

which is a simple Gaussian distribution with zero mean and variance $2D_c$. The asymptotic invariant density is applied in Chap. 3 to propagators which show a different temporal scaling function.

Experimentally, this asymptotic invariant distribution can be obtained from an ensemble of trajectories by scaling them with the scaling function $h(t)$ of the process time t and binning them into a properly normalized histogram. These trajectories do not necessarily have to start at the same position. But first the scaling function $h(t)$ has to be obtained. For normal diffusion processes $h(t) = \sqrt{t}$ is a useful guess. If the process diffuses not normally the scaling function may be obtained as well from asymptotic growth of the mean squared displacement or from asymptotic growth of the variance of the process. Both should asymptotically be $\propto h(t)^2$. The correct scaling can be checked easily, since the asymptotic invariant density should converge to a density with a constant finite width and a constant center of mass.

3. Results I: One-dimensional systems with state-dependent diffusion coefficient

As explained in Chap. 2, Sec. 2.3, the question of the proper interpretation of the Langevin equation with multiplicative noise or the proper form of the Fokker-Planck equation is still open for many physical systems. Thus, from an experimentalist point of view it is useful to know the impact of the stochastic interpretation, i.e. the value of α, on the behavior of propagator and other statistical quantities like mean and variance of the measured process in order to identify the proper probabilistic description. Hence, in this chapter several one-dimensional processes with state-dependent diffusion coefficient are evaluated and, if possible, a general propagator is calculated which is valid for any $0 \leq \alpha \leq 1$ and, thus, for any stochastic interpretation of the related Langevin equation. Furthermore, for those systems mean and variance are computed and the influence of the value of α on this quantities is studied.

3.1. Geometric Brownian motion or Black-Scholes model

The Black-Scholes model [68] assumes that the logarithm of a stock price $S(t)$ behaves like a Wiener process, which means the stock price itself behaves like geometric Brownian motion given by the Langevin equation

$$\frac{\mathrm{d}S}{\mathrm{d}t} = \mu S + \sigma S \xi(t). \quad (\alpha\text{-Interpretation}) \tag{3.1}$$

Here $S(t)$ remains positive for all times. Thus, after conversion to Stratonovich interpretation the equation reads

$$\frac{\mathrm{d}S}{\mathrm{d}t} = \left[\mu + (\alpha - \frac{1}{2})\sigma^2\right] S + \sigma S \xi(t), \quad (\text{Stratonovich}) \tag{3.2}$$

using $g(S) = \sigma S$ and $(\alpha - \frac{1}{2})g'(S)g(S) = (\alpha - \frac{1}{2})\sigma^2 S$. In the original version Eq. (3.1) is interpreted using the Itô ($\alpha = 0$) interpretation [68]. After applying the transformation $\tilde{S} = \frac{\log(S)}{\sigma} = \int^S \mathrm{d}S' \frac{1}{g(S')}$, the Langevin equation becomes a Wiener Process with constant drift

$$\frac{\mathrm{d}\tilde{S}}{\mathrm{d}t} = \frac{1}{\sigma}\left[\mu + (\alpha - \frac{1}{2})\sigma^2\right] + \xi(t). \tag{3.3}$$

The propagator of such a process is

$$\tilde{p}(\tilde{S}, t|\tilde{S}', t') = \frac{1}{\sqrt{2\pi(t-t')}} \exp\left\{ -\frac{\left[\tilde{S} - \tilde{S}' - \frac{1}{\sigma}(\mu + (\alpha - \frac{1}{2})\sigma^2)(t-t')\right]^2}{2(t-t')} \right\} \tag{3.4}$$

and, thus, after the transformation $\tilde{S} \to S$ the propagator of the original process reads

$$p(S, t|S', t') = \frac{1}{\sigma S\sqrt{2\pi(t-t')}} \exp\left\{ -\frac{\left[\log(S) - \log(S') - (\mu + (\alpha - \frac{1}{2})\sigma^2)(t-t')\right]^2}{2\sigma^2(t-t')} \right\}. \tag{3.5}$$

Hence, $S(t)$ is a log-normally distributed variable with mean $\langle S(t)\rangle = S_0 \exp\left\{[\mu + (\alpha - \frac{1}{2})\sigma^2]t\right\}$ and variance $\left\langle (S(t) - \langle S(t)\rangle)^2 \right\rangle = S_0^2 \exp\left\{2[\mu + (\alpha - \frac{1}{2})\sigma^2]t\right\} [\exp(\sigma^2 t) - 1]$ using $S_0 = S'(t' = 0)$. Consequently, the mean and the variance of the process grow exponentially in time. Only if $\mu + (\alpha - \frac{1}{2})\sigma^2$ is smaller than zero, the mean value and variance may not grow exponentially. An example is for the Itô case ($\alpha = 0$) and with $\mu = 0$, then $\lim_{t\to\infty} \langle S(t)\rangle = 0$ and $\lim_{t\to\infty} \left\langle (S(t) - \langle S(t)\rangle)^2 \right\rangle = S_0^2$.

3.2. Brownian motion with diffusion coefficient $\mathbf{D(x) = D_0(1 + \sigma|x|)^2}$

A possible generalization for the geometric Brownian motion can be found by setting $g(x) = \sqrt{2D_0}(1 + \sigma|x|)$, with D_0 and σ positive constants. Thus, heterogeneous diffusion with diffusion coefficient $D(x) = D_0(1 + \sigma|x|)^2$. The corresponding Langevin equation is

$$\frac{\mathrm{d}x}{\mathrm{d}t} = \sqrt{2D_0}(1 + \sigma|x|)\xi(t). \quad (\alpha\text{-Interpretation}) \tag{3.6}$$

After the variable transformation $\tilde{x} = \Phi(x) = \int^x \mathrm{d}x' \frac{1}{\sqrt{2D_0}(1+\sigma|x'|)} = \mathrm{sign}(x)\frac{\log(1+\sigma|x|)}{\sqrt{2D_0}\sigma}$, the transformed process is given by

$$\frac{\mathrm{d}\tilde{x}}{\mathrm{d}t} = -c\,\mathrm{sign}(\tilde{x}) + \xi(t), \tag{3.7}$$

with $c = (\frac{1}{2} - \alpha)\sqrt{2D_0}\sigma$. The back-transformation is given by $\Phi^{-1}(\tilde{x}) = -\mathrm{sign}(\tilde{x})\left(\frac{1-\exp(\sqrt{2D_0}\sigma|\tilde{x}|)}{\sigma}\right)$. Hence, the transformed process describes diffusion in the potential $V(\tilde{x}) = (\frac{1}{2} - \alpha)\log(h'(\tilde{x}))$ and $h'(\tilde{x}) = \frac{\partial\Phi^{-1}(\tilde{x})}{\partial\tilde{x}} = \sqrt{2D_0}\exp(\sqrt{2D_0}\sigma|\tilde{x}|)$ and, thus, $V(\tilde{x}) = c|\tilde{x}| + \frac{1}{2}(\frac{1}{2} - \alpha)\log(2D_0)$. Consequently, the propagator $\tilde{p}(\tilde{x}, t|\tilde{x}_0, t = 0) = \tilde{p}(\tilde{x}, t|\tilde{x}_0)$ describes the diffusion in a wedge potential and fulfills the Fokker-Planck equation Eq. (2.55). If the propagator is written in the form $\tilde{p}(\tilde{x}, t|\tilde{x}_0) = \exp(-V(\tilde{x}))\Psi(\tilde{x}, t|\tilde{x}_0)$, then $\Psi(\tilde{x}, t|\tilde{x}_0)$ solves the imaginary-time Schrödinger equation Eq. (2.58). The corresponding Schrödinger potential $V_\mathrm{S}(\tilde{x}) = V'(\tilde{x})^2 - V''(\tilde{x}) = c^2 - 2c\delta(\tilde{x})$ is obtained by utilizing $\frac{\partial|x|}{\partial x} = \mathrm{sign}(x)$ and $\frac{\partial^2|x|}{\partial x^2} = 2\delta(x)$. The wave function $\Psi(\tilde{x}, t)$ can be expressed in terms of eigenfunctions $\psi_k(\tilde{x})$ and corresponding eigenvalues λ_k, which are solutions to the equation $\hat{H}_\mathrm{S}\psi_k(\tilde{x}) = \lambda_k\psi_k(\tilde{x})$ (c.f. Eq. (2.61)) with the Hermitian operator $\hat{H}_\mathrm{S} = \frac{1}{2}\left[V_\mathrm{S}(\tilde{x}) - \frac{\partial^2}{\partial\tilde{x}^2}\right]$. The eigenfunctions are orthonormal (see Eq. (2.62)) and fulfill the completeness relation Eq. (2.63).

3.2.1. Case $c > 0$

For $c > 0$, there exists a single bound state for $\lambda_0 = 0$ with the eigenfunction

$$\psi_0(\tilde{x}) = \sqrt{c}\exp(-c|\tilde{x}|). \tag{3.8}$$

The eigenvalues $\frac{k^2}{2} = \lambda_k - \frac{c^2}{2} > 0$ for $\lambda_k > \frac{c^2}{2}$ form a continuum with the eigenfunctions [19, 108]

$$\begin{aligned}\psi_k^{\mathrm{odd}}(\tilde{x}) &= \frac{1}{\sqrt{\pi}}\sin(kx)\\ \psi_k^{\mathrm{even}}(\tilde{x}) &= \frac{1}{\sqrt{\pi(k^2 + c^2)}}\left[k\cos(kx) - c\sin(k|x|)\right].\end{aligned} \tag{3.9}$$

These eigenfunctions are the solution to the Schrödinger equation

$$-\frac{1}{2}\frac{\partial^2\psi_k(\tilde{x})}{\partial\tilde{x}^2} - c\,\delta(\tilde{x})\psi_k(\tilde{x}) = \frac{k^2}{2}\psi_k(\tilde{x}) \tag{3.10}$$

and describe the scattering caused by the δ Potential.

Now $\Psi(\tilde{x},t|\tilde{x}_0)$ can be written in terms of an eigenfunction expansion

$$\Psi(\tilde{x},t|\tilde{x}_0) = a_0\psi_0(\tilde{x}) + \exp\left(-\frac{c^2}{2}t\right)\int_0^\infty \mathrm{d}k \exp\left(-\frac{k^2}{2}t\right)\left[a_k^{\mathrm{even}}\psi_k^{\mathrm{even}}(\tilde{x}) + a_k^{\mathrm{odd}}\psi_k^{\mathrm{odd}}(\tilde{x})\right] \quad (3.11)$$

with the coefficients a_k given from the initial conditions of $p(\tilde{x},t=0|\tilde{x}_0) = \delta(\tilde{x}-\tilde{x}_0)$ via

$$a_k^{\mathrm{even,odd}} = \int_{-\infty}^{\infty}\mathrm{d}\tilde{x}\frac{\psi_k^{\mathrm{even,odd}}(\tilde{x})}{\psi_0(\tilde{x})}p(\tilde{x},t=0|\tilde{x}_0) = \frac{\psi_k^{\mathrm{even,odd}}(\tilde{x}_0)}{\psi_0(\tilde{x}_0)}. \quad (3.12)$$

Thus, with use of the completeness relation Eq. (2.63) the propagator

$$\begin{aligned}\tilde{p}(\tilde{x},t|\tilde{x_0}) = \psi_0^2(\tilde{x}) + \frac{\psi_0(\tilde{x})}{\psi_0(\tilde{x}_0)}\exp\left(-\frac{c^2}{2}t\right)\\ \times\int_0^\infty \mathrm{d}k\exp\left(-\frac{k^2}{2}t\right)\left[\psi_k^{\mathrm{even}}(\tilde{x}_0)\psi_k^{\mathrm{even}}(\tilde{x}) + \psi_k^{\mathrm{odd}}(\tilde{x}_0)\psi_k^{\mathrm{odd}}(\tilde{x})\right]\end{aligned} \quad (3.13)$$

is properly normalized.

The integration of Eq. (3.11) can be done with help of the density

$$\begin{aligned}\rho_k(\tilde{x},\tilde{x}_0) &= \psi_k^{\mathrm{even}}(\tilde{x}_0)\psi_k^{\mathrm{even}}(\tilde{x}) + \psi_k^{\mathrm{odd}}(\tilde{x}_0)\psi_k^{\mathrm{odd}}(\tilde{x})\\ &= \rho_k^1(\tilde{x},\tilde{x}_0) + \rho_k^2(\tilde{x},\tilde{x}_0) + \rho_k^3(\tilde{x},\tilde{x}_0)\end{aligned} \quad (3.14)$$

with

$$\rho_k^1(\tilde{x},\tilde{x}_0) = \frac{1}{\pi}\cos\left[k(\tilde{x}-\tilde{x}_0)\right] \quad (3.15)$$

$$\rho_k^2(\tilde{x},\tilde{x}_0) = -\frac{c^2}{\pi}\frac{1}{c^2+k^2}\cos\left[k(|\tilde{x}|+|\tilde{x}_0|)\right] \quad (3.16)$$

$$\rho_k^3(\tilde{x},\tilde{x}_0) = -\frac{c}{\pi}\frac{k}{c^2+k^2}\sin\left[k(|\tilde{x}|+|\tilde{x}_0|)\right]. \quad (3.17)$$

Thereby, the integral of the first density Eq. (3.15)

$$\int_0^\infty \mathrm{d}k\exp(-\frac{k^2}{2}t)\rho_k^1(\tilde{x},\tilde{x}_0) = \frac{1}{\sqrt{2\pi t}}\exp\left[-\frac{(\tilde{x}-\tilde{x}_0)^2}{2t}\right] \quad (3.18)$$

corresponds to the propagator of a free particle. The integration of Eq. (3.16) and Eq. (3.17) can be performed utilizing the cosine transform

$$\begin{aligned}\int_0^\infty \mathrm{d}x\frac{\exp(-\alpha^2x^2)}{x^2+\beta^2}\cos(xy) =\\ \frac{\pi}{4\beta}\exp(\alpha^2\beta^2)\left[\exp(-\beta y)\operatorname{erfc}\left(\alpha\beta-\frac{y}{2\alpha}\right) + \exp(\beta y)\operatorname{erfc}\left(\alpha\beta+\frac{y}{2\alpha}\right)\right]\end{aligned} \quad (3.19)$$

for $\mathrm{Re}(\alpha)>0$ and $\mathrm{Re}(\beta)>0$ from [109], p. 15, Eqn. (15) and the sine transform

$$\begin{aligned}\int_0^\infty \mathrm{d}x\frac{x\exp(-\alpha^2x^2)}{x^2+\beta^2}\sin(xy) =\\ \frac{\pi}{4}\exp(\alpha^2\beta^2)\left[\exp(-\beta y)\operatorname{erfc}\left(\alpha\beta-\frac{y}{2\alpha}\right) - \exp(\beta y)\operatorname{erfc}\left(\alpha\beta+\frac{y}{2\alpha}\right)\right]\end{aligned} \quad (3.20)$$

for $\mathrm{Re}(\alpha) > 0$ and $\mathrm{Re}(\beta) > 0$ from [109], p. 74, Eqn. (26). Here, $\mathrm{erfc}(x) = 1 - \int_0^x \mathrm{d}t \frac{2}{\sqrt{\pi}} \exp(-t^2)$ denotes the complementary error function. After simplification, the integration of $\rho_k^2(\tilde{x}, \tilde{x}_0)$ and $\rho_k^3(\tilde{x}, \tilde{x}_0)$ becomes

$$\int_0^\infty \mathrm{d}k \exp(-\frac{k^2}{2}t) \left[\rho_k^2(\tilde{x}, \tilde{x}_0) + \rho_k^3(\tilde{x}, \tilde{x}_0)\right] = \\ -\frac{1}{2}c \exp\left[\frac{c^2}{2}t - c(|\tilde{x}| + |\tilde{x}_0|)\right] \mathrm{erfc}\left(-\frac{|\tilde{x}| + |\tilde{x}_0| - ct}{\sqrt{2t}}\right). \quad (3.21)$$

After plugging Eq. (3.18) and Eq. (3.21) into Eq. (3.11) the wave equation for $c > 0$ becomes

$$\Psi(\tilde{x}, t|\tilde{x}_0) = \sqrt{c} \exp(-c|\tilde{x}|) + \frac{1}{\sqrt{2\pi t c}} \exp\left[-\frac{(\tilde{x} - \tilde{x}_0)^2}{2t} - \frac{c^2}{2}t + c|\tilde{x}_0|\right] \\ -\frac{1}{2}\sqrt{c} \exp\left(-c|\tilde{x}|\right) \mathrm{erfc}\left(-\frac{|\tilde{x}| + |\tilde{x}_0| - ct}{\sqrt{2t}}\right). \quad (3.22)$$

Hence, the corresponding propagator of $\tilde{x}$ reads

$$\tilde{p}(\tilde{x}, t|\tilde{x}_0) = c \exp(-2c|\tilde{x}|) + \frac{1}{\sqrt{2\pi t}} \exp\left[-\frac{(\tilde{x} - \tilde{x}_0)^2}{2t} - \frac{c^2}{2}t - c(|\tilde{x}| - |\tilde{x}_0|)\right] \\ -\frac{1}{2}c \exp\left(-2c|\tilde{x}|\right) \mathrm{erfc}\left(-\frac{|\tilde{x}| + |\tilde{x}_0| - ct}{\sqrt{2t}}\right) \quad (3.23)$$

with the stationary solution

$$\tilde{p}_{\mathrm{eq}}(\tilde{x}) = \lim_{t\to\infty} \tilde{p}(\tilde{x}, t|\tilde{x}_0) = c \exp(-2c|\tilde{x}|). \quad (3.24)$$

3.2.2. Case $c < 0$

Introducing the superpotential $W(\tilde{x})$, calculated from the ground state wave function of the $c > 0$ case [110]

$$W(\tilde{x}) = -\frac{\psi_0'(\tilde{x})}{\psi_0(\tilde{x})} = c\,\mathrm{sign}(\tilde{x}), \quad (3.25)$$

the Schrödinger potentials $V_{\mathrm{S}}^{\mp}(\tilde{x}) = W(\tilde{x})^2 \mp W'(\tilde{x}) = c^2 \mp 2c\delta(\tilde{x})$ form supersymmetric partner potentials. Hence, the case $c < 0$ is the supersymmetric partner to the case $c > 0$. The corresponding Hermitian operators read $\hat{H}_{\mathrm{S}}^{\mp} = \frac{1}{2}\left[V_{\mathrm{S}}^{\mp}(\tilde{x}) - \frac{\partial^2}{\partial \tilde{x}^2}\right]$. The operators can be written as $\hat{H}_{\mathrm{S}}^{-} = A^\dagger A$ and $\hat{H}_{\mathrm{S}}^{+} = A A^\dagger$ with the operators A and $A^\dagger$ given by

$$A = \sqrt{\frac{1}{2}}\frac{\partial}{\partial \tilde{x}} + \sqrt{\frac{1}{2}} W(\tilde{x}) \quad (3.26)$$

$$A^\dagger = -\sqrt{\frac{1}{2}}\frac{\partial}{\partial \tilde{x}} + \sqrt{\frac{1}{2}} W(\tilde{x}). \quad (3.27)$$

Thus, by applying the operator A to the time-independent Schrödinger equation $\hat{H}_{\mathrm{S}}^{-}\psi_k^{-}(\tilde{x}) = \lambda_k^{-}\psi_k^{-}(\tilde{x})$ the relation

$$A\hat{H}_{\mathrm{S}}^{-}\psi_k^{-}(\tilde{x}) = \hat{H}_{\mathrm{S}}^{+} A\psi_k^{-}(\tilde{x}) = \lambda_k^{-} A\psi_k^{-}(\tilde{x}) \quad (3.28)$$

is found and, similarly, the operator $A^\dagger$ applied to the time-independent Schrödinger equation for $\psi_k^+(\tilde{x})$ the equation reads

$$A^\dagger \hat{H}_{\rm S}^+ \psi_k^+(\tilde{x}) = \hat{H}_{\rm S}^- A^\dagger \psi_k^+(\tilde{x}) = \lambda_k^+ A^\dagger \psi_k^+(\tilde{x}). \tag{3.29}$$

Consequently, by using the equations above the relations

$$\lambda_k^+ = \lambda_{k+1}^-,\ \lambda_0^- = 0 \tag{3.30}$$

for the eigenvalues and

$$\psi_k^+(\tilde{x}) = \frac{A\psi_{k+1}^-(\tilde{x})}{\sqrt{\lambda_{k+1}^-}} \tag{3.31}$$

$$\psi_{k+1}^-(\tilde{x}) = \frac{A^\dagger \psi_k^+(\tilde{x})}{\sqrt{\lambda_k^+}} \tag{3.32}$$

for the eigenfunctions are found. Thereby, the eigenvalues and eigenfunctions for $\hat{H}_{\rm S}^-$ are already computed in the previous subsection and given by Eq. (3.8) for $\lambda_0^- = 0$ and Eq. (3.9) for $\lambda_k^- = \frac{k^2}{2} + \frac{c^2}{2}$. Thus, for the supersymmetric partner potential the eigenfunctions read

$$\begin{aligned}\psi_k^{\rm odd,+}(\tilde{x}) &= -\frac{1}{\sqrt{\pi}}\sin(k\tilde{x}) \\ \psi_k^{\rm even,+}(\tilde{x}) &= \frac{1}{\sqrt{\pi(k^2+\tilde{c}^2)}}\left[k\cos(k\tilde{x}) + \tilde{c}\sin(k|\tilde{x}|)\right],\end{aligned} \tag{3.33}$$

with $\tilde{c} = -c$ and $c < 0$ and the corresponding eigenvalues are $\lambda_k^+ = \frac{k^2}{2} + \frac{\tilde{c}^2}{2}$. The densities, needed for the computation of the propagator, read

$$\rho_k^{1,+}(\tilde{x},\tilde{x}_0) = \frac{1}{\pi}\cos\left[k(\tilde{x}-\tilde{x}_0)\right] \tag{3.34}$$

$$\rho_k^{2,+}(\tilde{x},\tilde{x}_0) = -\frac{\tilde{c}^2}{\pi}\frac{1}{\tilde{c}^2+k^2}\cos\left[k(|\tilde{x}|+|\tilde{x}_0|)\right] \tag{3.35}$$

$$\rho_k^{3,+}(\tilde{x},\tilde{x}_0) = \frac{\tilde{c}}{\pi}\frac{k}{\tilde{c}^2+k^2}\sin\left[k(|\tilde{x}|+|\tilde{x}_0|)\right]. \tag{3.36}$$

Here, the coefficients $a_k^{\rm even,odd,+} = \psi_k^{\rm even,odd,+}(\tilde{x}_0)\exp(V(\tilde{x}_0)) = \psi_k^{\rm even,odd,+}(\tilde{x}_0)\exp(-\tilde{c}|\tilde{x}_0|)$ are used. The wave equation for $c < 0$ is now computed via

$$\Psi^+(\tilde{x},t|\tilde{x}_0) = \exp(-\frac{c^2}{2}t)\int_0^\infty {\rm d}k\exp(-\frac{k^2}{2}t)\left[\rho_k^{1,+}(\tilde{x},\tilde{x}_0) + \rho_k^{2,+}(\tilde{x},\tilde{x}_0) + \rho_k^{3,+}(\tilde{x},\tilde{x}_0)\right] \tag{3.37}$$

Thus, by using the integrals Eq. (3.18), Eq. (3.19) and Eq. (3.20) the wave equation reads

$$\begin{aligned}\Psi^+(\tilde{x},t|\tilde{x}_0) = \frac{1}{\sqrt{2\pi t}}\exp\left[-\frac{(\tilde{x}-\tilde{x}_0)^2}{2t} - \frac{\tilde{c}^2}{2}t - \tilde{c}|\tilde{x}_0|\right] \\ - \frac{1}{2}\tilde{c}\exp\left(\tilde{c}|\tilde{x}|\right)\mathrm{erfc}\left(\frac{|\tilde{x}|+|\tilde{x}_0|+\tilde{c}t}{\sqrt{2t}}\right).\end{aligned} \tag{3.38}$$

Consequently, the propagator is given by $p^+(\tilde{x},t|\tilde{x}_0) = \exp(\tilde{c}|x|)\Psi^+(\tilde{x},t|\tilde{x}_0)$.

3.2.3. Propagator of diffusion in a wedge potential

Finally, the propagator for a general c and, thus, the propagator of diffusion in a potential $V(\tilde{x}) = c|\tilde{x}|$ reads

$$\tilde{p}(\tilde{x},t|\tilde{x}_0) = \frac{c}{2}\exp(-2c|\tilde{x}|)\,\mathrm{erfc}\left(\frac{|\tilde{x}|+|\tilde{x}_0|-ct}{\sqrt{2t}}\right) + \frac{1}{\sqrt{2\pi t}}\exp\left[-\frac{(\tilde{x}-\tilde{x}_0)^2}{2t} - \frac{c^2}{2}t - c(|\tilde{x}|-|\tilde{x}_0|)\right] \quad (3.39)$$

or by using $(\tilde{x}-\tilde{x}_0)^2 = (|\tilde{x}|-|\tilde{x}_0|)^2 - 2\tilde{x}\tilde{x}_0(1-\mathrm{sign}(\tilde{x})\mathrm{sign}(\tilde{x}_0))$, the propagator can be expressed as

$$\tilde{p}(\tilde{x},t|\tilde{x}_0) = \frac{c}{2}\exp(-2c|\tilde{x}|)\,\mathrm{erfc}\left(\frac{|\tilde{x}|+|\tilde{x}_0|-ct}{\sqrt{2t}}\right) + \frac{1}{\sqrt{2\pi t}}\exp\left[-\frac{(|\tilde{x}|-|\tilde{x}_0|+ct)^2 + 2|\tilde{x}||\tilde{x}_0|(1-\mathrm{sign}(\tilde{x})\mathrm{sign}(\tilde{x}_0))}{2t}\right]. \quad (3.40)$$

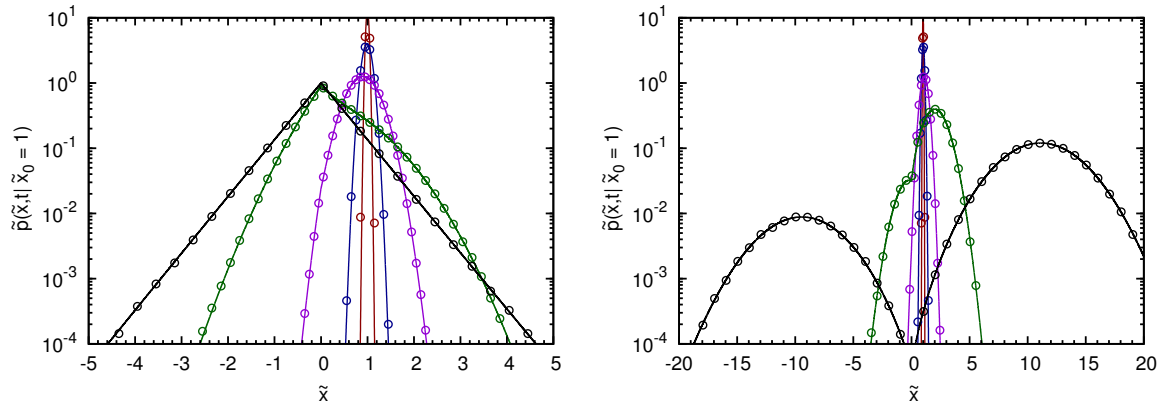

Figure 3.1.: The propagator of diffusion in a wedge potential with $c = 1$ (left) and $c = -1$ (right) for different times, $t = 0.001$, $t = 0.01$, $t = 0.1$, $t = 1$ and $t = 10$, with $D_0 = \sigma = 1$ and $x_0 = 1$. The numerical results (circles) and the respective analytical curve (lines) from Eq. (3.39) agree well. The process for a positive constant ($c = 1$, left) approaches the steady state given by Eq. (3.24).

In Fig. 3.1 a comparison between the analytic propagator Eq. (3.39) and the density obtained from the numerical implementation of the Langevin equation Eq. (3.7) is shown. Both probability density functions agree well for the simulated times and for $c > 0$ the approach to the equilibrium state Eq. (3.24) can be observed. Since the y-axis is scaled logarithmically, for $c > 0$ the crossover from the quadratic shape can be observed, which corresponds to a Gaussian PDF in the unscaled form, to a wedge shape, which corresponds to a pure exponential decay on both sides of zero in the unscaled form. For $c < 0$, the crossover goes from a single Gaussian peak for small times to two broadening Gaussian peaks moving in different direction away from zero.

It is also possible to calculate the characteristic function of the propagator

$$\tilde{G}(\tilde{k}) = \int_{-\infty}^{\infty} \mathrm{d}\tilde{x}\, \exp\left(\mathrm{i}\tilde{k}\tilde{x}\right)\tilde{p}(\tilde{x},t|\tilde{x}_0) = \tilde{G}^{+}(\tilde{k}) - \tilde{G}^{-}(\tilde{k}) \quad (3.41)$$

utilizing

$$\begin{aligned}\tilde{G}^{\pm}(\tilde{k}) &= \int_0^{\pm\infty} \mathrm{d}\tilde{x}\, \exp\left(\mathrm{i}\tilde{k}\tilde{x}\right) \tilde{p}(\tilde{x},t|\tilde{x}_0) \\ &= \frac{1}{2}\exp\left[\mp \mathrm{i}c\tilde{k}t + \mathrm{i}\tilde{k}\tilde{x}_0 - \frac{1}{2}\tilde{k}^2 t + c\left(|\tilde{x}_0| \mp \tilde{x}_0\right)\right]\left[\operatorname{erf}\left(\frac{\mathrm{i}\tilde{k}t + \tilde{x}_0 \mp ct}{\sqrt{2t}}\right) \pm 1\right] \\ \pm\frac{c}{4c \mp 2\mathrm{i}\tilde{k}}&\left[1 + \operatorname{erf}\left(\frac{ct - |\tilde{x}_0|}{\sqrt{2t}}\right) - \exp\left(\mp \mathrm{i}c\tilde{k}t \mp \mathrm{i}\tilde{k}|\tilde{x}_0 - \frac{1}{2}\tilde{k}^2 t + 2c|\tilde{x}_0|\right)\operatorname{erfc}\left(\frac{\mp\mathrm{i}\tilde{k}t + ct + |\tilde{x}_0|}{\sqrt{2t}}\right)\right]\end{aligned} \tag{3.42}$$

and from this characteristic function also the conditional moments of the propagator (see Sec. 2.1) can be computed. For instance, the first conditional moment reads

$$\begin{aligned}M^1_{\tilde{x}_0}(t) &= \frac{1}{\mathrm{i}}\left.\frac{\partial \tilde{G}(\tilde{k})}{\partial \tilde{k}}\right|_{\tilde{k}=0} \\ &= \frac{1}{2}\exp\left(c|\tilde{x}_0|\right)\left[(ct + \tilde{x}_0)\exp\left(c\tilde{x}_0\right)\operatorname{erfc}\left(\frac{ct + \tilde{x}_0}{\sqrt{2t}}\right) - (ct - \tilde{x}_0)\exp\left(-c\tilde{x}_0\right)\operatorname{erfc}\left(\frac{ct - \tilde{x}_0}{\sqrt{2t}}\right)\right].\end{aligned} \tag{3.43}$$

For asymptotic behavior of the first moment or mean for large t yields

$$M^1_{\tilde{x}_0}(t) \overset{t\to\infty}{\sim} \begin{cases} \sqrt{\frac{2}{\pi}}\frac{2\tilde{x}_0 t^{-\frac{3}{2}}}{c^3}\exp(c|\tilde{x}_0| - \frac{1}{2}c^2 t) & : \quad c > 0 \\ 2c\exp(c|\tilde{x}_0|)\sinh(c\tilde{x}_0)t & : \quad c < 0 \end{cases} \tag{3.44}$$

and for small t it yields

$$M^1_{\tilde{x}_0}(t) \overset{t\to 0}{\sim} \tilde{x}_0 - \operatorname{sign}(\tilde{x}_0)ct. \tag{3.45}$$

In the same fashion the second conditional moment of the propagator can be computed using $M^2_{\tilde{x}_0}(t) = -\left.\frac{\partial^2 \tilde{G}(\tilde{k})}{\partial \tilde{k}^2}\right|_{\tilde{k}=0}$ and also the variance of the process, which is given by $M^2_{\tilde{x}_0}(t) - \left(M^1_{\tilde{x}_0}(t)\right)^2$. The expression for the second moment can be found in the Appendix Eq. (A.1), nevertheless, the asymptotic behavior of the variance for large t yields

$$M^2_{\tilde{x}_0}(t) - \left(M^1_{\tilde{x}_0}(t)\right)^2 \overset{t\to\infty}{\sim} \begin{cases} \frac{1}{2c^2} & : \quad c > 0 \\ c^2\left[2\exp(2c|\tilde{x}_0|) - \exp(4c|\tilde{x}_0|)\right]t^2 & : \quad c < 0 \end{cases} \tag{3.46}$$

and for small t

$$M^2_{\tilde{x}_0}(t) - \left(M^1_{\tilde{x}_0}(t)\right)^2 \overset{t\to 0}{\sim} t. \tag{3.47}$$

In Fig. 3.2 a comparison between the analytical curves, their asymptotic behavior and the numerical values of mean and variance are shown. The latter was obtained from a random walk simulation with 5×10^5 walkers. All curves show a good agreement. For positive c mean and variance approach constant values as expected from the stationary distribution Eq. (3.24).

3.2.4. Propagator of the original process

The propagator of the Langevin equation Eq. (3.6) is now obtained using the transformation $\tilde{x} = \Phi(x) = \operatorname{sign}(x)\frac{\log(1+\sigma|x|)}{\sqrt{2D_0}\sigma}$, $\left|\frac{\partial\tilde{x}}{\partial x}\right| = \frac{1}{g(x)} = \left[\sqrt{2D_0}(1+\sigma|x|)\right]^{-1}$ and the propagator Eq. (3.40)

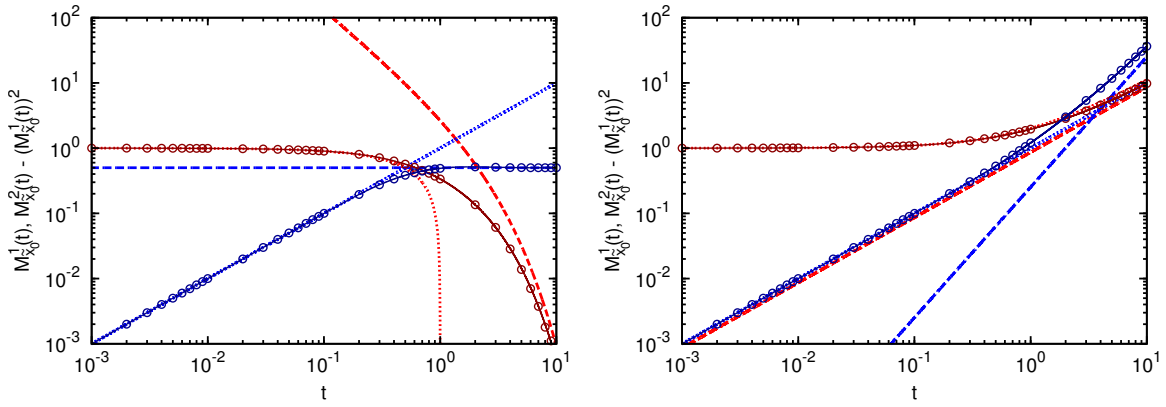

Figure 3.2.: Mean (red) and variance(blue) of a diffusion process in a wedge potential with $c = 1$ (left) and $c = -1$ (right) with $D_0 = \sigma = 1$ and $x_0 = 1$. The numerical results (circles) and the respective analytical curve (lines) agree well. Also the asymptotic behavior in the respective brighter colors for small t (dots) and for large t (dashes) agrees well. The mean for a positive constant ($c = 1$, left) approaches zero and the variance approaches a constant given by Eq. (3.46).

with $c = (\frac{1}{2} - \alpha)\sqrt{2D_0}\sigma$. Thus, it reads

$$\begin{aligned} p(x,t|x_0) &= \tilde{p}(\Phi(x),t|\Phi(x_0))\frac{1}{g(x)} = \\ &\frac{1}{2}(\frac{1}{2}-\alpha)\sigma(1+\sigma|x|)^{2\alpha-2}\,\mathrm{erfc}\left[\frac{(\alpha-\frac{1}{2})2D_0\sigma^2 t + \log(1+\sigma|x|) + \log(1+\sigma|x_0|)}{\sqrt{4D_0\sigma^2 t}}\right] \\ &+ \frac{1}{\sqrt{4\pi D_0 t}(1+\sigma|x|)}\exp\left\{-\frac{\left[\log\left(\frac{1+\sigma|x|}{1+\sigma|x_0|}\right) + (\frac{1}{2}-\alpha)2D_0\sigma^2 t\right]^2}{4D_0\sigma^2 t}\right\} \\ &\times \exp\left[-\frac{2\log(1+\sigma|x|)\log(1+\sigma|x_0|)(1-\mathrm{sign}(x)\mathrm{sign}(x_0))}{4D_0\sigma^2 t}\right]. \end{aligned} \tag{3.48}$$

For $\alpha < \frac{1}{2}$, e.g. for the Itô interpretation of Eq. (3.6), the propagator approaches an equilibrium state for $t \to \infty$

$$p_{\mathrm{eq}}(x) = \lim_{t\to\infty} p(x,t|x_0) = (\frac{1}{2}-\alpha)\sigma(1+\sigma|x|)^{2\alpha-2}. \tag{3.49}$$

In Fig. 3.3 a comparison between the analytic propagator Eq. (3.48) and the density obtained from the numerical implementation of the Langevin equation Eq. (3.6) is shown. This is done on the one hand for the Itô interpretation of this Langevin equation (left) and on the other hand for the Klimontovich-Hänggi interpretation of this Langevin equation (right). Both probability density functions agree well for the simulated times and also the approach to the equilibrium state Eq. (3.49) in the Itô case can be observed.

The conditional moments of the original process Eq. (3.6) can be computed either from the propagator of the original process Eq. (3.48) or from the propagator of the diffusion in the wedge

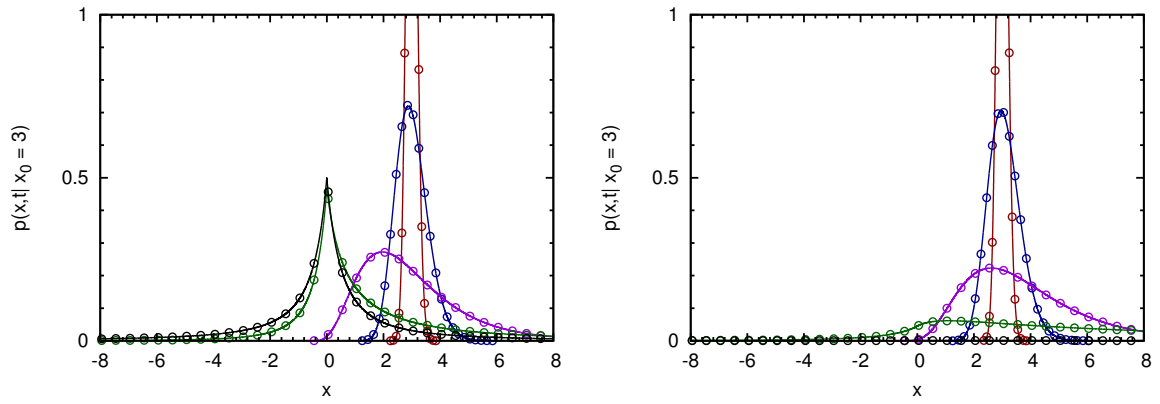

Figure 3.3.: The propagator of the Itô process ($\alpha = 0$, left) and of the Klimontovich-Hänggi process ($\alpha = 1$, right) for different times, $t = 0.001$, $t = 0.01$, $t = 0.1$, $t = 1$ and $t = 10$, with $D_0 = \sigma = 1$ and $x_0 = 3$. The numerical results (circles) and the respective analytical curve (lines) from Eq. (3.48) agree well. The Itô process approaches the steady state given by Eq. (3.49).

potential Eq. (3.39) via

$$M^m_{x_0}(t) = \langle x^m \rangle_{x_0} = \int_{-\infty}^{\infty} \mathrm{d}x\, x^m p(x,t|x_0) \tag{3.50}$$

$$= \int_{-\infty}^{\infty} \mathrm{d}\tilde{x} \left(\Phi^{-1}(\tilde{x})\right)^m \tilde{p}(\tilde{x}_0, t|\Phi(x_0)) \tag{3.51}$$

using the transformation function $\Phi(x) = \mathrm{sign}(x)\frac{\log(1+\sigma|x|)}{\sqrt{2D_0}\sigma}$ and its inverse $\Phi^{-1}(\tilde{x}) = -\mathrm{sign}(\tilde{x})\left(\frac{1-\exp(\sqrt{2D_0}\sigma|\tilde{x}|)}{\sigma}\right)$. The moments can be calculated explicitly by dividing the second integral into two parts,

$$\int_{-\infty}^{\infty} \mathrm{d}\tilde{x} \left(\Phi^{-1}(\tilde{x})\right)^m \tilde{p}(\tilde{x}_0, t|\Phi(x_0)) = \int_{0}^{\infty} \mathrm{d}\tilde{x} \left(\Phi^{-1}(\tilde{x})\right)^m \tilde{p}(\tilde{x}_0, t|\Phi(x_0)) - \int_{0}^{-\infty} \mathrm{d}\tilde{x} \left(\Phi^{-1}(\tilde{x})\right)^m \tilde{p}(\tilde{x}_0, t|\Phi(x_0)). \tag{3.52}$$

Nevertheless, the expressions are too large to be shown here, but the expression for the first moment can be found in the Appendix. For large t it can be shown that $M^1_{\tilde{x}_0}(t) \propto x_0 \exp(\alpha 2 D_0 \sigma^2 t)$ and for the Itô case the mean value simplifies to $M^1_{x_0}(t) = x_0$ as expected for an Itô process without drift (see Sec. 2.4.2). The same can be done for the variance of the process, which is for large t proportional to $\exp\left[(2\alpha+1)2D_0\sigma^2 t\right]$. Since the exponential growth in mean and variance directly depend on the value of α, and, thus on the stochastic interpretation, mean and variance can be used to distinguish the different cases of the stochastic interpretation or the form of the respective Fokker-Planck equation.

In Fig. 3.4 the mean and variance of the three most commonly used interpretations of the Langevin equation Eq. (3.6) is presented. Mean and variance obtained analytically and obtained from an ensemble of 10^7 random walkers performing the discrete Langevin equation show a good agreement. For large times there are slight deviations in the variance of Itô case between numerical and analytical results, which are caused by the numerical limits in the simulation.

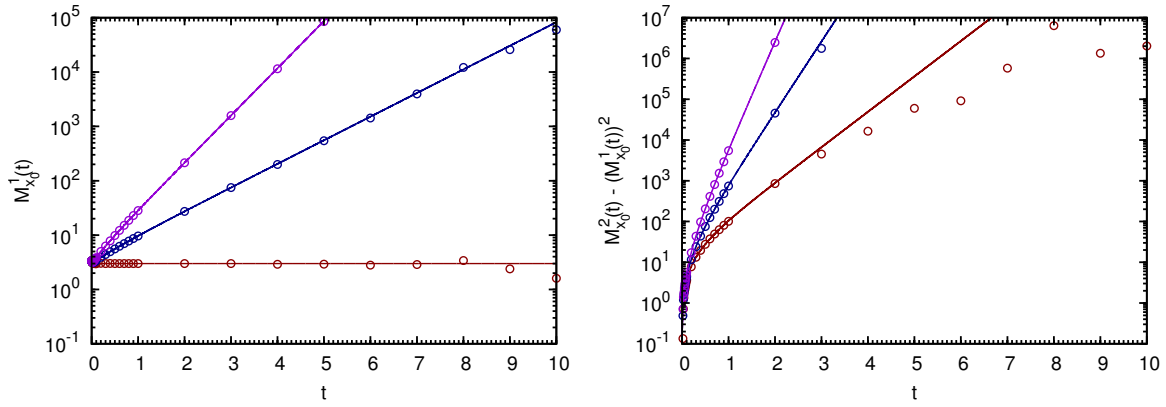

Figure 3.4.: Mean and variance of the diffusion process with $D(x) = D_0(1 + \sigma|x|)^2$ for the Itô interpretation (red), for the Stratonovich interpretation (blue) and for the Klimontovich-Hänggi interpretation (purple). The numerical results (circles) and the respective analytical curve (lines) agree well. Only for large times and the Itô process there are slight deviations which are caused by the numeric implementation and can be get rid of by simulating more walkers with a smaller time step. The Mean for the Itô process remains stationary.

It should be noted that in the Itô case the mean, i.e. the center of mass of the density, stays constant although the equilibrium or steady-state distribution Eq. (3.49) in this case has its center of mass in zero. This is a clear indicator that the steady-state solution is not reached in any finite time. Furthermore, each of the three stochastic interpretations can be clearly distinguished by their different exponential growth in mean and variance. For instance it can be used that $\lim_{t\to\infty} \frac{\log(M^1_{\tilde{x}_0}(t))}{\log(M^2_{\tilde{x}_0}(t))} = \frac{\alpha}{1+2\alpha}$ to infer the value of α.

3.3. Brownian motion with diffusion coefficient $\mathbf{D(x) = D_0 x^\kappa}$

A further generalization of the geometric Brownian motion (see Sec. 3.1) can be found by setting $D(x) = D_0 x^\kappa$ for $x > 0$, thus a process defined by the Langevin equation

$$\frac{\mathrm{d}x}{\mathrm{d}t} = \sqrt{2D_0} x^{\frac{\kappa}{2}} \xi(t) \quad (\alpha\text{-Interpretation}) \tag{3.53}$$

with $x(t) > 0$, $D_0 > 0$ and $\kappa \leq 2$ to fulfill the growth condition [58]. This algebraic dependency of the diffusion coefficient on the position is of high relevance in both mathematical finance and physics. As an example from finance, the above equation interpreted in the Itô, i.e. $\alpha = 0$ corresponds to the constant elasticity of variance (CEV)-model [111, 112], which is an expansion to the Black-Scholes model, and adds a leverage effect to the volatility, e.g. for $\kappa < 0$ the variance of a stock-price $x(t)$ increases as the stock-price falls. As example for physical systems, with $\kappa = 1$ and the Klimontovich-Hänggi interpretation of the Langevin equation above, i.e. $\alpha = 1$, this process describes the diffusion of a colloidal particle in the proximity of two walls, where one wall is slightly tilted against the other and, thus, building a wedge [72, 74]. Furthermore, Cherstvy *et al.* [113] already analyzed the Stratonovich-interpretation ($\alpha = \frac{1}{2}$) of this Langevin equation and showed that the process obeys anomalous diffusion of the form $\langle x^2(t) \rangle \simeq t^{\frac{2}{2-\kappa}}$

and weak ergodicity breaking (see also [114]). The general Langevin equation Eq. (3.53) after a transformation to an Itô-interpreted SDE reads

$$\frac{\mathrm{d}x}{\mathrm{d}t} = \alpha D_0 \kappa x^{\kappa-1} + \sqrt{2D_0} x^{\frac{\kappa}{2}} \xi(t). \quad \text{(Itô)} \tag{3.54}$$

It can be shown that this process can be transformed to a huge class of other highly relevant processes (see last subsection of Sec. 3.3.3). One example is the transformation $y = \Phi_{(\mathrm{BESQ})}(x) = \frac{2}{D_0(\kappa-2)^2} x^{2-\kappa}$ which leads to the squared Bessel process [115]. Thus, by applying Itôs Lemma Eq. (2.38), the SDE for $y(t)$ gives

$$\frac{\mathrm{d}y}{\mathrm{d}t} = \delta + 2\sqrt{y}\xi(t), \quad \text{(Itô)} \tag{3.55}$$

with $\delta = \frac{2(1+(\alpha-1)\kappa)}{2-\kappa}$. For positive integer δ, the process $y(t)$ is distributed as the sum of independent, squared Wiener processes, i.e. $y(t) \sim \sum_{i=1}^{\delta} W_i^2(t)$. Alternatively, $y(t)$ can be seen as the square of the norm of a δ-dimensional Wiener process. Since a Wiener process is a Gaussian distributed variable with variance t and mean $W_i(t=0)$, $y(t)$ follows a rescaled non-central χ^2 distribution. But even for a general positive δ, the propagator of the squared Bessel process follows such a non-central χ^2 distribution and is given by

$$p^{(\mathrm{BESQ})}(y,t|y_0) = \frac{1}{2t}\left(\frac{y}{y_0}\right)^{\frac{\delta}{4}-\frac{1}{2}} \exp\left(-\frac{y+y_0}{2t}\right) I_{\frac{\delta}{2}-1}\left(\frac{\sqrt{yy_0}}{t}\right), \tag{3.56}$$

where $I_\nu(x)$ denotes the modified Bessel of the first kind of order ν. Thus, after back-transformation the propagator of the process Eq. (3.54), or Eq. (3.53) respectively, reads

$$p(x,t|x_0) = \frac{x^{\frac{1}{2}(1+(\alpha-2)\kappa)} x_0^{\frac{1}{2}-\frac{\alpha\kappa}{2}}}{(2-\kappa)D_0 t} \exp\left[-\frac{x^{2-\kappa}+x_0^{2-\kappa}}{(2-\kappa)^2 D_0 t}\right] I_{\frac{1-\alpha\kappa}{\kappa-2}}\left[\frac{2(xx_0)^{1-\frac{\kappa}{2}}}{(2-\kappa)^2 D_0 t}\right]. \tag{3.57}$$

The propagator holds for $(1-\alpha)\kappa < 1$ and, thus, with a positive δ. Especially for the Itô case ($\alpha = 0$) the value of κ should not exceed unity. Furthermore, since the squared Bessel process is allowed to reach the boundary at $y = 0$ for $0 < \delta < 2$ and reaches it almost surely for $\delta < 1$ [see 115, chap. XI], this boundary has to be treated carefully in the original process too. As the diffusion coefficient at this point is zero, it behaves like an absorbing boundary in the original process. Thus, in order to keep the propagator Eq. (3.57) valid, the diffusion coefficient has to be slightly modified to

$$D(x) = \begin{cases} D_0 x^\kappa & : \quad x \geq \epsilon \\ \frac{D_0}{8}\epsilon^{\kappa-4}(\epsilon^2(4-\kappa)+\kappa x^2)^2 & : \quad x < \epsilon \end{cases} \tag{3.58}$$

for a small positive ϵ which can be chosen arbitrarily close to zero. Especially for computer-simulations $D(\epsilon)$ should not exceed the numerical ranges. Furthermore, the reflecting boundary itself has to be treated carefully, especially for negative κ, since in this case the noise-induced drift reaches high negative values. Thus, if a specular reflection is used, this will lead to an unphysical drift in positive direction. Hence, it is better to use a rejection method [116] for the simulation.

In Fig. 3.5 a comparison between the analytic propagator Eq. (3.57) for a positive $\kappa = 0.6$ and the density obtained from the numerical implementation of the Langevin equation Eq. (3.53) is shown. This is done for the Itô interpretation of this Langevin equation (left) and for the

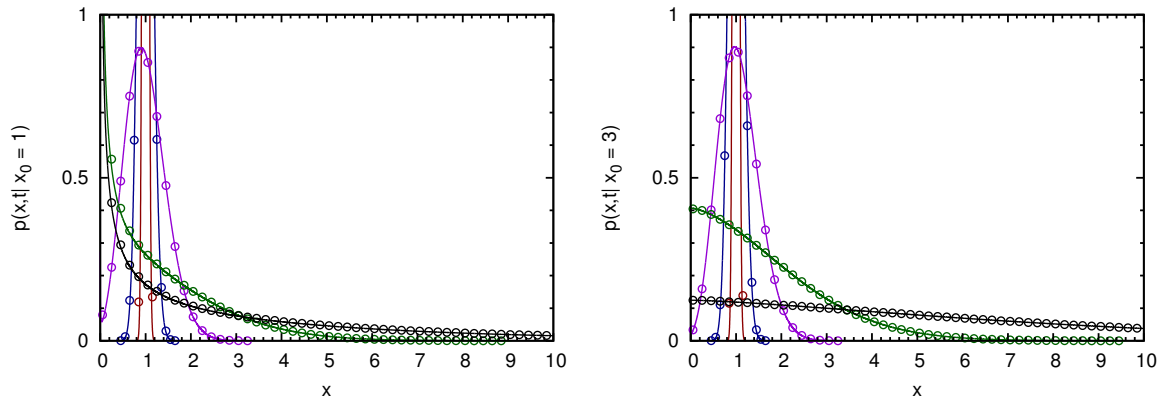

Figure 3.5.: The propagator of the Itô process ($\alpha = 0$, left) and of the Klimontovich-Hänggi process ($\alpha = 1$, right) for different times, $t = 0.001$, $t = 0.01$, $t = 0.1$, $t = 1$ and $t = 10$, with $D_0 = 1$, $\kappa = 0.6$ and $x_0 = 1$. The numerical results (circles) and the respective analytical curve (lines) from Eq. (3.57) agree well.

Klimontovich-Hänggi interpretation of this Langevin equation (right), respectively. Both probability density functions agree well for the simulated times. It should be noted that propagator for positive κ and for $\alpha < 1$ diverges at $x = 0$ for larger times as it can be seen in the figure.

In Fig. 3.6 a comparison between the analytic propagator Eq. (3.57) and the density obtained from the numerical implementation of the Langevin equation Eq. (3.53) is shown, but now for a negative $\kappa = -0.6$. This is done for the Itô interpretation of this Langevin equation (left) and for the Klimontovich-Hänggi interpretation of this Langevin equation (right), respectively. Both probability density functions agree well for the simulated times. The main difference between both PDFs is found for small values of x, where the propagator in the Itô case approaches zero and the propagator in the Klimontovich-Hänggi case approaches a time-dependent positive value. This holds also in general, hence, the propagator for $\alpha < 1$ approaches zero for negative κ or diverges at zero for positive κ. Thus, the propagator for the Klimontovich-Hänggi interpretation is special in that sense that it always approaches a positive time-dependent value given by $\exp\left[-\frac{x_0^{2-\kappa}}{(2-\kappa)^2 t}\right] t^{\frac{1}{\kappa-2}} (2-\kappa)^{\frac{\kappa}{\kappa-2}} \Gamma\left(\frac{1}{2-\kappa}\right)^{-1}$ for any $\kappa < 2$.

3.3.1. Moments

The conditional moments of the original process Eq. (3.53) can be computed either from the propagator of the original process Eq. (3.57) or from the propagator of the squared Bessel process Eq. (3.56) via

$$M_{x_0}^m(t) = \langle x^m \rangle_{x_0} = \int_0^\infty \mathrm{d}x\, x^m p(x,t|x_0) \tag{3.59}$$

$$= \int_0^\infty \mathrm{d}y \left(\Phi_{\mathrm{BESQ}}^{-1}(y)\right)^m p^{(\mathrm{BESQ})}(y,t|\Phi_{\mathrm{BESQ}}(x_0)) \tag{3.60}$$

using the inverse transformation function $\Phi_{(\mathrm{BESQ})}^{-1}(y) = \left[\frac{D_0}{2}(2-\kappa)^2 y\right]^{\frac{1}{2-\kappa}}$. Hence, the m-th moment of the original process is given as fractional moment of the propagator of the squared Bessel process. Although, the characteristic function as well as the Laplace transform of the propagator of the squared Bessel process are well known [115], using fractional derivatives like

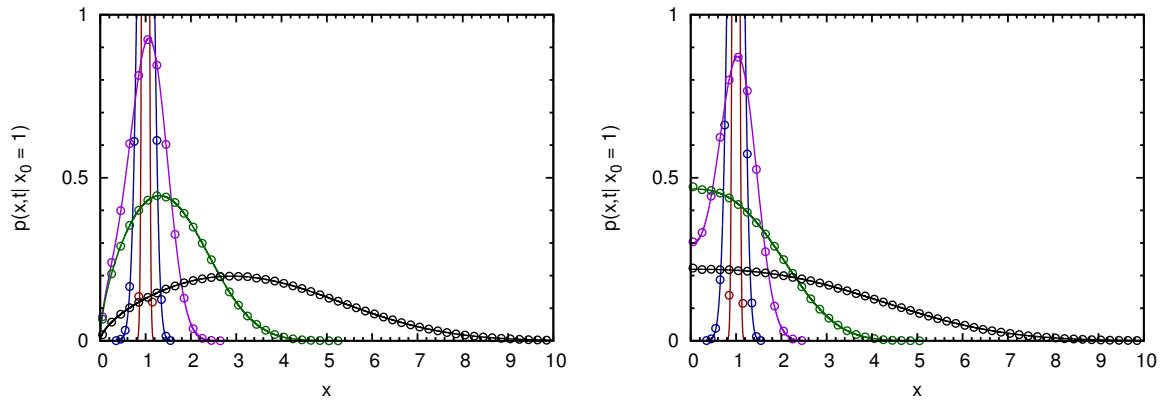

Figure 3.6.: The propagator of the Itô process ($\alpha = 0$, left) and of the Klimontovich-Hänggi process ($\alpha = 1$, right) for different times, $t = 0.001$, $t = 0.01$, $t = 0.1$, $t = 1$ and $t = 10$, with $D_0 = 1$, $\kappa = -0.6$ and $x_0 = 1$. The numerical results (circles) and the respective analytical curve (lines) from Eq. (3.57) agree well.

in Eqs. (2.7) to (2.8) does not lead to a simple expression for the fractional moments, but a direct integration leads to

$$M_{x_0}^m(t) = \left[D_0(2-\kappa)^2 t\right]^{\frac{m}{2-\kappa}} \frac{\Gamma(\frac{m+1+(\alpha-1)\kappa}{2-\kappa})}{\Gamma(\frac{1+(\alpha-1)\kappa}{2-\kappa})} {}_1F_1\left(-\frac{m}{2-\kappa}; \frac{1+(\alpha-1)\kappa}{2-\kappa}; -\frac{x_0^{2-\kappa}}{D_0(\kappa-2)^2 t}\right). \tag{3.61}$$

Here, ${}_1F_1(a;b;z) = \sum_{k=0}^{\infty} \frac{\Gamma(a+k)\Gamma(b)}{\Gamma(b+k)\Gamma(a)} \frac{z^k}{k!}$ is the Kummer confluent hypergeometric function.

The asymptotic behavior of the the conditional moments for large t yields

$$M_{x_0}^m(t) \overset{t\to\infty}{\sim} \left[D_0(2-\kappa)^2 t\right]^{\frac{m}{2-\kappa}} \frac{\Gamma(\frac{m+1+(\alpha-1)\kappa}{2-\kappa})}{\Gamma(\frac{1+(\alpha-1)\kappa}{2-\kappa})} \propto t^{\frac{m}{2-\kappa}}. \tag{3.62}$$

Thus, the moments become independent from the initial position for large t. Furthermore, it can be shown that the variance of all interpretations of the process for large t grows $\propto t^{\frac{2}{2-\kappa}}$, the same was also found already for the Stratonovich process [113]. Thus, for $\kappa > 0$ the variance of the processes asymptotically grows superdiffusively and for $\kappa < 0$ the variance asymptotically grows subdiffusively. The asymptotic growth of mean and variance does not depend on the value of α, i.e. on the stochastic interpretation of the Langevin equation Eq. (3.53). Thus, this cannot be used to distinguish the different interpretations.

In Fig. 3.7 the mean and variance of the three most commonly used interpretations of the Langevin equation Eq. (3.53) for the superdiffusive case, i.e. $\kappa = 0.6$, is presented. The analytical mean and variance and the values obtained from an ensemble of 5×10^6 random walkers, performing the discrete Langevin equation, show a good agreement. The crossover from the diffusive behavior in the variance for small times to the superdiffusive growth for large times can be seen. And the crossover from a constant mean for small times to an algebraic growth of the mean for large times can be observed as well for each type of stochastic interpretation. The distinction between the different types of the stochastic interpretations can only hardly be made by the asymptotic growth of mean and variance, as each obeys the same law. Only the prefactor is different and grows with increasing α, which may be used when the value of α has to be deduced.

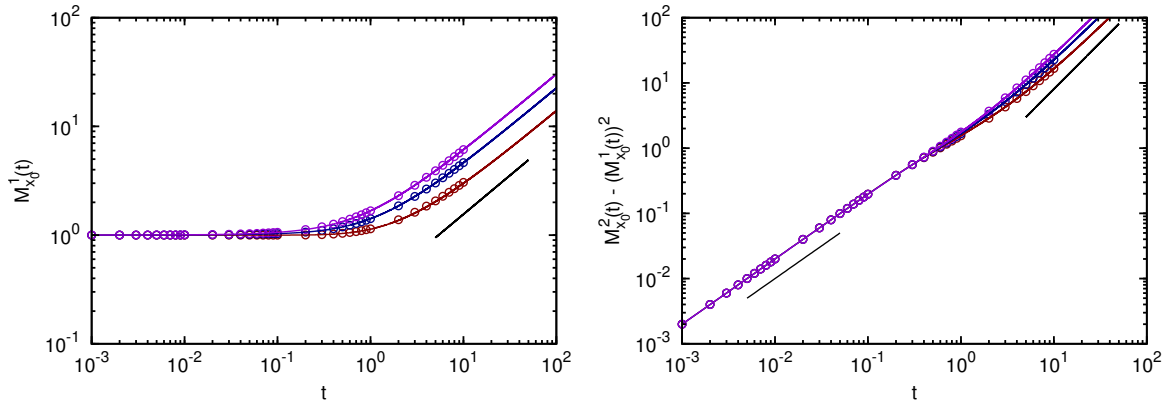

Figure 3.7.: Mean and variance of the diffusion process with $D(x) = x^{0.6}$ for the Itô interpretation (red), for the Stratonovich interpretation (blue) and for the Klimontovich-Hänggi interpretation (purple). The numerical results (circles) and the respective analytical curve (lines) obtained from Eq. (3.61) agree well. The mean shows a crossover from a constant behavior for small times to an algebraic growth $\propto t^{\frac{1}{2-0.6}}$ (black line as guide to the eye) as predicted from Eq. (3.62). The variance shows a crossover from a linear growth or diffusive behavior for small times to an algebraic superdiffusive growth $\propto t^{\frac{2}{2-0.6}}$ (black lines as guide to the eye) for large times.

In Fig. 3.8 mean and variance of the three most commonly used interpretations of the Langevin equation Eq. (3.53) for the subdiffusive case, i.e. $\kappa = -0.6$ are shown. The analytically obtained mean and variance and the values obtained from an ensemble of 5×10^6 random walkers, performing the discrete Langevin equation, show a good agreement. Again, the crossover from the diffusive behavior in the variance for small times to the subdiffusive growth for large times can be seen. Also the crossover from a constant mean for small times to an algebraic growth of the mean for large times can be observed for each type of stochastic interpretation. The distinction between the different types of the stochastic interpretations can only hardly be made by the asymptotic growth of mean and variance, as each obeys the same law. Only the prefactor is different and grows with increasing α, which may be of use if the value of α should be calculated.

3.3.2. Asymptotic invariant density

Since the moments of the process scale with $t^{\frac{m}{2-\kappa}}$, the propagator or density of the process converges to an invariant density for large t, if it is properly scaled. Thus, by introducing a new variable $\hat{x} = \frac{x}{t^{\frac{1}{2-\kappa}}}$, this asymptotic invariant density is found via

$$p_{\mathrm{AID}}(\hat{x}) = \lim_{t\to\infty} p(\hat{x}t^{\frac{1}{2-\kappa}}, t|x_0)t^{\frac{1}{2-\kappa}} = \lim_{t\to\infty} \left\langle \delta\left(\hat{x} - \frac{x}{t^{\frac{1}{2-\kappa}}}\right)\right\rangle_{x_0} \tag{3.63}$$

$$= \frac{D_0^{\frac{1-(\alpha-1)\kappa}{\kappa-2}}(2-\kappa)^{\frac{(2\alpha-1)\kappa}{\kappa-2}}}{\Gamma\left(\frac{(1-\alpha)\kappa-1}{\kappa-2}\right)}\hat{x}^{(\alpha-1)\kappa}\exp\left(-\frac{\hat{x}^{2-\kappa}}{D_0(\kappa-2)^2}\right). \tag{3.64}$$

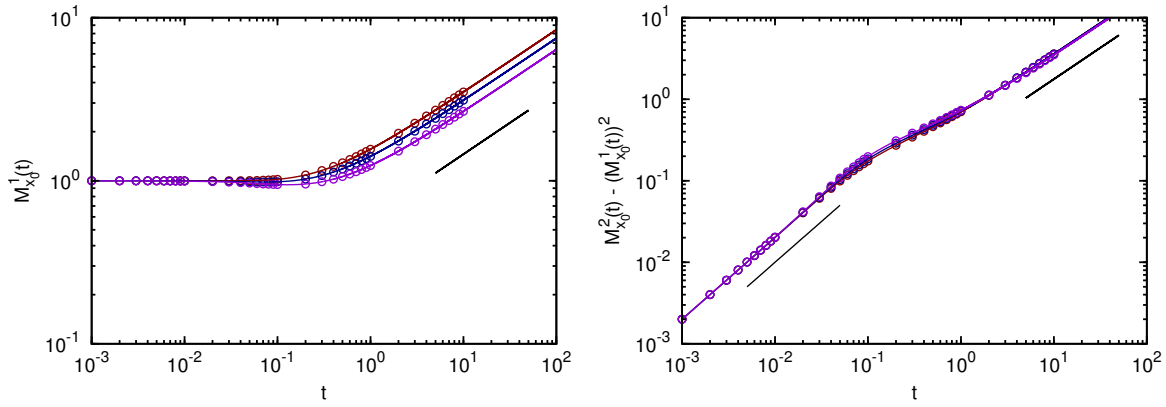

Figure 3.8.: Mean and variance of the diffusion process with $D(x) = x^{-0.6}$ for the Itô interpretation (red), for the Stratonovich interpretation (blue) and for the Klimontovich-Hänggi interpretation (purple). The numerical results (circles) and the respective analytical curve (lines) obtained from Eq. (3.61) agree well. The mean shows a cross-over from a constant behavior for small times to an algebraic growth $\propto t^{\frac{1}{2+0.6}}$ (black line as guide to the eye) as predicted from Eq. (3.62). The variance shows a crossover from a linear growth or diffusive behavior for small times to an algebraic subdiffusive growth $\propto t^{\frac{2}{2+0.6}}$ (black lines as guide to the eye) for large times.

And the moments of this density, which yield

$$\langle \hat{x}^m \rangle = \int_0^\infty \mathrm{d}\hat{x}\, \hat{x}^m p_{\mathrm{AID}}(\hat{x}) \tag{3.65}$$

$$= (D_0(2-\kappa)^2)^{\frac{m}{2-\kappa}} \frac{\Gamma(\frac{m+1+(\alpha-1)\kappa}{2-\kappa})}{\Gamma(\frac{1+(\alpha-1)\kappa}{2-\kappa})}, \tag{3.66}$$

are the rescaled asymptotic moments of the propagator, i.e. $\langle \hat{x}^m \rangle = \lim_{t\to\infty} \frac{M^m_{x_0}(t)}{t^{\frac{m}{2-\kappa}}}$. Furthermore, the value of α may be calculated, if κ is known, via the fraction

$$\frac{\langle \hat{x} \rangle^2}{\langle \hat{x}^2 \rangle} = \frac{\Gamma\left(1+\frac{\alpha\kappa}{2-\kappa}\right)}{\Gamma\left(\frac{3+(\alpha-1)\kappa}{\kappa-2}\right)\Gamma\left(\frac{1+(\alpha-1)\kappa}{\kappa-2}\right)}. \tag{3.67}$$

The value of κ can easily be determined with help of the mean of the process. Thus, by scaling the mean with a test value κ_{T}, the scaled mean $\frac{M^m_{x_0}(t)}{t^{\frac{m}{2-\kappa_{\mathrm{T}}}}}$ is still growing for large t if $\kappa_{\mathrm{T}} < \kappa$ and decreasing if $\kappa_{\mathrm{T}} > \kappa$. Only if $\kappa_{\mathrm{T}} = \kappa$, the scaled mean approaches a constant.

In Fig. 3.9 the approach of the density of a the scaled process $\hat{x} = \frac{x(t)}{t^{\frac{1}{2-\kappa}}}$ to the asymptotic invariant density is shown. The larger the process time, the better is the agreement between the measured density (dashed lines) and the asymptotic invariant density (black line).

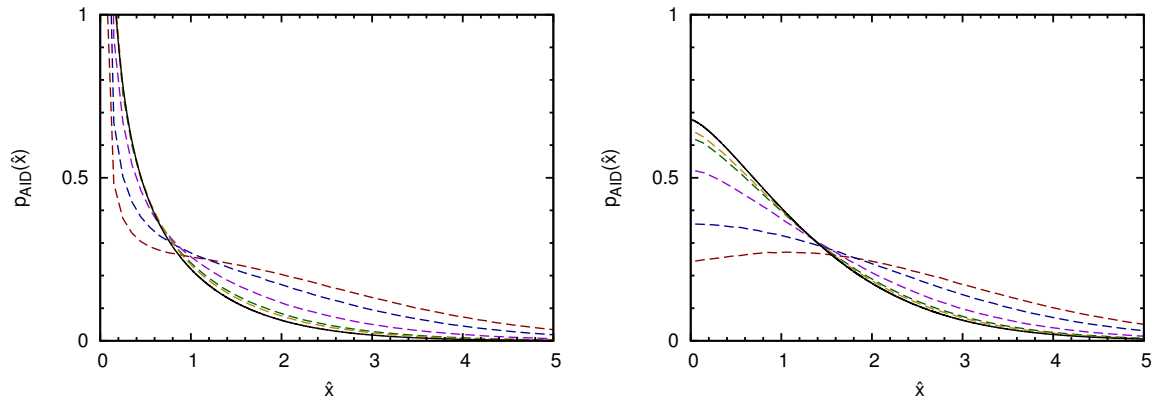

Figure 3.9.: The approach to the asymptotic invariant density for the Itô process ($\alpha = 0$, left) and of the Klimontovich-Hänggi process ($\alpha = 1$, right) for different times, $t = 0.5$, $t = 0.8$, $t = 2$, $t = 6$ and $t = 10$, with $D_0 = 1$ and $\kappa = 0.6$. The scaled densities from numerical evaluated Langevin equations (dashed lines) approach the asymptotic invariant density (black line) from Eq. (3.63) with increasing time t.

3.3.3. Other related processes

By applying another transformation $\tilde{x} = \sqrt{y}$ on the squared Bessel process Eq. (3.55) the Bessel process with the Langevin equation

$$\frac{\mathrm{d}\tilde{x}}{\mathrm{d}t} = \frac{\delta - 1}{2}\frac{1}{\tilde{x}} + \xi(t) \tag{3.68}$$

is obtained and, thus, diffusion in a logarithmic potential. This process is also obtained via the direct transformation $\tilde{x} = \Phi(x) = \sqrt{\frac{2}{D_0}}\frac{x^{1-\frac{\kappa}{2}}}{2-\kappa}$ of the original process Eq. (3.53). And the potential $V(\tilde{x}) = (\frac{1}{2} - \alpha)\log\left(\frac{\partial\Phi^{-1}(\tilde{x})}{\partial\tilde{x}}\right)$, obtained from the derivative of inverse function of $\Phi(x)$, is up to an unimportant constant the same as $V(\tilde{x}) = -\int \mathrm{d}\tilde{x}\frac{\delta-1}{2}\frac{1}{\tilde{x}}$ with $\delta = \frac{2(1+(\alpha-1)\kappa)}{2-\kappa}$ as above. With a reflection boundary at $\tilde{x} = 0$ and $\delta > 0$ the propagator of the Bessel process follows a noncentral χ-distribution and reads

$$p^{(\mathrm{BES})}(\tilde{x}, t|\tilde{x}_0) = \frac{1}{t}\left(\frac{\tilde{x}}{\tilde{x}_0}\right)^{\frac{\delta}{2}-1}\exp\left(-\frac{\tilde{x}^2 + \tilde{x}_0^2}{2t}\right) I_{\frac{\delta}{2}-1}\left(\frac{\tilde{x}\tilde{x}_0}{t}\right). \tag{3.69}$$

The diffusion process in a logarithmic potential is of high relevance in various physical fields and describes, for example, the momentum diffusion in dissipative optical lattices [117–120], the dynamics of particles in the proximity of a long, charged polymer [121] or of particles in a driven fluid field [122], long-range interacting systems [123–125] as well as the dynamics of local denaturation zones in DNA molecules [126, 127]. These systems usually have no reflecting boundaries at $\tilde{x} = 0$, thus, the propagator is not so easily calculated. Nevertheless, Kessler and Barkai [128] showed that the probability density in such systems approaches an infinite covariant density, if the process is scaled with the square root of t. Furthermore, it was shown that these systems obey a superaging correlation function and show ergodicity breaking [129–131].

Another related process is found via the transformation $z = \exp(bt)y\left\{\frac{c^2}{4b}[1 - \exp(-bt)]\right\}$ of

a squared Bessel process with $\delta = \frac{4a}{c^2}$. This leads to the Langevin equation [132]

$$\frac{\mathrm{d}z}{\mathrm{d}t} = a + bz + c\sqrt{|z|}\xi(t) \quad (\text{Itô}) \tag{3.70}$$

which is known as Feller process [133] and is originally used to describe population growth [134]. In finance this process is known as Cox-Ingersoll-Ross (CIR)-model [135] and is used to describe the short-time evolution of interest rates.

3.4. Brownian motion with periodically varying diffusion coefficient

As last example, a system with a diffusion coefficient $D(x) = \frac{D_1+D_2}{2} + \frac{D_1-D_2}{2}\cos(2\omega x)$ is considered and, thus, a system where the diffusion coefficient varies periodically between D_1 and D_2 with wave number $k = \frac{\pi}{\omega}$. Without loss of generality, $D_1 > D_2 > 0$ can be chosen. The general Langevin equation reads

$$\frac{\mathrm{d}x}{\mathrm{d}t} = \sqrt{D_1 + D_2 + (D_1 - D_2)\cos(2\omega x)}\xi(t). \quad (\alpha\text{-Interpretation}) \tag{3.71}$$

After a transformation $\tilde{x} = \Phi(x) = \frac{F(\omega x, 1-\frac{D_2}{D_1})}{\sqrt{2D_1}\omega}$, where $F(\phi, m) = \int_0^\phi \mathrm{d}\theta \left[1 - m\sin^2(\theta)\right]^{-\frac{1}{2}}$ denotes the elliptic integral of first kind, the Langevin equation for the transformed process reads

$$\frac{\mathrm{d}\tilde{x}}{\mathrm{d}t} = \frac{\left(\frac{1}{2} - \alpha\right)(D_1 - D_2)\sqrt{2}\omega\,\mathrm{cn}\left(\sqrt{2D_1}\omega\tilde{x}, 1 - \frac{D_2}{D_1}\right)\mathrm{sn}\left(\sqrt{2D_1}\omega\tilde{x}, 1 - \frac{D_2}{D_1}\right)}{\sqrt{D_1}\,\mathrm{dn}\left(\sqrt{2D_1}\omega\tilde{x}, 1 - \frac{D_2}{D_1}\right)} + \xi(t), \tag{3.72}$$

with the Jacobi elliptic functions $\mathrm{cn}(\phi, m) = \cos(\mathrm{am}(u, m))$, $\mathrm{sn}(\phi, m) = \sin(\mathrm{am}(u, m))$, $\mathrm{dn}(\phi, m) = \sqrt{1 - m\sin^2(\mathrm{am}(u, m))}$ and the Jacobi amplitude $\mathrm{am}(u, m)$ which is the inverse function to $u = F(\phi, m)$ [136]. The related potential reads $V(\tilde{x}) = \left(\frac{1}{2} - \alpha\right)\log\left[\sqrt{2D_1}\mathrm{dn}\left(\sqrt{2D_1}\omega\tilde{x}, 1 - \frac{D_2}{D_1}\right)\right]$. The Jacobi elliptic function $\mathrm{dn}\,(u, m)$ is in real space periodic with period $K(m) = F(\frac{\pi}{2}, m)$ which is the complete elliptic integral of first kind. Thus, also the potential $V(\tilde{x})$ and the stochastic force $f(\tilde{x}) = -\frac{\mathrm{d}V(\tilde{x})}{\mathrm{d}\tilde{x}}$ share the same periodicity.

3.4.1. Propagator and Moments

The propagator of the transformed process for a general α can not be found analytically. Nevertheless, it is known [137, 138] that the variance of processes with a periodic potential asymptotically grows linearly in time, thus

$$\tilde{D}_{\mathrm{eff}} = \lim_{t\to\infty} \frac{\left\langle \tilde{x}^2(t)\right\rangle - \left\langle \tilde{x}(t)\right\rangle^2}{2t} \tag{3.73}$$

gives an effective diffusion constant. This effective diffusion constant can be computed via [139]

$$\tilde{D}_{\mathrm{eff}} = \frac{L^2}{2\int_0^L \mathrm{d}x \exp(2V(x)) \int_0^L \mathrm{d}y \exp(-2V(y))} \tag{3.74}$$

for a general periodic potential with period L, i.e. $V(x + L) = V(x)$. Thereby $D_{\mathrm{eff}} \leq \frac{1}{2}$ and, thus, always smaller or equal than the diffusion coefficient of the Langevin equation Eq. (3.72) without the drift term.

For the potential $V(\tilde{x}) = \left(\frac{1}{2} - \alpha\right) \log\left[\sqrt{2D_1}\mathrm{dn}\left(\sqrt{2D_1}\omega\tilde{x}, 1 - \frac{D_2}{D_1}\right)\right]$ the integrals $\int_0^L \mathrm{d}\tilde{x} \exp(\pm 2V(\tilde{x}))$ with $L = \frac{2K(1-\frac{D_2}{D_1})}{\sqrt{2D_1}\omega}$ can be solved utilizing the variable transformation $\phi = \mathrm{am}(\tilde{x}, 1 - \frac{D_2}{D_1})$ and, thus,

$$\int_0^L \mathrm{d}\tilde{x} \exp(\pm 2V(\tilde{x})) = \frac{1}{\omega} \int_0^\pi \mathrm{d}\phi \left\{ 2D_1 \left[1 - \left(1 - \frac{D_2}{D_1} \right) \sin^2(\phi) \right] \right\}^{-\frac{1}{2} \pm (\frac{1}{2} - \alpha)}. \tag{3.75}$$

In the Itô and Klimontovich-Hänggi interpretation, i.e. $\alpha = 0$ or $\alpha = 1$, the effective diffusion coefficient simplifies to

$$\tilde{D}_{\mathrm{eff}} = \frac{2}{\pi^2} \sqrt{\frac{D_2}{D_1}} K \left(1 - \frac{D_2}{D_1} \right)^2. \tag{3.76}$$

For $D_1 \approx D_2$ the effective diffusion coefficient is approximated with

$$\tilde{D}_{\mathrm{eff}} \overset{D_1 \approx D_2}{\approx} \frac{1}{2} - \frac{(D_1 - D_2)^2}{64 D_2^2} + \mathcal{O}\left((D_1 - D_2)^3\right) \tag{3.77}$$

and for $D_2 \to 0$, or $D_1 \to \infty$ respectively, the effective diffusion coefficient is approximated with

$$\tilde{D}_{\mathrm{eff}} \overset{D_1 \gg D_2}{\approx} \sqrt{\frac{D_2}{D_1}} \frac{\log\left(\frac{16 D_1}{D_2}\right)^2}{2\pi^2} + \mathcal{O}\left(D_2^{-\frac{3}{2}} \right). \tag{3.78}$$

However, the knowledge of the effective diffusion coefficient in the transformed process $\tilde{x}(t)$ does not help to calculate the propagator of the original process from Eq. (3.71). Only in the Stratonovich interpretation a propagator is found (see also Sec. 2.4.3 in Chap. 2), which yields

$$p_{\mathrm{Strat}}(x, t|x_0) = \frac{\exp\left[-\frac{\left(F(\omega x, 1 - \frac{D_2}{D_1}) - F(\omega x_0, 1 - \frac{D_2}{D_1}) \right)^2}{4 D_1 \omega^2 t} \right]}{\sqrt{4\pi D_1 t \left[1 - \left(1 - \frac{D_2}{D_1} \right) \sin^2(\omega x) \right]}}. \tag{3.79}$$

In this case, also the conditional moments may be calculated using

$$M_{x_0}^m(t) = \int_{-\infty}^{\infty} \mathrm{d}x\, x^m p_{\mathrm{Strat}}(x, t|x_0) \tag{3.80}$$

$$= \int_{-\infty}^{\infty} \mathrm{d}\tilde{x} \left(\frac{\mathrm{am}(\sqrt{2D_1}\omega\tilde{x}, 1 - \frac{D_2}{D_1})}{\omega} \right)^m \frac{1}{\sqrt{2\pi t}} \exp\left[-\frac{\left(\tilde{x} - \frac{F(\omega x_0, 1 - \frac{D_2}{D_1})}{\sqrt{2D_1}\omega} \right)^2}{2t} \right] \tag{3.81}$$

utilizing the inverse transform $x = \Phi^{-1}(\tilde{x}) = \frac{\mathrm{am}(\sqrt{2D_1}\omega\tilde{x}, 1 - \frac{D_2}{D_1})}{\omega}$. For this conditional moments no explicit expression may be found, but the asymptotic behavior of the moments can be found. Therefore the same approach as for the asymptotic invariant density (see Chap. 2, Sec. 2.6.3) is

used, with a diffusive scaling function $f(t) = \sqrt{t}$, i.e.

$$\lim_{t\to\infty} \frac{M_{x_0}^m(t)}{t^{\frac{m}{2}}} = \lim_{t\to\infty} \int_{-\infty}^{\infty} \mathrm{d}\tilde{x} \left(\frac{\mathrm{am}(\sqrt{2D_1}\omega\tilde{x}, 1-\frac{D_2}{D_1})}{\sqrt{t}\omega} \right)^m \frac{1}{\sqrt{2\pi t}} \exp\left[-\frac{\left(\tilde{x} - \frac{F(\omega x_0, 1-\frac{D_2}{D_1})}{\sqrt{2D_1}\omega} \right)^2}{2t} \right]$$

$$= \lim_{t\to\infty} \int_{-\infty}^{\infty} \mathrm{d}\hat{x} \left(\frac{\mathrm{am}(\sqrt{2D_1}\omega\hat{x}\sqrt{t}, 1-\frac{D_2}{D_1})}{\sqrt{t}\omega} \right)^m \frac{\sqrt{t}}{\sqrt{2\pi t}} \exp\left[-\frac{\left(\hat{x}\sqrt{t} - \frac{F(\omega x_0, 1-\frac{D_2}{D_1})}{\sqrt{2D_1}\omega} \right)^2}{2t} \right] \tag{3.82}$$

with the transformed variable $\hat{x} = \frac{\tilde{x}}{\sqrt{t}}$ to obtain the asymptotic moment. Utilizing the Lambert series expansion of the Jacobi amplitude function

$$\mathrm{am}(\phi, m) = \frac{\pi\phi}{2K(m)} + 2\sum_{k=1}^{\infty} \frac{q(m)^k}{k(q(m)^{2k}+1)} \sin\left(\frac{k\pi\phi}{K(m)} \right) \tag{3.83}$$

with $q(m)$ the elliptic nome and taking the limit $t \to \infty$, the asymptotic moments are calculated

$$\lim_{t\to\infty} \frac{M_{x_0}^m(t)}{t^{\frac{m}{2}}} = \lim_{t\to\infty} \langle \hat{x}^m \rangle = \left(\frac{\pi\sqrt{2D_1}}{2K(1-\frac{D_2}{D_1})} \right)^m \int_{-\infty}^{\infty} \mathrm{d}\hat{x} \frac{\hat{x}^m}{\sqrt{2\pi}} \exp\left(-\frac{\hat{x}^2}{2} \right) \tag{3.84}$$

$$= \begin{cases} 0 & : \quad m \quad \text{odd} \\ \left(\frac{\pi\sqrt{D_1}}{2K(1-\frac{D_2}{D_1})} \right)^m \frac{m!}{(\frac{m}{2})!} & : \quad m \quad \text{even} \end{cases} . \tag{3.85}$$

In Fig. 3.10 (left) the propagator of the Stratonovich process is shown. The analytical propagator and the density obtained from the numerical simulation of the Langevin equation with 10^5 walkers agree well for the different times. Furthermore, in Fig. 3.10 (right) the first three moments of the time-scaled process $\hat{x}(t) = \frac{x(t)}{\sqrt{t}}$ are shown. The odd moments decay to zero and the second and, thus, even moment decays to a constant as predicted by Eq. (3.84). It should be noted that the odd moments decay $\propto t^{-\frac{1}{2}}$ to zero.

From the asymptotic moments Eq. (3.84) it may be assumed that the asymptotic invariant density is a Gaussian distribution with zero mean and variance $\frac{D_1\pi^2}{2K^2(1-\frac{D_2}{D_1})}$, but this is not the case for any finite time, as it can be seen in figure Fig. 3.11. With increasing t the periodic modulations of the scaled propagator get denser but they do not vanish for any finite time. Nevertheless, it may be assumed that this Gaussian distribution is an effective asymptotic invariant density also for large finite times, as it determines the asymptotic behavior of the moments of the propagator.

Since the asymptotic time-scaled moments may be computed with the propagator of the transformed process (see Eq. (3.82)), this ansatz can also be used for the general process, i.e. for an α-dependent interpretation of Eq. (3.71). But since the propagator of the transformed process Eq. (3.72) is unknown, an effective propagator

$$\tilde{p}_{\mathrm{eff}}(\tilde{x}, t|\tilde{x}_0) = \frac{\exp\left[-\frac{(\tilde{x}-\tilde{x}_0)^2}{4\tilde{D}_{\mathrm{eff}}t} \right]}{\sqrt{4\pi\tilde{D}_{\mathrm{eff}}t}} \tag{3.86}$$

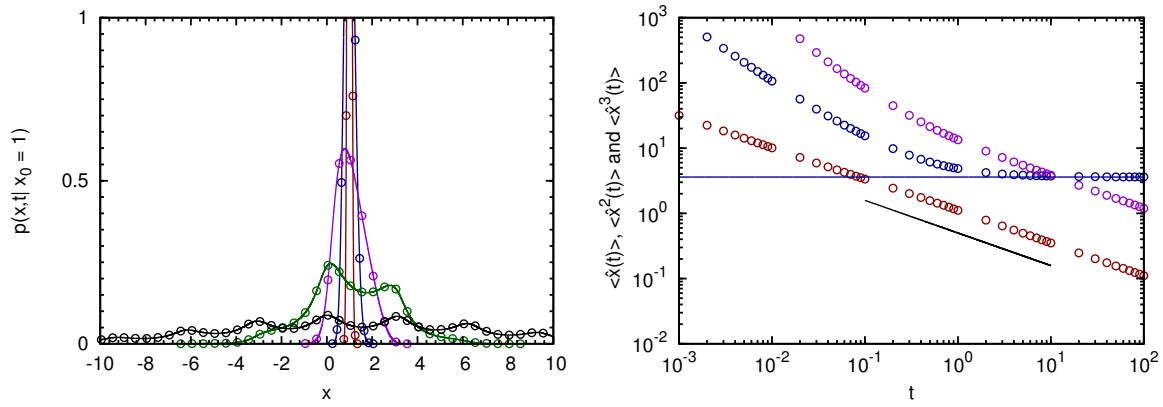

Figure 3.10.: The propagator (left) and its first three scaled moments (right) of the Stratonovich interpretation of Eq. (3.71). The propagator is shown for different times, $t = 0.001$, $t = 0.01$, $t = 0.1$, $t = 1$ and $t = 10$, with $D_1 = 3$, $D_2 = 1$, $\omega = 1$ and $x_0 = 1$. The numerical results (circles) and the respective analytical curve (lines) from Eq. (3.79) agree well. The moments $\langle \hat{x}^1 \rangle$, $\langle \hat{x}^2 \rangle$ and $\langle \hat{x}^3 \rangle$ of the time-scaled process $\hat{x}(t) = \frac{x(t)}{\sqrt{t}}$ are shown as circles. The second moment approaches the constant predicted by Eq. (3.84) and shown as blue line, whereas the odd moments decay to zero. The decay of the odd moments is $\propto t^{-\frac{1}{2}}$ (black line as guide to the eye).

may be used, with the effective diffusion coefficient given by Eq. (3.74) for the calculation of the asymptotic moments for a general α. After plugging the effective propagator in Eq. (3.82) the asymptotic moments are calculated

$$\lim_{t\to\infty} \frac{M_{x_0}^m(t)}{t^{\frac{m}{2}}} = \langle \hat{x}^m \rangle = \begin{cases} 0 & : \quad m \quad \text{odd} \\ \left(\frac{\pi \sqrt{D_1} \sqrt{2\tilde{D}_{\text{eff}}}}{2K(1-\frac{D_2}{D_1})} \right)^m \frac{m!}{(\frac{m}{2})!} & : \quad m \quad \text{even} \end{cases} . \tag{3.87}$$

In the Itô and Klimontovich-Hänggi case, where the effective diffusion coefficient is known explicitly (see Eq. (3.76)), the asymptotic moments simplify to

$$\lim_{t\to\infty} \frac{M_{x_0}^m(t)}{t^{\frac{m}{2}}} = \langle \hat{x}^m \rangle = \begin{cases} 0 & : \quad m \quad \text{odd} \\ (D_1 D_2)^{\frac{m}{4}} \frac{m!}{(\frac{m}{2})!} & : \quad m \quad \text{even} \end{cases} . \tag{3.88}$$

In Fig. 3.12 the approach of the time-scaled second moments $\langle \hat{x}^2(t) \rangle$ of Itô, Stratonovich and Klimontovich-Hänggi interpretation of Eq. (3.71) to their asymptotic values predicted from Eqs. (3.84) and (3.88) is shown. The numerical values (circles) and the predicted values (lines) agree well for large times. The remaining deviation is due to the finite time of the simulation. It should be noted that the time-scaled variances of theses processes $\langle (\hat{x} - \langle \hat{x} \rangle)^2 \rangle$ approach the same value as the time-scaled second moments since the time-scaled mean values approach zero for large times. Furthermore, since the asymptotic behavior of the time-scaled moments of all possible interpretations of Eq. (3.71) is nearly the same, the different interpretations cannot be distinguished with help of these moments.

Finally, since the diffusion coefficient of the original process Eq. (3.71) is periodic, the stationary solution of the corresponding Fokker-Planck equation with periodic boundary conditions at $x = -\frac{\pi}{2\omega}$ and $x = \frac{\pi}{2\omega}$ can be calculated. The equilibrium or steady state distribution with

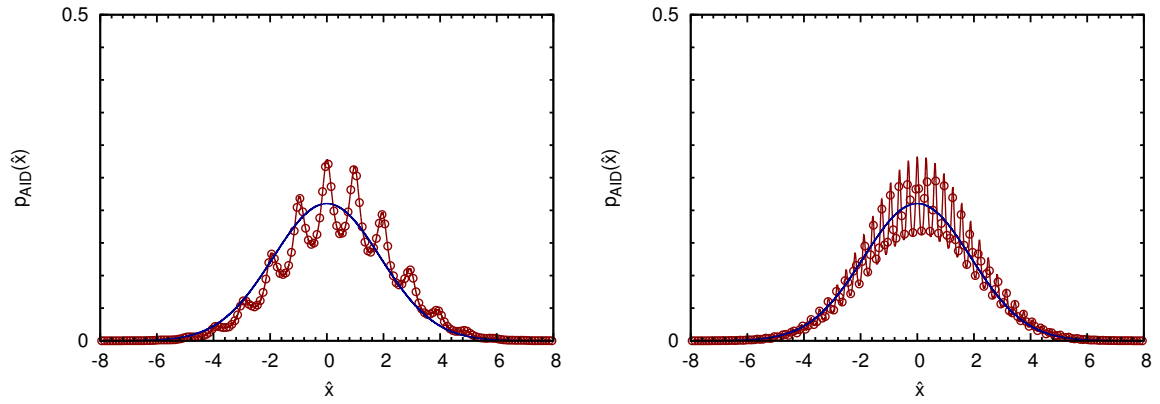

Figure 3.11.: The scaled propagator of the Stratonovich process ($\alpha = \frac{1}{2}$) for $t = 10$ left and $t = 100$ right. The scaled analytical propagator (red line) and the density from scaled trajectories (red circles) agree well and approach the effective asymptotic invariant density (blue line) for $t = 100$.

periodic boundary conditions is computed as

$$\begin{aligned} p_{\mathrm{eq}}(x) &= g(x)^{2\alpha-2}\left(\int_{-\frac{\pi}{2\omega}}^{\frac{\pi}{2\omega}} 0\,\mathrm{d}x\, g(x)^{2\alpha-2}\right)^{-1} \\ &= \omega\frac{[D_1+D_2+(D_1-D_2)\cos(2\omega x)]^{\alpha-\frac{1}{2}}}{(2D_2)^{\alpha-1}{}_2F_1(\frac{1}{2};1-\alpha;1;1-\frac{D_1}{D_2})} \end{aligned} \tag{3.89}$$

with ${}_2F_1(a;b;c;z) = \sum_{k=0}^{\infty}\frac{\Gamma(a+k)\Gamma(b+k)\Gamma(c)}{\Gamma(c+k)\Gamma(a)\Gamma(b)}\frac{z^k}{k!}$ a hypergeometric function. The steady state distribution simplifies in the three main interpretations of Eq. (3.71), thus in the Itô interpretation ($\alpha = 0$) it yields

$$p_{\mathrm{eq}}^{\mathrm{Itô}}(x) = \frac{2\sqrt{D_1D_2}\omega}{\pi\left[D_1+D_2+(D_1-D_2)\cos(2\omega x)\right]}. \tag{3.90}$$

In the Stratonovich interpretation ($\alpha = \frac{1}{2}$) it yields

$$p_{\mathrm{eq}}^{\mathrm{Strat}}(x) = \frac{\sqrt{D_2}\omega}{\sqrt{2\left[D_1+D_2+(D_1-D_2)\cos(2\omega x)\right]}K(1-\frac{D_1}{D_2})} \tag{3.91}$$

and for the Klimontovich-Hänggi interpretation ($\alpha = 1$) it reads

$$p_{\mathrm{eq}}^{\mathrm{KH}}(x) = \frac{\omega}{\pi}. \tag{3.92}$$

The difference in these steady state distributions is obvious, especially the Klimontovich-Hänggi can now be identified easily with help of the probability density of the process, as it approaches a uniform distribution. Interestingly, when averaging the Langevin equation for the second moment of the Itô case (see Eq. (2.44)) with the steady state distribution of the Itô case

$$\frac{\mathrm{d}\left\langle x^2\right\rangle}{\mathrm{d}t} = \left\langle g^2(x)\right\rangle_{p_{\mathrm{eq}}^{\mathrm{Itô}}(x)} = \left\langle 2D(x)\right\rangle_{p_{\mathrm{eq}}^{\mathrm{Itô}}(x)} = 2\sqrt{D_1D_2}, \tag{3.93}$$

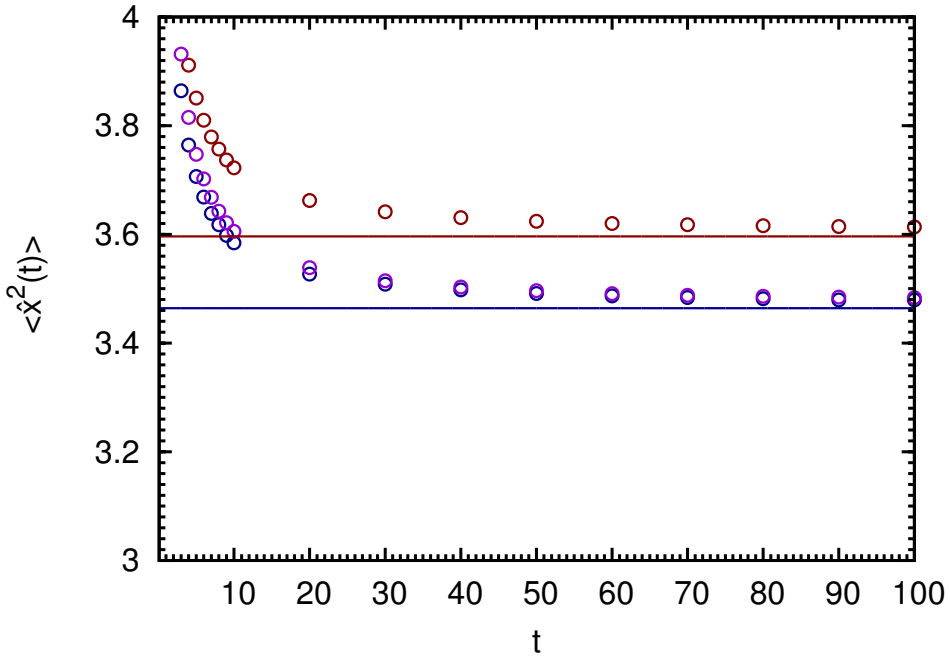

Figure 3.12.: The second moments of the scaled processes interpreted in Itô sense (red), Stratonovich sense (blue) and, respectively, in Klimontovich-Hänggi sense (purple) and the respective asymptotic values shown as lines. The time-scaled second moment of the Stratonovich process approaches the value predicted by Eq. (3.84) and the time-scaled second moments of the Itô and Klimontovich-Hänggi processes approach the same value as predicted by Eq. (3.88). The remaining deviation is due to the finite time of the process.

the same quantity as with the effective asymptotic density approach Eq. (3.88) is obtained. However, this is not the case in the Stratonovich and Klimontovich-Hänggi case, where the equation also includes an average over the noise-induced drift term. Whether this holds in general for drift free Itô processes cannot be concluded by the author.

4. Results II: Anisotropic systems with state-dependent diffusion tensor

Since many real world systems are not one-dimensional and may also not be isotropic, in this chapter systems with state-dependent diffusion tensor are considered. For a few examples, which are inspired by real heterogeneous liquid crystal systems, the temporal behavior of measurable quantities like mean squared displacement and distribution of diffusivities obtained from simulations is shown and compared with analytical predictions. At first, Sec. 4.1 considers a system with twist distortion of director field. Here the stochastic interpretation of the Langevin equation plays no role. Secondly, Sec. 4.2 considers an inhomogeneous director field after a Fréedericksz transition [140]. Here, the system is analyzed in both Itô and Stratonovich interpretation. They show a qualitatively completely different behavior for large times, which is here explored for the first time. Then, in Sec. 4.3 a system with undulation in the director field is examined. Here only prediction for the Itô interpretation may be given. And finally, in Sec. 4.4 some general assertions for diffusion with state-dependent diffusion tensor are given.

4.1. Twist system or translational diffusion of a two-dimensional ellipsoid

As first example for an anisotropic system with state-dependent diffusion tensor the twist system is considered. A paradigmatic experimental system would be the tracer diffusion in a chiral nematic or cholesteric liquid crystal [141] where the director or the orientation of the liquid crystal molecules undergoes a helical distortion along a single axis. A schematic illustration can be found in the left image of Fig. 4.1. The related diffusion tensor in such a system is given by

$$\mathbf{D}(z) = \begin{pmatrix} D_1\cos^2(\omega z) + D_2\sin^2(\omega z) & (D_2 - D_1)\cos(\omega z)\sin(\omega z) & 0 \\ (D_2 - D_1)\cos(\omega z)\sin(\omega z) & D_1\sin^2(\omega z) + D_2\cos^2(\omega z) & 0 \\ 0 & 0 & D_3 \end{pmatrix} \tag{4.1}$$

with D_1, D_2 and D_3 the diffusion coefficients related to the principal axes of the local diffusion tensor. In uniaxial systems D_3 is equal to either D_1 or D_2. The tensor may be written as $\mathbf{D}(z) = \mathbf{O}^\mathsf{T}(z)\hat{\mathbf{D}}\mathbf{O}(z)$, with $\hat{\mathbf{D}} = \mathrm{diag}(D_1, D_2, D_3)$ a constant diagonal tensor and $\mathbf{O}(z)$ an orthogonal tensor describing a rotation around the z-axis about by angle ωz.

If, like in the most experimental setups, only the two-dimensional diffusion in the x-y-plane is observed, the motion can be interpreted as the translational diffusion of a two-dimensional ellipsoid [142, 143] or rod-like particle [144]. Here the diffusion in z-direction is replaced by the rotational diffusion of the ellipsoid with the continuous orientation angle $\theta = \frac{1}{2}\omega z$ and the rotational diffusion coefficient $D_\theta = \frac{\omega^2}{4}D_3$. The Fokker-Planck equation of the system may be expressed as

$$\frac{\partial p(\mathbf{x},\theta,t)}{\partial t} = \frac{\partial}{\partial \mathbf{x}} \cdot \left(\mathbf{D}_{xy}(\theta) \cdot \frac{\partial}{\partial \mathbf{x}} p(\mathbf{x},\theta,t) \right) + \frac{\partial^2}{\partial \theta^2} D_\theta p(\mathbf{x},\theta,t) \tag{4.2}$$

with $\mathbf{D}_{xy}(\theta)$ the upper left 2×2 submatrix of the tensor $\mathbf{D}(\theta)$. Since the tensor $\mathbf{D}_{xy}(\theta)$ is independent of $\mathbf{x}$ and D_θ, it can be placed outside of the derivatives, thus, the related Langevin

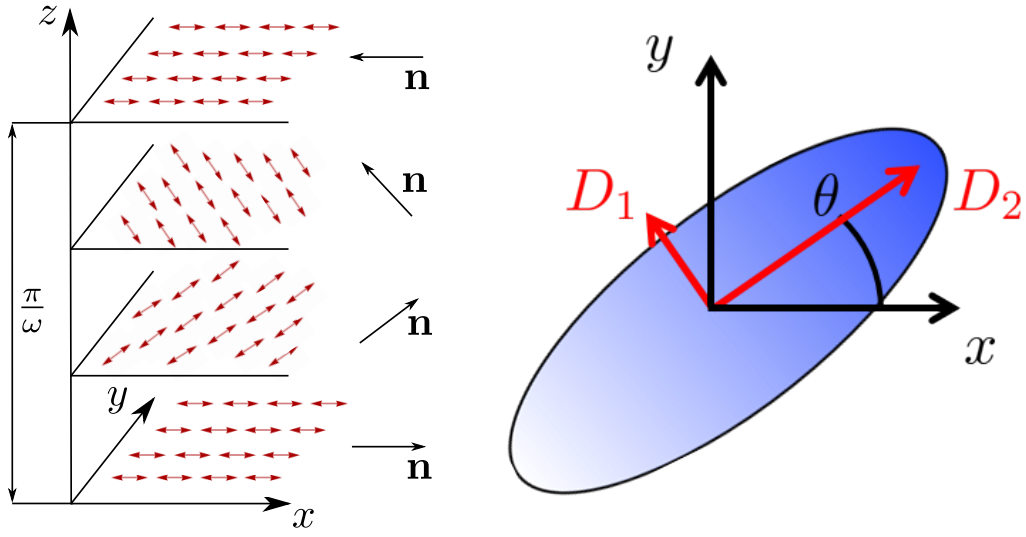

Figure 4.1.: Illustration of a twist system (left) and of the connection between orientation of a ellipsoid and the principal axes of its diffusion tensor (right). The left figure shows schematically the orientation change of the molecules in a twist system with a spatial periodicity ω. In the right figure a single ellipsoid is shown and the connection between its current orientation, given as angle θ, and the principal axes of its diffusion tensor are presented.

equations show no ambiguity with respect to the stochastic interpretation. Furthermore, since the orientational motion is independent of the translational motion, express the probability density $p(\mathbf{x}, \theta, t)$ of the process can be expressed as product of the marginal densities of the orientation $p_\theta(\theta, t)$ and of the position $p_\mathbf{x}(\mathbf{x}, t)$, i.e. $p(\mathbf{x}, \theta, t) = p_\mathbf{x}(\mathbf{x}, t)p_\theta(\theta, t)$. Hence, it can be integrated over x and y in order to obtain the Fokker-Planck equation for the orientation probability density

$$\frac{\partial p_\theta(\theta, t)}{\partial t} = \frac{\partial^2}{\partial \theta^2} D_\theta p(\mathbf{x}, \theta, t), \tag{4.3}$$

which is a simple homogeneous one-dimensional diffusion equation. Thus, the propagator for the angle θ can be written, with help of an angular displacement $\Delta\theta = \theta - \theta'$ during some time $\tau = t - t'$, in terms of a Gaussian displacement distribution (see also Eq. (2.17))

$$p_{\Delta\theta}(\Delta\theta, \tau) = \frac{\exp\left(-\frac{\Delta\theta^2}{4D_\theta \tau}\right)}{\sqrt{4\pi D_\theta \tau}}, \tag{4.4}$$

which is now independent of the initial orientation and initial time. For the position density $p_\mathbf{x}(\mathbf{x}, t)$, the integration over the angular coordinate can be performed, already plugging in the angular displacement propagator Eq. (4.4) and also performing a coordinate transformation to positional displacement $\mathbf{r} = \mathbf{x} - \mathbf{x}'$ and temporal displacement $\tau = t - t'$. Thus, the Fokker-Planck equation for the positional displacement reads

$$\frac{\partial p_\mathbf{r}(\mathbf{r}, \tau)}{\partial \tau} = \frac{\partial}{\partial \mathbf{r}} \cdot \underbrace{\left(\int_{-\infty}^{\infty} \mathrm{d}\theta\, \mathbf{D}(\Delta\theta) p_{\Delta\theta}(\Delta\theta, \tau) \right)}_{\tilde{\mathbf{D}}(\tau)} \cdot \frac{\partial}{\partial \mathbf{r}} p_\mathbf{r}(\mathbf{r}, \tau). \tag{4.5}$$

Since the averaged diffusion tensor depends now on temporal displacement τ, the displacement distribution is obtained in the same way as the propagator of a system with time-dependent diffusion coefficient [19] and reads

$$p_{\mathbf{r}}(\mathbf{r},\tau) = \frac{(2\pi)^{-\frac{d}{2}}}{\sqrt{\det \boldsymbol{\Sigma}(\tau)}} \exp\left(-\frac{1}{2}\mathbf{r}^{\mathsf{T}}\boldsymbol{\Sigma}^{-1}(\tau)\mathbf{r}\right), \tag{4.6}$$

with an effective covariance tensor $\boldsymbol{\Sigma}(\tau) = 2\int_0^\tau \mathrm{d}s\tilde{\mathbf{D}}(s) = 2\int_0^\tau \mathrm{d}s \int_{-\infty}^{\infty} \mathrm{d}\Delta\theta \mathbf{D}(\Delta\theta) p_{\Delta\theta}(\Delta\theta, s)$. Thus, the effective diffusion tensor reads

$$\begin{aligned}\mathbf{D}_{\mathrm{eff}}(\tau) &\equiv \frac{\boldsymbol{\Sigma}(\tau)}{2\tau} \\ &= \begin{pmatrix} \frac{D_2 - D_1 + (D_1 - D_2)\exp(-4D_\theta\tau) + 4D_\theta(D_1+D_2)}{8D_\theta\tau} & 0 \\ 0 & \frac{D_1 - D_2 + (D_2 - D_1)\exp(-4D_\theta\tau) + 4D_\theta(D_1+D_2)}{8D_\theta\tau} \end{pmatrix}.\end{aligned} \tag{4.7}$$

Since this tensor is already diagonal, the effective τ-dependent diffusion coefficients corresponding to the principal axes of the system are given by the diagonal elements. It should be noted that the correlations between the x and y component is zero due to the averaging over all possible angular displacements, thus the solutions above give only an averaged propagator. For the full propagator and, thus, the solution of Eq. (4.2) with initial conditions $\mathbf{r}_0$ and θ_0 this is not the case and the computation of the full propagator is more complicated. A solution for the full problem was given by Munk *et al.* [144], which computed the intermediate scattering function, i.e. the Fourier transform of the propagator.

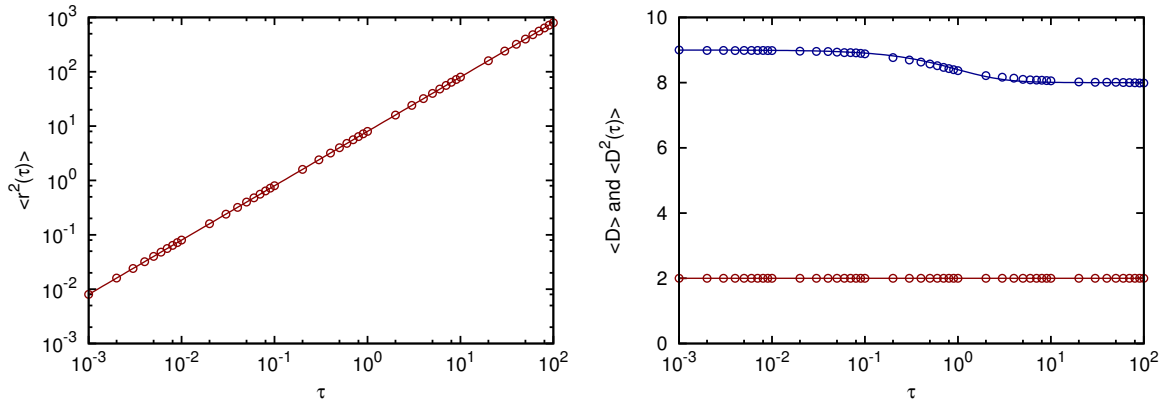

Figure 4.2.: The mean squared displacement (left) and the first two moments of the distribution of diffusivities (right) for a twist system with $D_1 = 3$, $D_2 = 1$, $D_3 = 1$ and $\omega = 1$, i.e. $D_\theta = \frac{\omega^2}{4}D_3 = \frac{1}{4}$. The MSD obtained from random walk simulation of the Langevin equation (circles) and the analytical value (lines) agree well. The MSD grows linearly in time like for an isotropic system with the same mean diffusion coefficient. The first two moments of the distribution of diffusivities are shown in the right figure. Here the first moment (red) is constant as predicted and has the value $\langle D\rangle = \frac{D_1+D_2}{2} = 2$. The second moment shows a crossover from small τ to large τ and the time-dependence agrees well with the analytical prediction from Eq. (4.10) (blue line).

From the effective covariance tensor or the effective diffusion tensor the mean squared displacement of the process can be computed, which is given by

$$\left\langle \mathbf{r}^2(\tau) \right\rangle = 2\,\mathrm{tr}(\mathbf{D}_{\mathrm{eff}}(\tau))\tau = \mathrm{tr}(\mathbf{\Sigma}(\tau)) = 2(D_1 + D_2)\tau. \tag{4.8}$$

Thus, the MSD is not sufficient to determine the values of the effective diffusion coefficients [98–100]. Heidernätsch *et al.* [36] already showed that the distribution of diffusivities is the superior method in anisotropic systems to determine the eigenvalues of the diffusion tensor (see also Chap. 2, Sec. 2.6.2). This method can be easily applied to the twist system with the τ-dependent effective diffusion coefficients. In Eqs. (2.106) and (2.107) already the relation between the eigenvalues and the first two moments of the distribution of diffusivities of a two-dimensional system are given. The first moment in the twist system now reads

$$\langle D \rangle = M^1 = \frac{1}{2}(D_1 + D_2), \tag{4.9}$$

which is constant and gives also the mean diffusion coefficient and the second moment reads

$$\left\langle D^2 \right\rangle(\tau) = M^2(\tau) \tag{4.10}$$

$$= \frac{(D_1 - D_2)^2 - 2(D_1 - D_2)^2 \exp(-4D_\theta\tau) + \left[D_1 - D_2)^2 + 32D_1 + D_2)^2 D_\theta^2 \tau^2\right]}{64 D_\theta^2 \tau^2}, \tag{4.11}$$

which is now τ-dependent, in contrast to homogeneous diffusion systems. If these two moments are measured, the effective τ-dependent diffusion coefficients belonging to the principal axes of the system are determined via Eq. (2.108). In left part of Fig. 4.2 the behavior of the MSD can be observed, which grows linearly in time and matches perfectly with the analytical prediction from Eq. (4.8). And in the right part it can be seen that the first moment of the diffusivities remains constant, as predicted from Eq. (4.9), and the second moment obtained from a set of 10^5 trajectories of the process (blue circles) shows a good agreement with the analytical prediction from Eq. (4.10) (blue line).

Furthermore, since the explicit expressions for these moments are known, the behavior of the anisotropy measure Eq. (2.109) can be predicted, which also becomes τ-dependent and reads

$$\eta(\tau) = \frac{\sqrt{M^2(\tau) - 2(M^1)^2}}{M^1} = \frac{|D_1 - D_2|}{(D_1 + D_2)} \frac{[1 - \exp(-4D_\theta\tau)]}{4D_\theta\tau}. \tag{4.12}$$

For small τ the anisotropy measure reads $\eta(\tau) \overset{\tau\to 0}{\sim} \frac{|D_1 - D_2|}{D_1 + D_2}$ and is equal to the anisotropy measure of a homogeneous two-dimensional anisotropic system and for large τ the anisotropy measure $\eta(\tau) \overset{\tau\to\infty}{\sim} \frac{|D_1 - D_2|}{D_1 + D_2} \frac{1}{4D_\theta\tau}$ decays algebraically to zero. Thus, for large times the system behaves identically to a homogeneous isotropic system with diffusion constant $D_c = \frac{1}{2}(D_1 + D_2)$.

In Fig. 4.3 the τ-dependence of the distribution of diffusivities (left) and of the anisotropy measure η is shown. For $\tau < 0.1$ the distributions obtained from the simulated trajectories agree well with a distribution of a homogeneous anisotropic system with the same eigenvalues as from $\mathbf{D}(z)$ (black line). For $\tau > 10$ the distribution agrees well with that of a homogeneous isotropic system with diffusion coefficient $D_c = \langle D \rangle$ (black dashed line). For the anisotropy measure both time-average and ensemble average are shown. The first was obtained from a single trajectory of length $t = 10^5$ with time increment $\Delta t = 10^{-3}$ and the second was obtained from 10^5 trajectories of length $t = 10^2$ and the same time-increment. The time-averaged values (blue line) agree much better with the predicted curve (black dashed line) from Eq. (4.12),

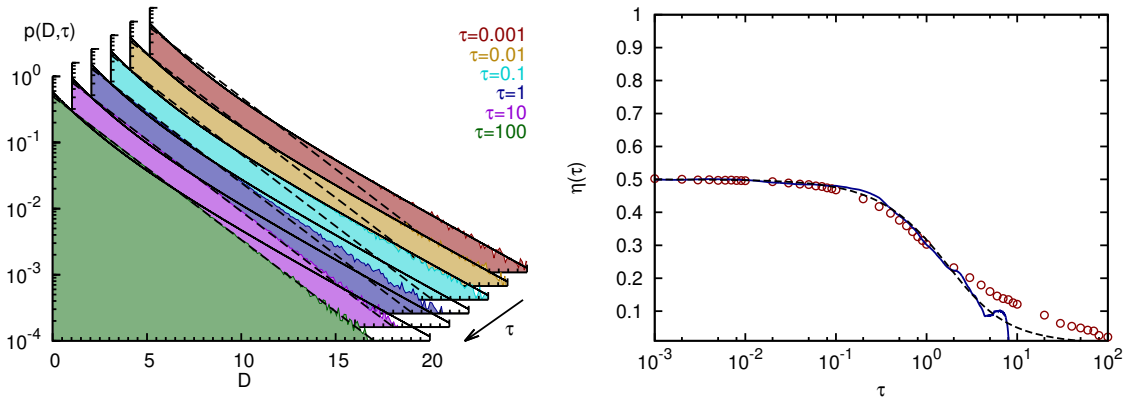

Figure 4.3.: The time-dependence of the distribution of diffusivities (left) and of the anisotropy measure η (right) for a twist system with $D_1 = 3$, $D_2 = 1$, $D_3 = 1$ and $\omega = 1$, i.e. $D_\theta = \frac{\omega^2}{4} D_3 = \frac{1}{4}$. The distribution of diffusivities is shown for different values of τ. For $\tau < 0.1$ the distributions obtained from the simulated trajectories agree well with a distribution of a homogeneous anisotropic system with the same eigenvalues as from $\mathbf{D}(z)$ (black line). For $\tau > 10$ the distribution agrees well with that of a homogeneous isotropic system with diffusion coefficient $D_c = \langle D \rangle$ (black dashed line). The anisotropy measure (right) is calculated with help of the moments of the diffusivities obtained from simulation of the Langevin equation of this system. Here both time-average (blue line) and ensemble average (red circles) are shown and compared with the analytical prediction from Eq. (4.12) (black dashed line). The time-average values seem to agree better with the analytical prediction than the ensemble average values.

although the values for large τ are less reliable in the time-average since the amount of data is heavily reduced (e.g for $\tau = 10$ only 10^4 data point are available). The ensemble average curve seems to decay slower than predicted to the asymptotic value, although the time-dependence of the second moment agrees well with the predicted behavior (see Fig. 4.2).

4.2. Deformed director field caused by a Fréedericksz transition

Another example which is considered in this thesis is also inspired from an experimental accessible formation of liquid crystal director field namely the Fréedericksz transition [140]. The Fréedericksz transition usually describes the transition from a uniform director field to a deformed one caused by the application of a strong electric or magnetic field [141]. One example of such a distorted director field is illustrated in the left part of Fig. 4.4. Here, without the magnetic field the director field would be uniformly oriented as the the molecules at the boundary. With the magnetic field perpendicular to the boundary orientation the director field is deformed and shows a continuous orientation change from one boundary to the other. Of course, depending on the preferred orientation at the boundary or on the direction of the applied magnetic or, respectively, electric field a whole bunch of different deformed director fields may be prepared in such a way.

The left part of Fig. 4.4 shows the director field which is considered in this section. It is a continuous extension of the field without the boundaries. This causes an heterogeneity in the x-

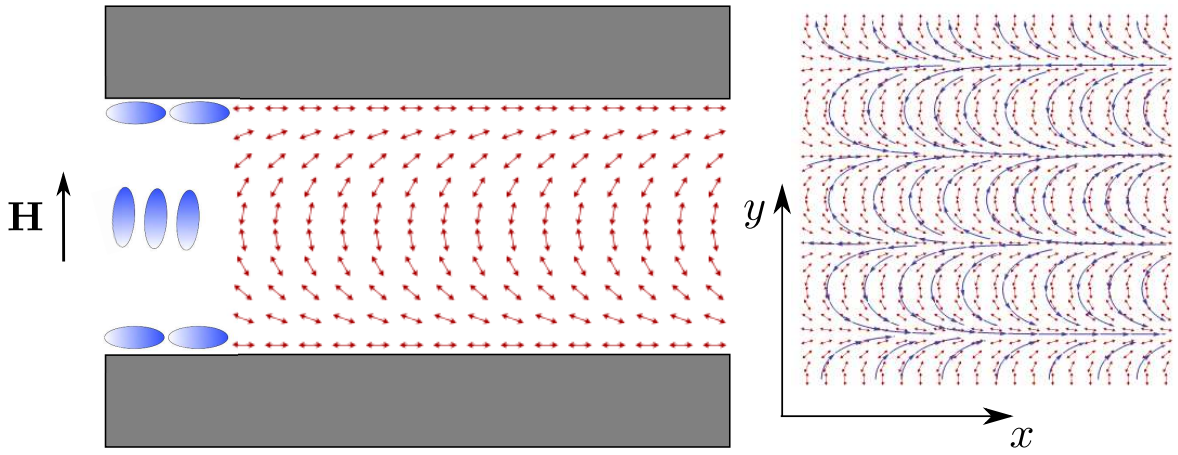

Figure 4.4.: Illustration of the deformed director field after a Fréedericksz transition (left) and the continuous inhomogeneous director field considered for the calculation. The left figure shows exemplarily the deformation of the director field caused by the applied magnetic field $\boldsymbol{H}$. Without the field the director field would be uniform and the mean orientation of the liquid crystal would be determined purely by the boundary. In this example a planar alignment at the boundary is preferred, but also homeotropic, i.e. perpendicular, or tilted alignment would be possible, which one depends on the type of liquid crystal and on the boundary. The right figure shows the considered director field (the blue stream lines are as guide to the eye) for the analysis which is now continuous and has natural boundary conditions.

y-plane, which only depends on the coordinate y. The third direction is independent and, thus, the diffusion in this direction is decoupled. Consequently, only the diffusion in the x-y-plane is considered and the diffusion tensor may be written

$$\mathbf{D}(y) = \begin{pmatrix} D_1\cos^2(\omega y) + D_2\sin^2(\omega y) & (D_2 - D_1)\cos(\omega y)\sin(\omega y) \\ (D_2 - D_1)\cos(\omega y)\sin(\omega y) & D_1\sin^2(\omega y) + D_2\cos^2(\omega y) \end{pmatrix} \tag{4.13}$$

with D_1 and D_2 the constant diffusion coefficients related to the principal axes of the local diffusion tensor. The tensor may be written as $\mathbf{D}(y) = \mathbf{O}^{\mathsf{T}}(y)\hat{\mathbf{D}}\mathbf{O}(y)$, with $\hat{\mathbf{D}} = \mathrm{diag}(D_1, D_2)$ a diagonal tensor and $\mathbf{O}(y)$ an orthogonal tensor describing a rotation around the z-axis about an angle ωy. Although the tensor looks very similar to the projected diffusion tensor $\mathbf{D}_{xy}(z)$ of the twist system (see Sec. 4.1), the behavior is different since the dependent direction lies in the same plane as the affected orientation. Hence, when looking at the corresponding Langevin equation

$$\frac{\mathrm{d}}{\mathrm{d}t}\begin{pmatrix} x \\ y \end{pmatrix} = \sqrt{2\mathbf{D}(y)}\begin{pmatrix} \xi_x(t) \\ \xi_y(t) \end{pmatrix} \quad (\alpha\text{-Interpretation}) \tag{4.14}$$

with $\sqrt{2\mathbf{D}(y)} = \sqrt{2}\mathbf{O}^{\mathsf{T}}(y)\sqrt{\hat{\mathbf{D}}}\mathbf{O}(y)$ it should be noticed that the equation now depends on the stochastic interpretation. In this example, the Langevin equation for the y-coordinate includes multiplicative noise, thus, the equation for the projection on this coordinate can be expressed as (see Chap. 2, Sec. 2.5.1, Eq. (2.87))

$$\frac{\mathrm{d}y(t)}{\mathrm{d}t} = \sqrt{2D_{yy}(y)} = \hat{g}(y)\hat{\xi}(t). \quad (\alpha\text{-Interpretation}) \tag{4.15}$$

Furthermore, the projected state-dependent diffusion coefficient $D_{yy}(y)$ has the same form as the example with the periodically varying diffusion coefficient given in Chap. 3, Sec. 3.4. Only the diffusion coefficients are interchanged. Thus, the propagator of the Stratonovich interpretation Eq. (3.79) and the asymptotic behavior of the scaled moments for an arbitrary interpretation may be calculated (see Eq. (3.87)).

4.2.1. Itô interpretation

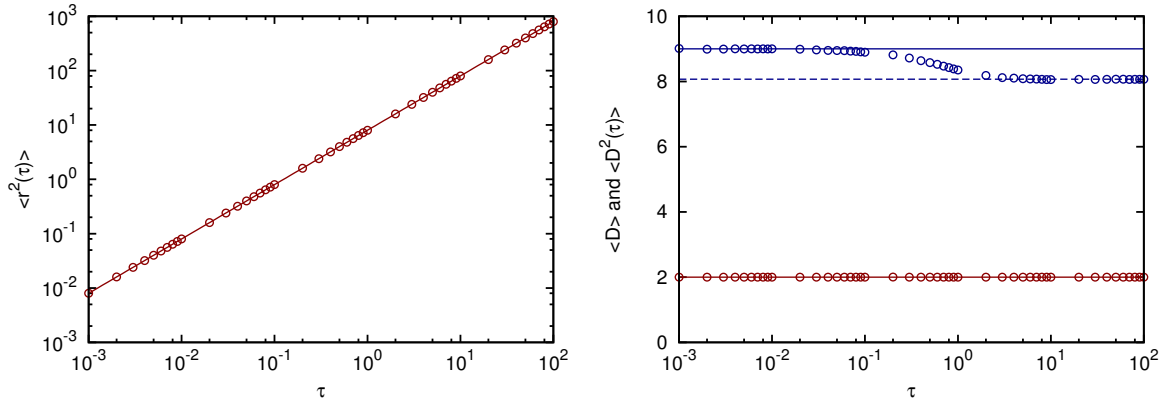

Figure 4.5.: The mean squared displacement (left) and the first two moments of the distribution of diffusivities (right) for a system after Fréedericksz transition interpreted in Itô sense with $D_1 = 1$, $D_2 = 3$ and $\omega = \frac{1}{2}$. The MSD obtained from random walk simulation of the Langevin equation Eq. (4.14) (circles) and the analytical value (lines) agree well. The MSD grows linear in time like for an isotropic system with the same mean diffusion coefficient. The first two moments of the distribution of diffusivities are shown in the left figure. Here the first moment (red) is constant as predicted and has the value $\langle D \rangle = \frac{D_1+D_2}{2} = 2$. The second moment shows a crossover from small τ to large τ. In both cases it takes the value of the homogeneous anisotropic system Eq. (2.107), but with different values, i.e. $\lim_{\tau\to 0} \langle D^2(\tau) \rangle = 9$ (blue line) and $\lim_{\tau\to\infty} \langle D^2(\tau) \rangle \approx 8.0718$ (blue dashed line).

For the Itô interpretation of the full process, it is already known from Eq. (2.83) that the mean square of the process is found via a simple ODE

$$\frac{\mathrm{d}\langle r^2 \rangle}{\mathrm{d}t} = \frac{\mathrm{d}\langle (x^2 + y^2) \rangle}{\mathrm{d}t} = 2 \operatorname{tr} \mathbf{D} = 2(D_1 + D_2). \tag{4.16}$$

Thus, the first moment of the diffusivity distribution $\langle D(\tau) \rangle = \frac{D_1+D_2}{2}$ and the MSD $\langle r^2(\tau) \rangle = 2(D_1 + D_2)\tau$ can be predicted, immediately. This can be observed in the left part of Fig. 4.5, which shows a good agreement of the analytic MSD (line) and the values obtained form a numerical implementation of the Langevin equation Eq. (4.14) interpreted in the Itô sense (circles).

Furthermore, the displacement distribution for $\tau \to 0$ is a bivariate Gaussian distribution with zero mean and covariance tensor $\mathbf{\Sigma} = 2\mathbf{D}(y)\tau$ [19]. Also, it is known that the distribution of diffusivities for a multivariate Gaussian displacement distribution depends only on the eigenvalues of the diffusion tensor [36]. Since the eigenvalues of $\mathbf{D}(y)$ are constant and independent of y, the distribution of diffusivities for $\tau \to 0$ is identical to that of a homogeneous anisotropic system with the same eigenvalues and given by Eq. (2.105). For large τ the process in y-direction has

asymptotically an effective diffusion coefficient $D_{y,\text{eff}} = \lim_{\tau\to\infty} \frac{\langle \Delta y\rangle}{2\tau} = \sqrt{D_1 D_2}$ (see Eq. (3.88)). Since the mean diffusivity $\langle D(\tau)\rangle = \frac{D_1+D_2}{2}$ is constant, it follows immediately that the effective diffusion coefficient in x direction must yield $D_{x,\text{eff}} = \lim_{\tau\to\infty} \frac{\langle \Delta x\rangle}{2\tau} = D_1 + D_2 - \sqrt{D_1 D_2}$. The same result can be obtained if the diffusion tensor Eq. (4.13) is averaged with the equilibrium distribution Eq. (3.90) in a periodic system. Thus, the effective diffusion tensor for large τ is $\mathbf{D}_\text{eff} = \text{diag}(D_1 + D_2 - \sqrt{D_1 D_2}, \sqrt{D_1 D_2})$. By plugging the effective diffusion coefficients into the equation for the second moment of the diffusivities for a two-dimensional system Eq. (2.107),

$$\lim_{\tau\to\infty} \left\langle D^2(\tau)\right\rangle = \frac{1}{4}\left[(3D_1 + D2)(D_1 + 3D_2) - 4\left(\sqrt{D_1^3 D_2} + \sqrt{D_1 D_2^3}\right)\right] \tag{4.17}$$

is obtained. This can be observed in the right part of Fig. 4.5, which shows the first two moments of the numerical implementation of the process as circles. Here the mean diffusivity remains constant and agrees well with the predicted value (red line). For the second moment of the diffusivity the crossover from value of a homogeneous anisotropic system for small τ (line) to the value predicted by Eq. (4.17) (dashed line) can be observed. It should be noted that in this case with $D_1 = 1$ and $D_2 = 3$ the second moment for large τ, here with value of about 8.0718, is already very close to the value of an isotropic system where the second moment is $\left\langle D^2\right\rangle = 2\left\langle D\right\rangle^2 = 8$ and, hence, the system can hardly be identified as anisotropic for large τ (see also Fig. 4.6). Nevertheless, if the difference between the eigenvalues of the diffusion tensor $\mathbf{D}(y)$ is larger, then also the gap between the effective eigenvalues for large τ is larger and, consequently the anisotropy is easier to detect.

And now, by using the expressions for the first and second moment of the diffusivities for large τ, the anisotropy value can be calculated

$$\lim_{\tau\to\infty} \eta(\tau) = \lim_{\tau\to\infty} \frac{\left\langle D^2(\tau)\right\rangle - 2\left\langle D\right\rangle^2}{\langle D\rangle} = \frac{|D_{x,\text{eff}} - D_{y,\text{eff}}|}{D_{x,\text{eff}} + D_{y,\text{eff}}} = 1 - \frac{2\sqrt{D_1 D_2}}{D_1 + D_2}. \tag{4.18}$$

Consequently, the distribution of diffusivities for $\tau \to \infty$ should still be anisotropic, but now with the the effective diffusion eigenvalues $D_{x,\text{eff}}$ and $D_{y,\text{eff}}$.

In Fig. 4.6 the τ-dependence is shown for the distribution of diffusivities and for the anisotropy measure η for the Itô interpretation of the Langevin equation Eq. (4.14). A crossover from the distribution of the homogeneous anisotropic system (black line) to an anisotropic distribution with the effective diffusion coefficient $D_{x,\text{eff}}$ and $D_{y,\text{eff}}$ can be observed. Since the eigenvalues of $\mathbf{D}(y)$, D_1 and D_2, are already very close together, the distribution for large τ is still well approximated with an isotropic distribution with the same mean diffusivity (red line). If the difference between D_1 and D_2 is larger, also the remaining anisotropy for large τ is increased. This behavior can also be observed in the anisotropy measure η, which shows a crossover from the value of a homogeneous anisotropic system $\eta = \frac{|D_1 - D_2|}{D_1 + D_2}$ to a value which now depends on the effective diffusion coefficients, given by Eq. (4.18).

4.2.2. Stratonovich interpretation

For the Stratonovich interpretation the situation is different than in the Itô case. The time-derivative of the mean square norm is not necessarily constant as in the Itô case due to the noise induced drift (see Eq. (2.83)). Nevertheless, for $\tau \to 0$ the displacement distribution is still a bivariate Gaussian distribution with covariance tensor $\mathbf{\Sigma} = 2\mathbf{D}(y)\tau$ [19], but now with the noise induced drift $\mathbf{f}^\alpha(y(t))\tau$, with $\alpha = \frac{1}{2}$. The noise induced drift is calculated with help of

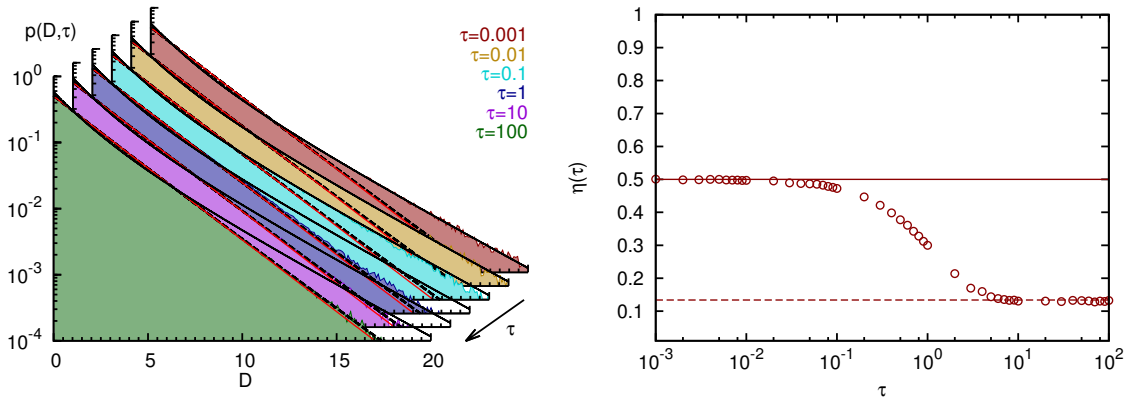

Figure 4.6.: The distribution of diffusivities for different time (left) and the anisotropy measure η (right) for a system after Fréedericksz transition interpreted in Itô sense with $D_1 = 1$, $D_2 = 3$ and $\omega = \frac{1}{2}$. The distribution of diffusivities obtained from random walk simulation of the Langevin equation Eq. (4.14) (colored densities) for different τ are shown. For $\tau < 0.1$ the distribution agrees well with that from the homogeneous anisotropic system with the same eigenvalues (black line) and for $\tau > 1$ it agrees well with that from a homogeneous anisotropic system (black dashed line) with the effective eigenvalues $D_{x,\text{eff}} = D_1 + D_2 - \sqrt{D_1 D_2} \approx 2.26795$ and $D_{y,\text{eff}} = \sqrt{D1D2} \approx 1.73205$. For comparison the distribution of diffusivities for a homogeneous isotropic system with the same mean diffusion coefficient $\langle D \rangle = D_c = \frac{D_1+D_2}{2} = 2$ is shown (red line) which can hardly be distinguished from true distribution for large τ. In the right figure the τ-dependence for the anisotropy measure η is shown. The values from the numerical implementation agree well for small times with the anisotropy value of a homogeneous anisotropic system with $\eta = \frac{|D_1-D_2|}{D_1+D_2} = \frac{1}{2}$ (red line) and for large times it agrees with the predicted value $\eta = 1 - \frac{2\sqrt{D_1 D_2}}{D_1+D_2} \approx 0.133975$ (red dashed line).

$\mathbf{g}(y) = \sqrt{2\mathbf{D}(y)} = \sqrt{2}\mathbf{O}^{\mathsf{T}}(y)\sqrt{\hat{\mathbf{D}}}\mathbf{O}(y)$ (see Chap. 2,Sec. 2.5) and yields

$$\mathbf{f}^{\alpha}(y) = \alpha \begin{pmatrix} \omega \left[D_1 + D_2 - 2\sqrt{D_1 D_2} + (D_2 - D_1)\cos(2\omega y) \right] \\ \omega(D_1 - D_2)\sin(2\omega y) \end{pmatrix}. \tag{4.19}$$

Thus, in the limit $\tau \to 0$ the distribution of diffusivities may be calculated via

$$\begin{aligned} \lim_{\tau\to 0} p(D,\tau) &= \lim_{\tau\to 0} \int \mathrm{d}^2 r \int \mathrm{d}^2 r\, \delta\left(D - \frac{\mathbf{r}^2}{4\tau}\right) p(\mathbf{x}+\mathbf{r}, t+\tau|\mathbf{x},t) p(\mathbf{x},t) \\ &= \lim_{\tau\to 0} \int \mathrm{d}^2 r \int \mathrm{d}^2 r\, \delta\left(D - \frac{\mathbf{r}^2}{4\tau}\right) \frac{\exp\left[-\frac{1}{4\tau}(\mathbf{r} - \mathbf{f}^{\alpha=\frac{1}{2}}(y(t))\tau)^{\mathsf{T}}\mathbf{D}^{-1}(y)(\mathbf{r} - \mathbf{f}^{\alpha=\frac{1}{2}}(y(t))\tau)\right]}{4\pi\tau D_1 D_2} p(\mathbf{x},t). \end{aligned} \tag{4.20}$$

By introducing the time-scaled variable $\hat{\mathbf{r}} = \frac{\mathbf{r}}{2\sqrt{\tau}}$ and taking the limit $\tau \to 0$ the calculation simplifies to

$$\lim_{\tau\to 0} p(D,\tau) \approx \int \mathrm{d}^2 \hat{r} \int \mathrm{d}^2 x\, \delta\left(D - \hat{\mathbf{r}}^2\right) \frac{\exp\left[-\hat{\mathbf{r}}^{\mathsf{T}}\mathbf{D}^{-1}(y)\hat{\mathbf{r}}\right]}{\pi D_1 D_2} p(\mathbf{x},t). \tag{4.21}$$

Now the integration over $\hat{\mathbf{r}}$ may be performed and yields the distribution of diffusivities of the homogeneous anisotropic case which depends only on the eigenvalues of $\mathbf{D}(y)$ which are independent of y. Thus, the integration over $\mathbf{x}$ does not influence the result. These steps can be performed for any system described by a Fokker-Planck equation with time-independent drift and state-dependent diffusion tensor with constant eigenvalues and consequently the distribution of diffusivities in the limit of small τ depends only on these eigenvalues and, thus, approaches an invariant distribution in that limit. This should not be underestimated, since this means, the local diffusion coefficients can be identified independently of applied time-independent forces and also independently of the form of the Fokker-Planck equation with respect to the stochastic interpretations. Accordingly, it is impossible to distinguish the stochastic interpretations with help of the distribution of diffusivities in the limit of small τ.

For large τ the situation is different, since now the drift term plays a role. Nevertheless, from Eq. (3.79) the exact propagator for the y-component is known, in this example only D_1 and D_2 are interchanged. And from Eq. (3.84) it is derived that the scaled variable $\hat{y}(t) = \frac{y(t)}{\sqrt{t}}$ in the limit $\tau \to \infty$ is effectively distributed like a Gaussian variable with zero mean and variance $\frac{D_2\pi^2}{2K^2(1-\frac{D_1}{D_2})}$. With this variance it is already assumed that $D_2 > D_1$, which is without loss of generality, i.e. if $D_1 > D_2$ the diffusion coefficients in the variance have to be interchanged. Thus, the moments of scaled displacement $\hat{r}_y = \frac{r_y(\tau)}{\sqrt{\tau}} = \frac{y(t+\tau)-y(t)}{\sqrt{\tau}}$ should approach the same values for large τ. Consequently, the moments of the projected diffusivity read

$$\lim_{\tau\to\infty} \langle D_y(\tau)^m \rangle = \lim_{\tau\to\infty} \left(\frac{1}{2}\right)^m \langle \hat{r}_y^{2m}(\tau) \rangle = \left(\frac{D_2\pi^2}{8K(1-\frac{D_1}{D_2})^2}\right)^m \frac{(2m)!}{m!} \tag{4.22}$$

and, hence correspond to a one-dimensional isotropic distribution of diffusivities with diffusion constant $D_c = \frac{D_2\pi^2}{4K(1-\frac{D_1}{D_2})^2}$. For the estimation of the mean diffusivity the mean projected diffusivity in x-direction is needed, since $\langle D(\tau) \rangle = \frac{1}{2}(\langle D_x(\tau) \rangle + \langle D_y(\tau) \rangle)$ and, thus, the behavior of the scaled displacement $\hat{r}_x = \frac{r_x(\tau)}{\sqrt{\tau}} = \frac{x(t+\tau)-x(t)}{\sqrt{\tau}}$ is known. The mean value of $x(t)$ fulfills the ODE $\frac{\mathrm{d}\langle x(t) \rangle}{\mathrm{d}t} = \left\langle f_x^{\alpha=\frac{1}{2}}(y) \right\rangle$, as can be seen in Eq. (2.84). Since the force-term of the right-hand side of the equation only depends on y, the average over the propagator of the projected coordinate $p(y,t|y_0)$, which is already known in the Stratonovich case (see Eq. (3.79)), may be calculated. Thus, the solution to this ODE reads

$$\langle x(t) \rangle_{x_0,y_0} = x_0 + \int_0^t \mathrm{d}s \int \mathrm{d}y f_x^{\frac{1}{2}}(y) p(y,s|y_0). \tag{4.23}$$

Unfortunately, this integrals cannot be performed explicitly. Nevertheless, the mean force $\left\langle f_x^{\frac{1}{2}}(y) \right\rangle(s) = \int \mathrm{d}y f_x^{\frac{1}{2}}(y) p(y,s|y_0)$ for large times s approaches a constant. Therefore, the integral

$$\lim_{s\to\infty} \left\langle f_x^{\frac{1}{2}}(y) \right\rangle(s) = \lim_{s\to\infty} \int_{-\infty}^{\infty} \mathrm{d}y \, \frac{\omega}{2} \left[D_1 + D_2 - 2\sqrt{D_1 D_2} + (D_2 - D_1)\cos(2\omega y) \right] p(y,s|y_0) \tag{4.24}$$

has to be solved. The integration over the constants can be performed without effort. For the integral over the cosine the coordinate transformation $\tilde{y} = \frac{F(\omega y, 1-\frac{D_1}{D_2})}{\sqrt{2D_2}\omega}$ is needed, where $F(\phi,m) = \int_0^\phi \mathrm{d}\theta \left[1 - m\sin^2(\theta)\right]^{-\frac{1}{2}}$ denotes the elliptic integral of first kind. And with the

knowledge that the initial value y_0 for large time becomes unimportant (see Sec. 3.4.1), the integration can be written as

$$\lim_{s\to\infty}\int_{-\infty}^{\infty}\mathrm{d}y\cos(2\omega y)p(y,s|y_0)\approx\lim_{s\to\infty}\int_{-\infty}^{\infty}\mathrm{d}\tilde{y}\left[1-2\,\mathrm{sn}(\sqrt{2D_2}\omega\tilde{y},1-\frac{D_1}{D_2})\right]\frac{\exp\left(-\frac{\tilde{y}^2}{2s}\right)}{\sqrt{2\pi s}} \quad (4.25)$$

with $\mathrm{sn}(\phi,m)=\sin(\mathrm{am}(u,m))$ and the Jacobi amplitude $\mathrm{am}(u,m)$, which is the inverse function to $u=F(\phi,m)$ [136]. After utilizing the Lambert series expansion of $\mathrm{sn}(\phi,m)$ and performing the square $\mathrm{sn}(\phi,m)^2$ reads

$$\begin{aligned}\mathrm{sn}(\phi,m)^2=\frac{4\pi^2}{mK(m)}\Bigg\{&\sum_{n=0}^{\infty}\frac{q(m)^{2n+1}}{(1-q(m)^{2n+1})^2}\sin^2\left[(2n+1)\frac{\pi\phi}{2K(m)}\right]\\&+2\sum_{n<l}^{\infty}\frac{q(m)^{n+\frac{1}{2}}q(m)^{l+\frac{1}{2}}}{(1-q(m)^{2n+1})(1-q(m)^{2l+1})}\sin\left[(2n+1)\frac{\pi\phi}{2K(m)}\right]\sin\left[(2l+1)\frac{\pi\phi}{2K(m)}\right]\Bigg\}\end{aligned} \quad (4.26)$$

with $q(m)$ the elliptic nome. Now the integration can be performed and after taking the limit $s\to\infty$, the mean acting force for large times s reads

$$\begin{aligned}f_x^{\mathrm{asy}}\equiv\lim_{s\to\infty}\left\langle f_x^{\frac{1}{2}}(y)\right\rangle(s)=\frac{\omega}{2}\Bigg[&D_1+D_2-2\sqrt{D_1D_2}\\&+(D_2-D_1)\left(1-\frac{4\pi^2}{(1-\frac{D_1}{D_2})K(1-\frac{D_1}{D_2})^2}\sum_{n=0}^{\infty}\frac{q(1-\frac{D_1}{D_2})^{2n+1}}{(1-q(1-\frac{D_1}{D_2})^{2n+1})^2}\right)\Bigg].\end{aligned} \quad (4.27)$$

The sum on the right side converges very rapidly and may be aborted after a few terms. If $D_2\gg D_1$, then $\cos\left[2\mathrm{am}(\sqrt{2D_2}\omega\tilde{y},1-\frac{D_1}{D_2})\right]\approx\cos\{4\tan^{-1}[\exp(\sqrt{2D_2}\omega\tilde{y})]-\pi\}$ and, thus,

$$\lim_{s\to\infty}\int_{-\infty}^{\infty}\mathrm{d}\tilde{y}\cos\left[2\mathrm{am}(\sqrt{2D_2}\omega\tilde{y},1-\frac{D_1}{D_2})\right]\frac{\exp\left(-\frac{\tilde{y}^2}{2s}\right)}{\sqrt{2\pi s}}\approx-1. \quad (4.28)$$

Then the mean force simplifies to

$$f_x^{\mathrm{asy}}=\lim_{s\to\infty}\left\langle f_x^{\frac{1}{2}}(y)\right\rangle(s)\overset{D_2\gg D_1}{\approx}\omega\left(D_1-\sqrt{D_1D_2}\right), \quad (4.29)$$

If $D_1\approx D_2$, then $\mathrm{sn}(\sqrt{2D_1}\omega\tilde{y},1-\frac{D_2}{D_1})\approx\sin(\sqrt{2D_1}\omega\tilde{y})$ and, consequently

$$\lim_{s\to\infty}\int_{-\infty}^{\infty}\mathrm{d}\tilde{y}\left[1-2\,\mathrm{sn}(\sqrt{2D_1}\omega\tilde{y},1-\frac{D_2}{D_1})\right]\frac{\exp\left(-\frac{\tilde{y}^2}{2s}\right)}{\sqrt{2\pi s}}\approx0. \quad (4.30)$$

Here the mean force simplifies to

$$f_x^{\mathrm{asy}}=\lim_{s\to\infty}\left\langle f_x^{\frac{1}{2}}(y)\right\rangle(s)\overset{D_2\approx D_1}{\approx}0, \quad (4.31)$$

which is the isotropic limit.

Another possibility to calculate the mean force is to use the equilibrium or steady-state distribution given by Eq. (3.91) instead of the propagator. Then the asymptotic mean force yields

$$f_x^{\mathrm{asy}}=\lim_{s\to\infty}\left\langle f_x^{\frac{1}{2}}(y)\right\rangle(s)=\int_{-\frac{\pi}{2\omega}}^{\frac{\pi}{2\omega}}\mathrm{d}y f_x^{\frac{1}{2}}(y)p_{\mathrm{eq}}(y)=-\omega\sqrt{D_1D_2}+\omega D_1\frac{E\left(1-\frac{D_2}{D_1}\right)}{K\left(1-\frac{D_2}{D_1}\right)} \quad (4.32)$$

with $K(m) = \int_0^{\frac{\pi}{2}} \mathrm{d}\theta \left(1 - m\sin^2(\theta)\right)^{-\frac{1}{2}}$ the complete elliptic integral of first kind and $E(m) = \int_0^{\frac{\pi}{2}} \mathrm{d}\theta \left(1 - m\sin^2(\theta)\right)^{\frac{1}{2}}$ the complete elliptic integral of second kind. By comparing Eq. (4.32) with Eq. (4.27)

$$\sum_{n=0}^{\infty} \frac{q(m)^{2n+1}}{(1-q(m)^{2n+1})^2} = \frac{K(m)}{2\pi^2}\left[\sqrt{\frac{1}{1-m}}K\left(\frac{m}{m-1}\right) - \sqrt{1-m}E\left(\frac{m}{m-1}\right)\right] \tag{4.33}$$

is obtained and, thus, by the way finds an explicit expression for this sum. Since the mean force is constant for large times, the mean and also the mean displacement grows asymptotically linear in time, i.e. $\lim_{t\to\infty} \frac{\langle x(t)-x(0)\rangle}{t} = \lim_{t\to\infty} \left\langle f_x^{\frac{1}{2}}(y)\right\rangle(t) = f_x^{\mathrm{asy}}$.

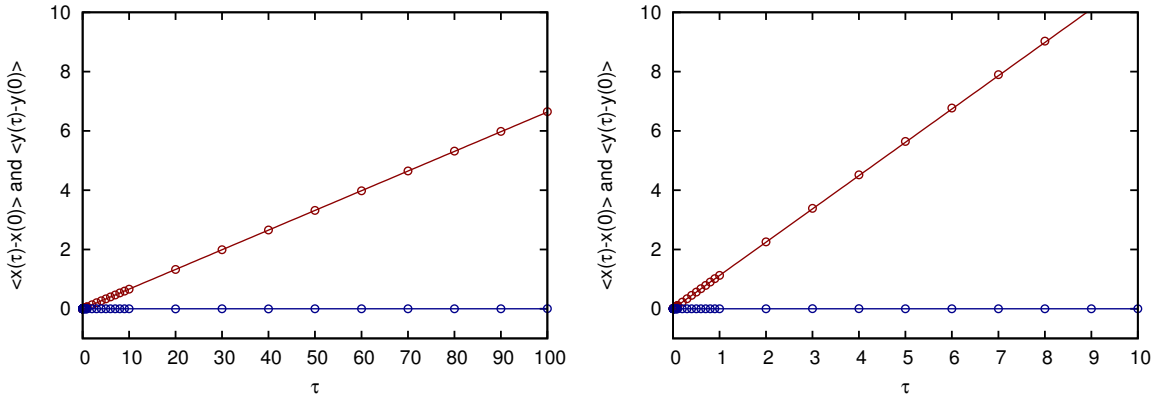

Figure 4.7.: Mean displacements for a system after Fréedericksz transition interpreted in Stratonovich sense with $D_1 = 1$, $D_2 = 3$ and $\omega = \frac{1}{2}$ (left) and with $D_1 = 1$, $D_2 = 10$ and $\omega = 1$ (right). The mean displacements in x direction (red) and in y-direction (blue) from a numerical evaluation of the Langevin equation Eq. (4.14) interpreted in Stratonovich sense (circles) are compared with the analytical predictions (lines) for two different parameter sets. In both cases the mean displacement in y direction is approximately zero. The mean displacement in x-direction grows linearly in time for large τ in both cases. The slope in both figures can be computed either with Eq. (4.27) or (4.32) and yields in the left figure $f_x^{\mathrm{asy}} \approx 0.06636$ and in the right figure $f_x^{\mathrm{asy}} \approx 1.12296$. The numerical results show a good agreement with the analytical predictions.

In Fig. 4.7 the mean displacements for a system after Fréedericksz transition interpreted in Stratonovich sense for two different parameter sets are shown. As predicted, the mean displacement in y-direction is zero, whereas in x-direction there exist a mean drift, which for large τ may be calculated with Eq. (4.27) or (4.32). The numerical results (circles) and the analytical prediction (lines) show a good agreement.

For the estimation of the mean square displacement, again the equation for the mean square of the process Eq. (2.83)

$$\begin{aligned}\frac{\mathrm{d}\left\langle r^2(t)\right\rangle}{\mathrm{d}t} &= \left\langle 2\mathbf{x}(t)^{\mathsf{T}}\mathbf{f}^{\frac{1}{2}}(\mathbf{x}(t))\right\rangle + 2\,\mathrm{tr}(\mathbf{D}) \\ &= 2\left\langle x(t)\right\rangle\left\langle f_x^{\frac{1}{2}}(y(t))\right\rangle + 2\left\langle y(t) f_y^{\frac{1}{2}}(y(t))\right\rangle + 2(D_1+D_2)\end{aligned} \tag{4.34}$$

may be taken, here already constant trace of $\mathbf{D}$ and the independence between the force $f_x^{\frac{1}{2}}(y(t))$ and the variable $x(t)$ is used. If the asymptotic behavior of $\langle x(t)\rangle$ and $\left\langle f_x^{\frac{1}{2}}(y(t))\right\rangle$ for large t is utilized and, furthermore, assumed that $\left\langle y(t) f_y^{\frac{1}{2}}(y(t))\right\rangle$ is zero for large times, then this ODE may be solved and yields

$$\left\langle r^2(t)\right\rangle \overset{t\to\infty}{\sim} (f_x^{\text{asy}})^2\, t^2 + 2(D_1 + D_2)t. \tag{4.35}$$

Consequently, the mean diffusivity for large τ should yield

$$\langle D(\tau)\rangle \overset{\tau\to\infty}{\approx} \frac{\left\langle r^2(\tau)\right\rangle}{4\tau} \overset{\tau\to\infty}{\sim} \left(\frac{1}{2} f_x^{\text{asy}}\right)^2 \tau + \frac{1}{2}(D_1 + D_2). \tag{4.36}$$

Hence, the mean diffusivity should grow asymptotically linearly with τ and, thus, the MSD grows with τ^2, i.e. with a ballistic exponent.

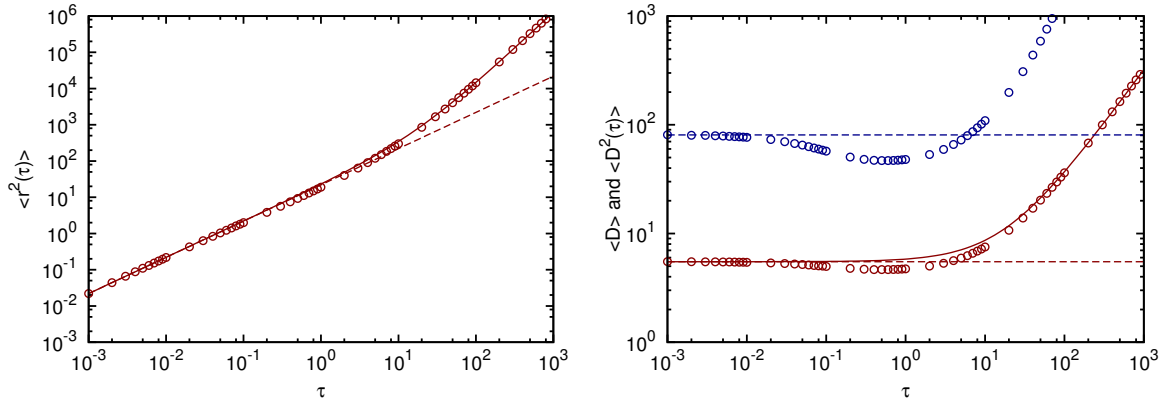

Figure 4.8.: MSD (left) and first two moments of the distribution of diffusivities (right) for a system after Fréedericksz transition interpreted in Stratonovich sense with $D_1 = 1$, $D_2 = 10$ and $\omega = 1$. The MSD from a numerical evaluation of the Langevin equation Eq. (4.14) interpreted in Stratonovich sense (circles) for small τ grows linearly with slope $2\,\mathrm{tr}(\mathbf{D}(y)) = 22$ (red dashed line) and for large τ it grows ballistically, i.e. with τ^2 and a slope of $(f_x^{\text{asy}})^2 \approx 1.261$. Overall it shows a good aggreement with Eq. (4.35) (red line). The first two moments of the distribution of diffusivities are shown in the right figure. The first moment (red circles) and the second moment (blue circles) of the simulation show a good agreement with the values of the homogeneous anisotropic case with the same eigenvalues D_1 and D_2 (dashed lines) for small τ. For increasing τ, the moments for an intermediate τ decrease, but then grow for large τ. The first moment for large τ grows linearly with τ, as predicted by Eq. (4.36), with a slope of $(\frac{1}{2} f_x^{\text{asy}})^2 \approx 0.315$. Except for intermediate τ, the numerical values (red circles) show a good agreement with curve of Eq. (4.36) (red line).

In Fig. 4.8 the MSD and the first two moments of a simulation of the Eq. (4.14) interpreted in Stratonovich sense are compared with the analytical results from Eqs. (4.35) and (4.36). Except for intermediate τ there is a good agreement between the numerical values (circles) and the analytical predictions (lines).

4.3. Undulation of the director field

The final example in this thesis considers an undulation in the director field. The undulation pattern was originally predicted by Helfrich [145, 146] to describe the orientation field of cholesteric liquid crystal between two conducting plates. The liquid crystal molecules have a parallel alignment to the plates without an applied electric field and with electric field the orientation layers tend to reorient with the electric field lines, but the free reorientation is hindered by the surface forces from the boundaries. As result the orientation layers show a periodic modulation, i.e. undulation. This undulation, also known as Helfrich-Hurault effect [141], can also be found for smectic A liquid crystals, which has a homeotropic texture between two glass plates, i.e. the molecules are aligned perpendicular to the plates, and with application of a magnetic field parallel to the plates the undulation pattern occurs [141]. Furthermore, this pattern was predicted by Clark and Meyer [147] and measured from Delaye *et al.* [148] for smectic A and cholesteric liquid crystals, which are subjected to dilative mechanical stress.

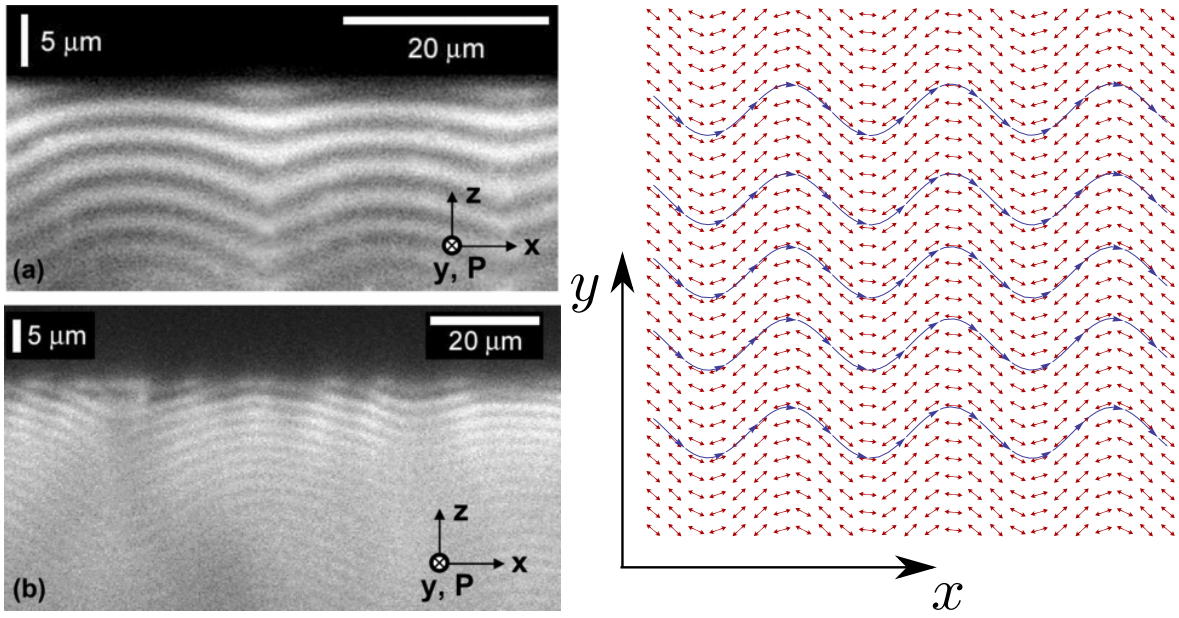

Figure 4.9.: Experimental example of a director field with undulation (from [50], Fig. 8) recorded with fluorescence confocal polarized microscopy technique and the illustration of the continuous director field considered for the calculation (the blue stream lines are as guide to the eye).

In Fig. 4.9 an experimentally observed undulation pattern is shown (left). This pattern was measured by Senyuk *et al.* [50] with help of fluorescence confocal polarized microscopy. In the right part of Fig. 4.9 the continuous director field which is considered in this thesis is shown. The corresponding state-dependent diffusion tensor reads

$$\mathbf{D}(x) = \begin{pmatrix} D_2 + \frac{D_1 - D_2}{1 + A^2 \cos^2(\omega x)} & \frac{2A(D_1 - D_2)\cos(\omega x)}{2 + A^2 + A^2 \cos(2\omega x)} \\ \frac{2A(D_1 - D_2)\cos(\omega x)}{2 + A^2 + A^2 \cos(2\omega x)} & D_1 + \frac{D_2 - D_1}{1 + A^2 \cos^2(\omega x)} \end{pmatrix} \tag{4.37}$$

with ω the period of the undulation and A its amplitude and with D_1 and D_2 the diffusion coefficients related to the principal axes of the local diffusion tensor. The tensor may be written

as $\mathbf{D}(x) = \mathbf{O}^\mathsf{T}(x)\hat{\mathbf{D}}\mathbf{O}(x)$, with $\hat{\mathbf{D}} = \mathrm{diag}(D_1, D_2)$ a constant diagonal tensor and

$$\mathbf{O}(x) = \begin{pmatrix} \mathbf{d}^\mathsf{T}(x) \\ \mathbf{n}^\mathsf{T}(x) \end{pmatrix} \tag{4.38}$$

an orthogonal tensor written in terms of the local director $\mathbf{d}(x)$ and its normal vector $\mathbf{n}(x)$ given by

$$\mathbf{d}(x) = \frac{1}{\sqrt{1 + A^2\cos^2(\omega x)}} \begin{pmatrix} 1 \\ A\cos(\omega x) \end{pmatrix} \text{ and } \mathbf{n}(x) = \frac{1}{\sqrt{1 + A^2\cos^2(\omega x)}} \begin{pmatrix} -A\cos(\omega x) \\ 1 \end{pmatrix}. \tag{4.39}$$

Again, the corresponding Langevin equation

$$\frac{\mathrm{d}}{\mathrm{d}t}\begin{pmatrix} x \\ y \end{pmatrix} = \sqrt{2\mathbf{D}(x)}\begin{pmatrix} \xi_x(t) \\ \xi_y(t) \end{pmatrix} \quad (\alpha\text{-Interpretation}) \tag{4.40}$$

for the x-component includes multiplicative noise. Unfortunately, no explicit transformation function $\Phi(x) = \int^x \mathrm{d}x' \frac{1}{\sqrt{2D_{xx}(x')}} = \int^x \mathrm{d}x' \frac{1}{\hat{g}(x')}$ is found up to now for the projected process. Furthermore, also the normalization constants of the equilibrium distributions for other than the Itô interpretation can not be computed explicitly. And, thus no analytical predictions for the behavior of the process for other than the Itô interpretation can be made. Nevertheless, the methods provided in Sec. 4.2.2 may still be used to predict the behavior numerically.

4.3.1. Itô interpretation

For the Itô interpretation of the full process it is known, from Eq. (2.83) and from Sec. 4.2.1, that the mean diffusivity is constant and the mean squared displacement grows linearly in time, i.e.

$$\langle D \rangle = \frac{D_1 + D_2}{2} \text{ and } \left\langle r^2(\tau) \right\rangle = 2(D_1 + D_2)\tau. \tag{4.41}$$

This can be observed in the left part of Fig. 4.10, which shows a good agreement of the analytic MSD (line) and the values obtained from a numerical implementation of the Langevin equation Eq. (4.40) interpreted in the Itô sense (circles).

Furthermore, independently of the stochastic interpretation and of external state-dependent forces, the distribution of diffusivities for small τ in case of constant eigenvalues of $\mathbf{D}(x)$ is always the same as in a homogeneous anisotropic case with the same eigenvalues (see first part of Sec. 4.2.2, especially Eq. (4.21)) and, consequently, given by Eq. (2.105) in this case.

Since the diffusion tensor is periodic in x, the same ansatz as in Sec. 4.2.1 for the calculation of the effective diffusion coefficients for large τ can be taken. Therefore, the equilibrium distribution of the projected x-coordinate of the system with periodic boundary conditions is needed, given by

$$p_{\mathrm{eq}}(x) = \frac{1}{D_{xx}(x)}\left(\int_{-\frac{\pi}{\omega}}^{\frac{\pi}{\omega}} \mathrm{d}x\, \frac{1}{D_{xx}(x)}\right)^{-1} = \frac{\omega D_2\sqrt{D_1(D_1 + A^2D_2)}}{2\pi(D_2 - D_1 + \sqrt{D_1(D_1 + A^2D_2)})\left(D_2 + \frac{D_1 - D_2}{1 + A^2\cos^2(\omega x)}\right)}. \tag{4.42}$$

With the knowledge of the equilibrium distribution of the dependent variable x, the effective diffusion tensor of the system, which determines the diffusive behavior of the system for large τ, is calculated via

$$\mathbf{D}_{\mathrm{eff}} = \int_{-\frac{\pi}{\omega}}^{\frac{\pi}{\omega}} \mathrm{d}x \mathbf{D}(x) p_{\mathrm{eq}}(x). \tag{4.43}$$

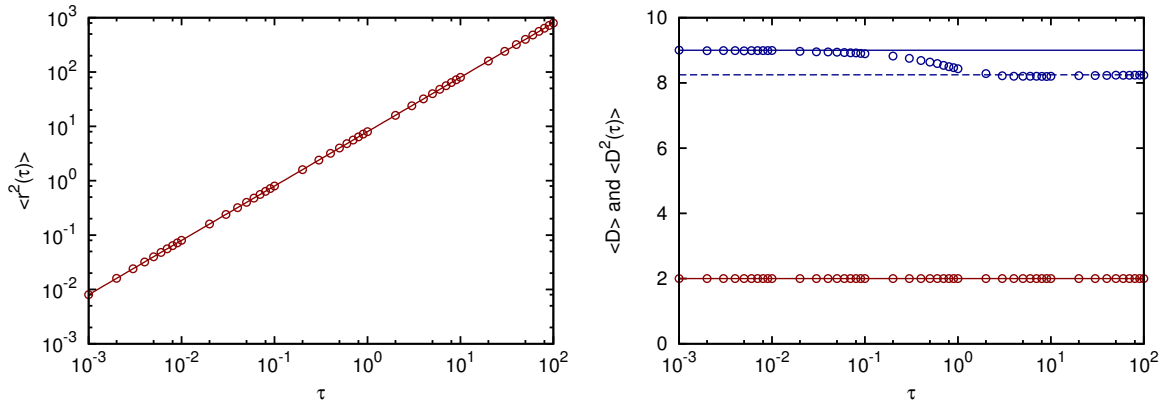

Figure 4.10.: The mean squared displacement (left) and the first two moments of the distribution of diffusivities (right) for an undulation system interpreted in Itô sense with $D_1 = 1$, $D_2 = 3$, $\omega = 1$ and $A = 1$. The MSD obtained from random walk simulation of the Langevin equation Eq. (4.40) (circles) and the analytical value (lines) agree well. The MSD grows linearly in time like for an isotropic system with the same mean diffusion coefficient. The first two moments of the distribution of diffusivities are shown in the left figure. Here the first moment (red) is constant as predicted and has the value $\langle D \rangle = \frac{D_1+D_2}{2} = 2$. The second moment shows a crossover from small τ to large τ. In both cases it takes the value of the homogeneous anisotropic system Eq. (2.107) but with different values, i.e. $\lim_{\tau\to 0} \langle D^2(\tau) \rangle = 9$ (blue line) and $\lim_{\tau\to\infty} \langle D^2(\tau) \rangle = 8.25$ (blue dashed line).

The eigenvalues of this effective tensor read

$$D_{x,\text{eff}} = \frac{D_2\sqrt{D_1(D_1 + A^2 D_2)}}{D_2 - D_1 + \sqrt{D_1(D_1 + A^2 D_2)}} \tag{4.44}$$

and

$$D_{y,\text{eff}} = \frac{D_2^2 - D_1^2 + D_1\sqrt{D_1(D_1 + A^2 D_2)}}{D_2 - D_1 + \sqrt{D_1(D_1 + A^2 D_2)}}. \tag{4.45}$$

By plugging the effective diffusion coefficients into the equation for the second moment of the diffusivities for a two-dimensional system Eq. (2.107), the asymptotic behavior of the second moment for large τ

$$\lim_{\tau\to\infty} \langle D^2(\tau) \rangle = \frac{1}{4}\left[3D_{x,\text{eff}}^2 + 2D_{x,\text{eff}}D_{y,\text{eff}} + 3D_{y,\text{eff}}^2\right] \tag{4.46}$$

is obtained. This can be observed in the right part of Fig. 4.5, which shows the first two moments of the numerical implementation of the process as circles. The mean diffusivity remains constant and agrees well with the predicted value (red line). For the second moment of the diffusivity the crossover from the value of a homogeneous anisotropic system for small τ (line) to the value predicted by Eq. (4.46) (dashed line) can be observed.

And now the expressions for the first and second moment of the diffusivities for large τ or the

effective eigenvalues may be used to calculate the anisotropy value

$$\lim_{\tau\to\infty}\eta(\tau) = \lim_{\tau\to\infty}\frac{\left\langle D^2(\tau)\right\rangle - 2\left\langle D\right\rangle^2}{\left\langle D\right\rangle} = \frac{|D_{x,\mathrm{eff}} - D_{y,\mathrm{eff}}|}{D_{x,\mathrm{eff}} + D_{y,\mathrm{eff}}} = \frac{\left|(D_1 - D_2)\left(D_1 + D_2 - \sqrt{D_1\left(D_1 + A^2 D_2\right)}\right)\right|}{(D_1 + D_2)\left(\sqrt{D_1\left(D_1 + A^2 D_2\right)} - D_1 + D_2\right)}. \tag{4.47}$$

Consequently, the distribution of diffusivities for $\tau \to \infty$ should still be anisotropic, but now with the the effective diffusion eigenvalues $D_{x,\mathrm{eff}}$ and $D_{y,\mathrm{eff}}$.

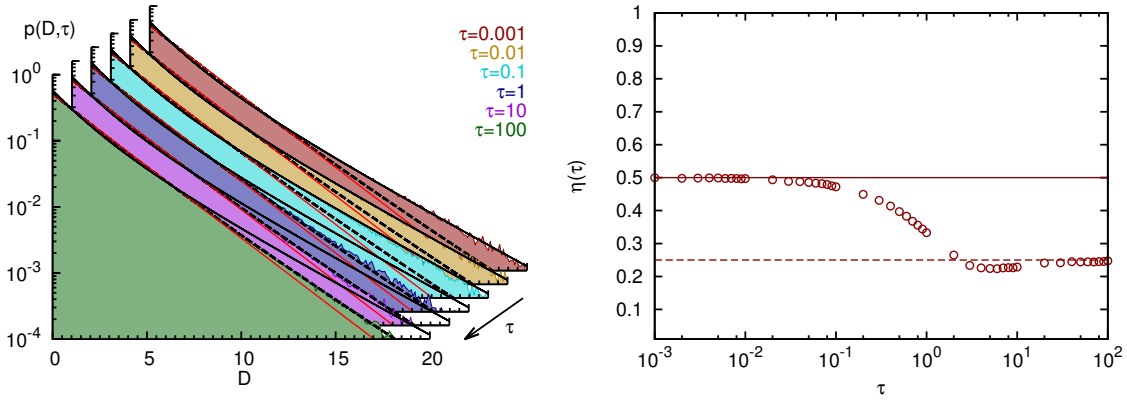

Figure 4.11.: The distribution of diffusivities for different times (left) and the anisotropy measure η (right) for an undulation in Itô sense with $D_1 = 1$, $D_2 = 3$, $\omega = 1$ and $A = 1$. The distribution of diffusivities obtained from random walk simulation of the Langevin equation Eq. (4.40) (colored densities) for different τ are shown. For $\tau < 0.1$ the distribution agrees well with that from the homogeneous anisotropic system with the same eigenvalues (black line) and for $\tau > 1$ it agrees well with that from a homogeneous anisotropic system (black dashed line) with the effective eigenvalues given by Eqs. (4.44) and (4.45) $D_{x,\mathrm{eff}} = \frac{3}{2}$ and $D_{y,\mathrm{eff}} = \frac{5}{2}$. For comparison the distribution of diffusivities for a homogeneous isotropic system with same mean diffusion coefficient $\langle D\rangle = D_c = \frac{D_1+D_2}{2} = 2$ is shown (red line). It can be well distinguished from true distribution for large τ, especially for large D. In the right figure the τ-dependence for the anisotropy measure η is shown. The values from the numerical implementation agree well for small times with the anisotropy value of a homogeneous anisotropic system with $\eta = \frac{|D_1-D_2|}{D_1+D_2} = \frac{1}{2}$ (red line) and for large times it agrees with the predicted value from Eq. (4.47) $\eta = \frac{1}{4}$ (red dashed line).

In Fig. 4.11 the τ-dependence of the distribution of diffusivities and of the anisotropy measure η for the Itô interpretation of the Langevin equation Eq. (4.40) is shown. One can observe the crossover from the distribution of the homogeneous anisotropic system (black line) to an anisotropic distribution with the effective diffusion coefficients $D_{x,\mathrm{eff}}$ and $D_{y,\mathrm{eff}}$ given by Eqs. (4.44) and (4.45). In the right part of Fig. 4.11 the temporal behavior of the anisotropy parameter η is presented. It shows a similar crossover as the distribution of diffusivities from a value which is determined by the eigenvalues of $\mathbf{D}(x)$, D_1 and D_2, for small τ to a value which is now stipulated by the effective eigenvalues $D_{x,\mathrm{eff}}$ and $D_{y,\mathrm{eff}}$.

4.4. Some general results

From the results obtained in the previous sections, some general assertions can be made. First, for anisotropic systems with a state-dependent diffusion tensor $\mathbf{D}(\mathbf{x})$ with constant eigenvalues and arbitrary state-dependent drift $\mathbf{f}(\mathbf{x})$, where the probability density function follows a general Fokker-Planck equation

$$\frac{\partial p(\mathbf{x},t)}{\partial t} = \sum_{i=1}^{d}\sum_{j=1}^{d} -\frac{\partial}{\partial x_i}\left(f_i(\mathbf{x})p(\mathbf{x},t) - \frac{\partial}{\partial x_j}D_{ij}(\mathbf{x})p(\mathbf{x},t)\right), \tag{4.48}$$

the distribution of diffusivities is a valuable tool to determine the eigenvalues of $\mathbf{D}(\mathbf{x})$. It has been established in the first part of Sec. 4.2.2, on the example of a two-dimensional system (see Eq. (4.21)), that the distribution of diffusivities only depends on the eigenvalues of $\mathbf{D}(\mathbf{x})$ for small τ and that prove can be easily extended to arbitrary dimensions. Furthermore, Heidernätsch *et al.* [36] already showed how these eigenvalues can be obtained from the moments of measured diffusivities. Consequently, for any system which follows the general Fokker-Planck equation Eq. (4.48) and has constant eigenvalues of $\mathbf{D}(\mathbf{x})$, these eigenvalues may be obtained by measuring the moments of the diffusivities for small time-increments τ. Of course, this also includes any stochastic interpretations of the Langevin equation Eq. (2.72), since the noise-induced drift term is also only state-dependent.

Secondly, if the same system is additionally drift-free, which corresponds to the Itô interpretation of Eq. (2.72), the mean diffusivity and the mean squared displacement is easily predicted and yield

$$\langle D\rangle = \frac{1}{d}\sum_{i=1}^{d} D_i \text{ and } \left\langle r^2(\tau)\right\rangle = 2\,\mathrm{tr}(\mathbf{D}(\mathbf{x}))\tau = 2d\,\langle D\rangle\,\tau. \tag{4.49}$$

And finally, if there is only one dependent direction, i.e. $\mathbf{D}(\mathbf{x}) = \mathbf{D}(x_i)$, and the equilibrium or steady distribution of the projected density can be calculated with

$$p_{\mathrm{eq}}(x_i) = \frac{\mathcal{N}^{-1}}{D_{ii}(x_i)}, \tag{4.50}$$

the effective diffusion tensor which applies for large τ may be calculated via

$$\mathbf{D}_{\mathrm{eff}} = \int \mathrm{d}x_i \mathbf{D}(x_i) p_{\mathrm{eq}}(x_i). \tag{4.51}$$

$\mathcal{N} = \int \mathrm{d}x_i \frac{1}{D_{ii}(x_i)}$ has to be a finite normalization constant as a necessary condition that the steady-state exists. Nevertheless, if the projected diffusion coefficient has a periodicity L, i.e. $D_{ii}(x_i) = D_{ii}(x_i \pm L)$, also the steady-state solution within one period can be used, which is easily normalized. Consequently, the distribution of diffusivities for large τ now only depends on the eigenvalues of the effective tensor Eq. (4.51).

5. Summary and Outlook

The diffusion with state-dependent diffusion coefficient or diffusion tensor, which is of high relevance in a wide variety of systems, was studied in this thesis. The dynamics of diffusing molecules or particles in such systems is usually described and modeled using a drift-free Langevin equation with multiplicative noise. This immediately leads to the question of the stochastic interpretation of the Langevin equation and, accordingly, to the question of the proper form of the Fokker-Planck equation, or diffusion equation respectively, describing the probability density function of the process. This question cannot be settled by theoretical consideration alone. Measurable quantities have to be found, e.g. the from the propagator or temporal behavior of moments of the processes, which allow to identify the proper description.

Thus, in Chap. 2 a brief recall of the stochastic description of diffusion processes was given, already highlighting the problems related to the stochastic interpretations and recalling analytical treatments to obtain the propagator of the stochastic differential equation modeling the process. This chapter was concluded by a short presentation of methods which are used in experiments to measure properties of diffusion processes and how they are related to the stochastic description. This was followed by the first result Chap. 3, which presented several examples of one-dimensional systems with state-dependent diffusion coefficient. For these examples for the first time the respective exact propagator was calculated for any possible stochastic interpretation. Furthermore, it was shown how the stochastic interpretation, i.e. the form of the Fokker-Planck equation, may be identified with help of mean and variance of the processes. This can only be done by assuming no additional drift in the system, i.e. the system is completely described by a state-dependent diffusion coefficient and a stochastic interpretation. Finally, in the second result Chap. 4 also heterogeneous anisotropic systems were treated. Here, for typical examples of experimentally highly relevant systems, predictions for the mean squared displacement and the distribution of diffusivities were given, which are both easily accessible in experiments.

One-dimensional systems with state-dependent diffusion coefficient

One-dimensional diffusion processes with state-dependent diffusion coefficient can be transformed into diffusion processes in a potential with constant diffusion coefficient. Since the transformation rule depends on the stochastic interpretation of the original process, the potential of the transformed process also depends on this stochastic interpretation. Nevertheless, if the potential is found, the powerful instruments of quantum mechanics may be applied to calculate the propagator of the transformed process and, thus, after back-transformation also the propagator of the original process is available. Furthermore, the potentials of the transformed Itô process and transformed Klimontovich-Hänggi process are supersymmetric partner-potentials and, consequently, the eigenvalues and eigenfunctions of the eigenfunction expansion of the propagator have a simple relation to one another. This knowledge was used in Chap. 3 to calculate the exact propagator of several experimentally relevant systems with state-dependent diffusion coefficient and for the very first time also for every possible stochastic interpretation. Furthermore, for these systems the influence of the stochastic interpretation on mean and variance of the processes was studied, providing hints to distinguish the interpretation based on these averages.

As first example a generalized geometric Brownian motion with state-dependent diffusion coefficient $D(x) = D_0(1 + \sigma|x|)^2$ was studied. The transformed process gives the diffusion in a wedge or V-shaped potential, which itself is an interesting system. And the related imaginary-time Schrödinger equation leads to a wave-function in a δ-potential, which is a textbook example in quantum mechanics. Although the eigenfunctions in such systems are well known, in this thesis for the first time the explicit propagator of the diffusion in a wedge potential was computed. Additionally, the characteristic function of the propagator was calculated, which allows to compute every moment of the propagator explicitly. After back-transformation to the original process, also the explicit propagator for diffusion with the state-dependent diffusion coefficient for any stochastic interpretation is known. For two interpretations of the Langevin equation, i.e. the Itô interpretation and the Klimontovich-Hänggi interpretation, the temporal behavior of the analytical propagator was presented and compared with numerical results, which showed a very good agreement. Both behave also qualitatively different. The propagator of the Itô interpretation approaches a steady-state distribution for large time t, whereas the propagator of the Klimontovich-Hänggi interpretation shows a broadening of the distribution and also a motion of the center of mass with increasing time. This can also be observed in mean and variance, which was presented for the three main interpretations, i.e. additionally including the Stratonovich interpretation. Here, mean and variance grow exponentially in time for large t with an exponent which depends, besides from the parameters D_0 and σ, on the interpretation value α. Hence, the value of α may be determined with help of mean and variance of the process under the assumption that no other drift exists and, thus, the stochastic interpretation may be identified.

The second example, which was presented, is the diffusion with an algebraically varying diffusion coefficient $D(x) = D_0 x^\kappa$, which may be used to describe the diffusion close to interfaces. It was shown that the process can be transformed to a square Bessel process and to diffusion in a logarithmic potential. For the Stratonovich interpretation of the corresponding Langevin equation the propagator is already known [114]. But in this thesis, additionally, the propagator for any other possible stochastic interpretation was calculated. Again, the temporal behavior of the analytical propagator for the Itô interpretation and the Klimontovich-Hänggi interpretation is compared with simulations of the corresponding Langevin equations and shows a good agreement. Furthermore, analytic expressions for the conditional moments of the process were presented, which show an algebraic growth with increasing time. Moreover, it was proved that the variance of these processes show a subdiffusive growth for negative κ and a superdiffusive growth for positive κ independent of the stochastic interpretation. Finally, it was shown that if these processes are scaled with $t^{\frac{1}{2-\kappa}}$, their density approaches an asymptotic invariant density for large t and the asymptotically constant scaled moments can be used to infer the value of α and, thus, the stochastic interpretation can be identified.

In the final example a periodically varying diffusion coefficient was presented, which was later used also for an anisotropic system. Here the exact propagator can only be given for the Stratonovich interpretation. Nevertheless, since the effective diffusion coefficient in the transformed process can be computed, the behavior of the time-scaled moments for large t of the original process for an arbitrary interpretation may still be predicted. Unfortunately, no explicit expressions for the moments for a general α can be computed and, thus, in this case no hint can be given how to obtain the value of α from moments of the process.

In summary, the stochastic interpretation, i.e. the value of α, has a huge impact on the temporal behavior of the propagator and on its moments. Although, how this manifests depends strongly on the considered system, i.e. on the explicit form of the state-dependent diffusion coefficient. In some of the presented systems, the influence of the stochastic interpretation can

directly be observed in the temporal behavior of the moments. In other examples, the moments show a similar scaling over time, but then the propagator takes a qualitatively different form. Nevertheless, many of the methods presented in this chapter may also be applied in future to other systems with state-dependent diffusion coefficient to identify the influence of the stochastic interpretation, to predict mean values, or to calculate the propagator.

Anisotropic systems with state-dependent diffusion tensor

Since many real world systems are not one-dimensional and, besides the state-dependence, the diffusion coefficient may also be direction dependent, in Chap. 4 systems with state-dependent diffusion tensor were considered. Inspired by real heterogeneous liquid crystal systems, for a few examples the temporal behavior of measurable quantities like mean squared displacement and distribution of diffusivities was presented and analytical predictions were given.

As first example, a system with twist distortion of director field was considered. The diffusive motion along the axis of rotation of the director may also be interpreted as rotational diffusion and, thus, the system can be related to the translational diffusive motion of a two-dimensional ellipsoid. Since the dependent direction, here the z-axis, and the affected directions, here the x-y-plane, are perpendicular to each other, the stochastic interpretation of the related Langevin equation plays no role. Furthermore, the independence of the motion in z-direction or the rotational motion from the motion in the x-y-plane can be used to compute the averaged time-dependent diffusion tensor of the system. With this computed tensor, the temporal behavior of the moments of the x-y-process was calculated and, thus, also the temporal behavior of measurable quantities like MSD, distribution of diffusivities, or anisotropy parameter are known explicitly. For this system, the MSD is insufficient to detect the heterogeneity, since it has a constant slope determined by the sum of the eigenvalues of the diffusion tensor $\mathbf{D}$ or, respectively, its trace. Nevertheless, the distribution of diffusivities and its moments are well suited to detect this heterogeneity, since it manifests in a dependence of the displacements or diffusivities, respectively, on the record time τ. Thereby, the distribution of diffusivities shows a crossover from a distribution of a homogeneous anisotropic system with the same eigenvalues for small τ to a distribution of a homogeneous isotropic system for large τ with a diffusion constant given by the arithmetic mean of the eigenvalues.

As second example, the diffusion in a system after a Fréedericksz transition was considered. Here, like in the twist system, the director rotates continuously around the z-axis, but the local orientation depends now on the y-direction. Consequently, since dependent direction, the y-axis, and affected directions, the x-y-plane, are not perpendicular, the stochastic interpretation of the Langevin equation now plays a role, in contrast to the twist system. Since like in the twist system no direction is distinguished, it may be assumed that the system for large τ behaves isotropically. But it was shown for the Itô interpretation of the corresponding Langevin equation, that this is not the case. For this system, the distribution of diffusivities shows a crossover from a distribution of a homogeneous anisotropic system with the same eigenvalues as the eigenvalues of the diffusion tensor $\mathbf{D}(y)$ for small τ to the distribution of another homogeneous anisotropic system for large τ, but now with effective eigenvalues. These effective eigenvalues may be computed by averaging the diffusion tensor $\mathbf{D}(y)$ with help of the equilibrium distribution of the projected process in the dependent direction y. Furthermore, the system was also interpreted in Stratonovich sense, which leads to a qualitatively completely different behavior, which was here explored for the first time. In contrast to the Itô interpretation, for the Stratonovich interpretation the noise-induced drift term is important for the temporal behavior of MSD and the moments of the diffusivities. Nevertheless, it was proved that for small τ the distribution of

diffusivities is again the same as for a homogeneous anisotropic system with the same eigenvalues and, consequently, this distribution for small τ can be used to determine the eigenvalues. For large τ, the behavior is completely determined by the noise induced drift and, thus, the mean squared displacement grows quadratically with τ and the first moment of diffusivities grows linearly with τ. This is surprising, since this ballistic growth of the MSD is observed in a natural drift free system and is only caused by the Stratonovich interpretation of the related Langevin equation modeling the diffusion process. Furthermore, it was shown that this effective drift can be computed explicitly with help of the propagator or equilibrium distribution of the projected process of the dependent direction.

As last example, a system with undulation in the director field was in the focus. Here only the prediction for the Itô interpretation was given. Again, the mean squared displacement grows linearly in time with a slope determined by the trace of the diffusion tensor $\mathbf{D}$ or, respectively, the sum of its eigenvalues. Thus, the MSD is insufficient to determine the eigenvalues of $\mathbf{D}$ and to detect the heterogeneity. Again, the distribution of diffusivities for small τ can be used to determine the eigenvalues of the tensor and for large τ it can be used to determine the effective diffusion coefficients in the system.

In the last section of Chap. 4 some general assertions for diffusion with state-dependent diffusion tensor were given. Summarized, the distribution of diffusivities for small τ depends only on the eigenvalues of the diffusion tensor, if the state-dependent diffusion tensor has constant eigenvalues and additional drifts are also only state-dependent. Thus, distribution of diffusivities is the superior method to determine the local diffusion coefficients for this huge class of heterogeneous diffusion systems, which also includes all possible stochastic interpretations of the multidimensional Langevin equation with state-dependent drift and state-dependent diffusion tensor with constant eigenvalues. Furthermore, for the drift-free Itô-interpreted multidimensional Langevin equation also the MSD and the first moment of diffusivities was given explicitly. Furthermore, if such systems have only one dependent direction, the equilibrium distribution of that direction may be used to determine the effective diffusion coefficients in the system, which applies for large τ and manifests also in the distribution of diffusivities.

To summarize, it was shown on experimentally relevant systems, how the state-dependence of the diffusion tensor manifests in measurable quantities. Furthermore, it was shown how these quantities may be predicted by analytical means. Finally, for the system after Fréedericksz transition also a different stochastic interpretation and its impact on the MSD and first moment of diffusivities was studied. Like in Chap. 3, the stochastic interpretation has a huge impact on these quantities and should not be neglected when considering heterogeneous systems.

Future work and open questions

Many of the obtained results were driven by the question of the importance of the stochastic interpretation of the Langevin equation, or, equivalently, by the question of the proper form of the diffusion equation. As pointed out in Chap. 2, this questions cannot be answered by theoretical considerations alone. The experimental system has to be considered explicitly. However, this thesis predicts the impact of the stochastic interpretation on measurable quantities for many systems and demonstrates how they can be calculated. The methods presented here may be easily transferred to other systems. Nevertheless, to answer the question of the proper diffusion equation in systems with state-dependent diffusion coefficient or tensor, a system has to be prepared, where the dependence is explicitly known in order to compare analytical predictions with experimental results. Especially, tracer diffusion in liquid crystalline systems may be perfectly suited for such studies, since the director field may be influenced by magnetic or

electric fields without necessarily affecting the diffusion of the tracer. Another possibility are molecular dynamic simulations, where the system may also be prepared in a configuration where the state-dependence of the diffusion coefficient can be given explicitly. Up to now only a few experiments [17, 18, 64, 65] were performed in heterogeneous systems which focus on the form of the diffusion equation. In liquid crystalline system no such experiments are known to the author, but especially in such systems a inhomogeneous director field is often found and as shown in this thesis, analytical predictions are possible.

A. Appendix

A.1. Second moment of the propagator of the wedge potential

The second moment of the propagator Eq. (3.39) reads

$$
\begin{aligned}
M^2_{\tilde{x}_0}(t) = \frac{1}{4}\Bigg\{ & 2\exp\left[c(|\tilde{x}_0| - \tilde{x}_0)\right]\left(c^2t^2 - 2ct\tilde{x}_0 + t + \tilde{x}_0^2\right)\operatorname{erf}\left(\frac{\tilde{x}_0 - ct}{\sqrt{2t}}\right) \\
& + \frac{2}{c}\,|\tilde{x}_0|\exp\left[-\frac{(|\tilde{x}_0| - ct)^2}{2t}\right]\left(\sqrt{\frac{2t}{\pi}}c - \left(2c^2t - 1\right)\exp\left[\frac{(|\tilde{x}_0| + ct)^2}{2t}\right]\operatorname{erfc}\left(\frac{|\tilde{x}_0| + ct}{\sqrt{2t}}\right)\right) \\
& - 2\exp\left[c(|\tilde{x}_0| + \tilde{x}_0)\right]\left(c^2t^2 + 2ct\tilde{x}_0 + t + \tilde{x}_0^2\right)\left(\operatorname{erf}\left(\frac{ct + \tilde{x}_0}{\sqrt{2t}}\right) - 1\right) \\
& + 2\exp\left[-\frac{(ct + \tilde{x}_0)^2}{2t}\right]\left(c^2t^2 - 2ct\tilde{x}_0 + t + \tilde{x}_0^2\right)\exp\left[c\,|\tilde{x}_0| + \frac{c^2t}{2} + \frac{\tilde{x}_0^2}{2t}\right] \\
& - \frac{2}{c^2}\exp\left[-\frac{(ct + \tilde{x}_0)^2}{2t}\right]\left(\sqrt{\frac{2t}{\pi}}c\left(c^2t + 1\right)\exp\left[c(|\tilde{x}_0| + \tilde{x}_0)\right] + \exp\left[\frac{(ct + \tilde{x}_0)^2}{2t}\right]\right) \\
& + \frac{1}{c^2}\exp\left[2c\,|\tilde{x}_0|\right]\left(2c^4t^2 + 2c^2\tilde{x}_0^2 + 1\right)\left(\operatorname{erf}\left(\frac{|\tilde{x}_0| + ct}{\sqrt{2}\sqrt{t}}\right) - 1\right) + \operatorname{erf}\left(\frac{ct - |\tilde{x}_0|}{\sqrt{2}\sqrt{t}}\right) - 1\Bigg\}. \qquad \text{(A.1)}
\end{aligned}
$$

A.2. First moment of the propagator for Brownian motion with diffusion coefficient $\mathbf{D(x) = D_0(1 + \sigma|x|)^2}$

The first moment of the propagator Eq. (3.48) reads

$$
\begin{aligned}
M^1_{x_0}(t) = \frac{1}{2\sigma}\left(\frac{\sigma x_0}{\operatorname{sign}(x_0)} + 1\right)^{\frac{1}{2} - \alpha - \left(\alpha + \frac{1}{2}\right)\operatorname{sign}(x_0)} & \\
\times \Bigg\{ & (\sigma|x_0| + 1)^{\operatorname{sign}(x_0)}\operatorname{erfc}\left[\frac{\operatorname{sign}(x_0)\log(\sigma\,|x_0| + 1) + (1 - 2\alpha)D_0\sigma^2t}{2\sigma\sqrt{D_0t}}\right] \\
& + (\sigma|x_0| + 1)^{2\alpha\operatorname{sign}(x_0)}\left(\operatorname{erfc}\left(\frac{\operatorname{sign}(x_0)\log(\sigma\,|x_0| + 1) + (2\alpha - 1)D_0\sigma^2t}{2\sigma\sqrt{D_0t}}\right) - 2\right) \\
+ \exp[2\alpha D_0\sigma^2t]\Bigg[& (\sigma|x_0| + 1)^{(2\alpha+1)\operatorname{sign}(x_0)}\left(1 + \operatorname{erf}\left(\frac{\operatorname{sign}(x_0)\log(\sigma\,|x_0| + 1) + (2\alpha + 1)D_0\sigma^2t}{2\sigma\sqrt{D_0t}}\right)\right) \\
& - \operatorname{erfc}\left(\frac{\operatorname{sign}(x_0)\log(\sigma\,|x_0| + 1) - (2\alpha + 1)D_0\sigma^2t}{2\sigma\sqrt{D_0t}}\right)\Bigg]\Bigg\}. \qquad \text{(A.2)}
\end{aligned}
$$

Bibliography

[1] R. Brown, "A brief account of microscopical observations made in the months of june, july and august, 1827, on the particles contained in the pollen of plants; and on the general existence of active molecules in organic and inorganic bodies." in *The miscellaneous botanical works of Robert Brown.*, edited by J. J. Bennet (Published for the Ray society by R. Hardwicke, London, 1866) pp. 463–486.

[2] A. Fick, "Über Diffusion," Ann. Phys. **170**, 59–86 (1855).

[3] A. Einstein, "Über die von der molekularkinetischen Theorie der Wärme geforderte Bewegung von in ruhenden Flüssigkeiten suspendierten Teilchen," Ann. Phys. **322**, 549–560 (1905).

[4] M. von Smoluchowski, "Zur kinetischen Theorie der Brownschen Molekularbewegung und der Suspensionen," Ann. Phys. **326**, 756–780 (1906).

[5] N. G. van Kampen, "Diffusion in inhomogeneous media," J. Phys. Chem. Solids **49**, 673–677 (1988).

[6] M. Christensen and J. B. Pedersen, "Diffusion in inhomogeneous and anisotropic media," J. Chem. Phys. **119**, 5171–5175 (2003).

[7] E. Bringuier, "Particle diffusion in an inhomogeneous medium," Eur. J. Phys. **32**, 975 (2011).

[8] A. Pérez-Madrid, J. Rubí, and P. Mazur, "Brownian motion in the presence of a temperature gradient," Physica A **212**, 231–238 (1994).

[9] S. Duhr and D. Braun, "Thermophoretic depletion follows boltzmann distribution," Phys. Rev. Lett. **96**, 168301 (2006).

[10] D. Rings, R. Schachoff, M. Selmke, F. Cichos, and K. Kroy, "Hot Brownian motion," Phys. Rev. Lett. **105**, 090604 (2010).

[11] D. Täuber, M. Heidernätsch, M. Bauer, G. Radons, J. Schuster, and C. von Borczyskowski, "Single molecule tracking of the molecular mobility in thinning liquid films on thermally grown sio2," Diff. Fund. J. **11**, 1–11 (2009).

[12] A. Schob and F. Cichos, "Single molecule diffusion at step edges," Chem. Phys. Lett. **484**, 192–196 (2010).

[13] S. Krause, M. Hartmann, I. Kahle, M. Neumann, M. Heidernätsch, S. Spange, and C. von Borczyskowski, "Optical tracking of single Ag clusters in nanostructured water films," J. Phys. Chem. C **117**, 24822–24829 (2013).

[14] D. Täuber, I. Trenkmann, and C. von Borczyskowski, "Influence of van der Waals interactions on morphology and dynamics in ultrathin liquid films at silicon oxide interfaces," Langmuir **29**, 3583–3593 (2013).

[15] J. Mittal, T. M. Truskett, J. R. Errington, and G. Hummer, "Layering and position-dependent diffusive dynamics of confined fluids," Phys. Rev. Lett. **100**, 145901 (2008).

[16] P. Lançon, G. Batrouni, L. Lobry, and N. Ostrowsky, "Brownian walker in a confined geometry leading to a space-dependent diffusion coefficient," Physica A **304**, 65–76 (2002).

[17] B. P. van Milligen, P. D. Bons, B. A. Carreras, and R. Sánchez, "On the applicability of Fick's law to diffusion in inhomogeneous systems," Eur. J. Phys. **26**, 913 (2005).

[18] B. P. van Milligen, B. A. Carreras, and R. Sánchez, "The foundations of diffusion revisited," Plasma Phys. and Contr. F. **47**, B743 (2005).

[19] H. Risken, *The Fokker-Planck Equation: Methods of Solution and Applications*, 2nd ed., Springer Series in Synergetics, Vol. 18 (Springer, Berlin, 1989).

[20] C. Hellriegel, J. Kirstein, C. Bräuchle, V. Latour, T. Pigot, R. Olivier, S. Lacombe, R. Brown, V. Guieu, C. Payrastre, A. Izquierdo, and P. Mocho, "Diffusion of single streptocyanine molecules in the nanoporous network of sol-gel glasses," J. Phys. Chem. B **108**, 14699–14709 (2004).

[21] A. Zürner, J. Kirstein, M. Döblinger, C. Bräuchle, and T. Bein, "Visualizing single-molecule diffusion in mesoporous materials," Nature **450**, 705–708 (2007).

[22] M. Dentz, P. Gouze, A. Russian, J. Dweik, and F. Delay, "Diffusion and trapping in heterogeneous media: An inhomogeneous continuous time random walk approach," Adv. Water Res. **49**, 13–22 (2012).

[23] B. P. English, V. Hauryliuk, A. Sanamrad, S. Tankov, N. H. Dekker, and J. Elf, "Single-molecule investigations of the stringent response machinery in living bacterial cells," PNAS **108**, E365–E373 (2011).

[24] T. Kühn, T. O. Ihalainen, J. Hyväluoma, N. Dross, S. F. Willmann, J. Langowski, M. Vihinen-Ranta, and J. Timonen, "Protein diffusion in mammalian cell cytoplasm," PLoS ONE **6**, e22962 (2011).

[25] M. J. Saxton and K. Jacobson, "Single-particle tracking: Applications to membrane dynamics," Annu. Rev. Biophys. Biomol. Struct. **26**, 373–399 (1997).

[26] M. Dahan, S. Lévi, C. Luccardini, P. Rostaing, B. Riveau, and A. Triller, "Diffusion dynamics of glycine receptors revealed by single-quantum dot tracking," Science **302**, 442–445 (2003).

[27] N. Ruthardt, D. C. Lamb, and C. Bräuchle, "Single-particle tracking as a quantitative microscopy-based approach to unravel cell entry mechanisms of viruses and pharmaceutical nanoparticles," Mol. Ther. **19**, 1199–1211 (2011).

[28] T. G. Mason, K. Ganesan, J. H. van Zanten, D. Wirtz, and S. C. Kuo, "Particle tracking microrheology of complex fluids," Phys. Rev. Lett. **79**, 3282–3285 (1997).

[29] D. T. Chen, E. R. Weeks, J. C. Crocker, M. F. Islam, R. Verma, J. Gruber, A. J. Levine, T. C. Lubensky, and A. G. Yodh, "Rheological Microscopy: Local Mechanical Properties from Microrheology," Phys. Rev. Lett. **90**, 108301 (2003).

[30] K. McHale, A. J. Berglund, and H. Mabuchi, "Quantum dot photon statistics measured by three-dimensional particle tracking," Nano Lett. **7**, 3535–3539 (2007).

[31] Y. Katayama, O. Burkacky, M. Meyer, C. Bräuchle, E. Gratton, and D. C. Lamb, "Real-time nanomicroscopy via three-dimensional single-particle tracking," Chem. Phys. Chem. **10**, 2458–2464 (2009).

[32] J.-H. Spille, T. Kaminski, H.-P. Königshoven, and U. Kubitscheck, "Dynamic three-dimensional tracking of single fluorescent nanoparticles deep inside living tissue," Opt. Express **20**, 19697–19707 (2012).

[33] S.-L. Liu, J. Li, Z.-L. Zhang, Z.-G. Wang, Z.-Q. Tian, G.-P. Wang, and D.-W. Pang, "Fast and high-accuracy localization for three-dimensional single-particle tracking," Sci. Rep. **3**, 2462 (2013).

[34] B. Schulz, D. Täuber, F. Friedriszik, H. Graaf, J. Schuster, and C. von Borczyskowski, "Optical detection of heterogeneous single molecule diffusion in thin liquid crystal films," Phys. Chem. Chem. Phys. **12**, 11555–11564 (2010).

[35] M. Bauer, R. Valiullin, G. Radons, and J. Kärger, "How to compare diffusion processes assessed by single-particle tracking and pulsed field gradient nuclear magnetic resonance," J. Chem. Phys. **135**, 144118 (2011).

[36] M. Heidernätsch, M. Bauer, and G. Radons, "Characterizing N-dimensional anisotropic Brownian motion by the distribution of diffusivities," J. Chem. Phys. **139**, 184105 (2013).

[37] F. Perrin, "Mouvement brownien d'un ellipsoide - I. Dispersion diélectrique pour des molécules ellipsoidales," J. Phys. Radium **5**, 497–511 (1934).

[38] R. Gans, "Zur Theorie der Brownschen Molekularbewegung," Ann. Phys. **391**, 628–656 (1928).

[39] B. Schulz, D. Täuber, J. Schuster, T. Baumgärtel, and C. von Borczyskowski, "Influence of mesoscopic structures on single molecule dynamics in thin smectic liquid crystal films," Soft Matter **7**, 7431–7440 (2011).

[40] M. Pumpa and F. Cichos, "Slow single-molecule diffusion in liquid crystals," J. Phys. Chem. B **116**, 14487–14493 (2012).

[41] D. Täuber and C. von Borczyskowski, "Single molecule studies on dynamics in liquid crystals," Int. J. Mol. Sci. **14**, 19506–19525 (2013).

[42] P. Bräuer, A. Brzank, L. A. Clark, R. Q. Snurr, and J. Kärger, "Guest-specific diffusion anisotropy in nanoporous materials: Molecular dynamics and dynamic Monte Carlo simulations," Adsorption **12**, 417–422 (2006).

[43] R. Grima, S. N. Yaliraki, and M. Barahona, "Crowding-induced anisotropic transport modulates reaction kinetics in nanoscale porous media," J. Phys. Chem. B **114**, 5380–5385 (2010).

[44] M. Arrio-Dupont, G. Foucault, M. Vacher, P. F. Devaux, and S. Cribier, "Translational diffusion of globular proteins in the cytoplasm of cultured muscle cells," Biophys. J. **78**, 901–907 (2000).

[45] M. K. Aliev and A. N. Tikhonov, "Obstructed metabolite diffusion within skeletal muscle cells in silico," Mol. Cell. Biochem. **358**, 105–119 (2011).

[46] A. Illaste, M. Laasmaa, P. Peterson, and M. Vendelin, "Analysis of molecular movement reveals latticelike obstructions to diffusion in heart muscle cells," Biophys. J. **102**, 739–748 (2012).

[47] B. A. Smith, W. R. Clark, and H. M. McConnell, "Anisotropic molecular motion on cell surfaces," PNAS **76**, 5641–5644 (1979).

[48] Y. Bouligand, "Liquid crystals and biological morphogenesis: Ancient and new questions," Compt. Rendus Chem. **11**, 281–296 (2008).

[49] I. Dierking, *Textures of Liquid Crystals* (WILEY-VCH Verlag, Weinheim, 2003).

[50] B. I. Senyuk, I. I. Smalyukh, and O. D. Lavrentovich, "Undulations of lamellar liquid crystals in cells with finite surface anchoring near and well above the threshold," Phys. Rev. E **74**, 011712 (2006).

[51] O. D. Lavrentovich, "Transport of particles in liquid crystals," Soft Matter **10**, 1264–1283 (2014).

[52] B. Senyuk, D. Glugla, and I. I. Smalyukh, "Rotational and translational diffusion of anisotropic gold nanoparticles in liquid crystals controlled by varying surface anchoring," Phys. Rev. E **88**, 062507 (2013).

[53] P. J. Smith, "A recursive formulation of the old problem of obtaining moments from cumulants and vice versa," Amer. Stat. **49**, 217–218 (1995).

[54] M. N. Berberan-Santos, "Computation of one-sided probability density functions from their cumulants," J. Math. Chem. **41**, 71–77 (2007).

[55] G. Cottone and M. D. Paola, "On the use of fractional calculus for the probabilistic characterization of random variables," Probabilist. Eng. Mech. **24**, 321–330 (2009).

[56] S. Wolfe, "On moments of probability distribution functions," in *Fractional Calculus and Its Applications*, Lecture Notes in Mathematics, Vol. 457, edited by B. Ross (Springer Berlin Heidelberg, 1975) pp. 306–316.

[57] A. Marchaud, "Sur des derivées et sur les différences des fonctions de variable réeles," J. Math. Pure Appl. **6**, 337–425 (1927).

[58] C. W. Gardiner, *Handbook of Stochastic Methods*, 2nd ed., Springer Series in Synergetics, Vol. 13 (Springer, Berlin, 1985).

[59] N. G. van Kampen, "Itô versus stratonovich," J. Stat. Phys. **24**, 175–187 (1981).

[60] K. Itô, "Stochastic integral," Proc. Imp. Acad. **20**, 519–524 (1944).

[61] R. L. Stratonovich, "A new representation for stochastic integrals and equations," SIAM J. Control **4**, 362–371 (1966).

[62] D. Ryter and U. Deker, "Properties of the noise-induced "spurious" drift. I," J. Math. Phys. **21**, 2662–2665 (1980).

[63] D. Ryter and U. Deker, "Properties of the noise-induced "spurious" drift. II. simplifications of Langevin equations," J. Math. Phys. **21**, 2666–2669 (1980).

[64] G. Volpe, L. Helden, T. Brettschneider, J. Wehr, and C. Bechinger, "Influence of noise on force measurements," Phys. Rev. Lett. **104**, 170602 (2010).

[65] T. Brettschneider, G. Volpe, L. Helden, J. Wehr, and C. Bechinger, "Force measurement in the presence of Brownian noise: Equilibrium-distribution method versus drift method," Phys. Rev. E **83**, 041113 (2011).

[66] M. Yang and M. Ripoll, "Drift velocity in non-isothermal inhomogeneous systems," J. Chem. Phys. **136**, 204508 (2012).

[67] R. Manella and P. V. E. McClintock, "Itô versus Stratonovich: 30 years later," Fluct. Noise Lett. **11**, 1240010 (2012).

[68] F. Black and M. Scholes, "The pricing of options and corporate liabilities," J. Polit. Econ. **81**, 637–654 (1973).

[69] D. Nelson, "ARCH models as diffusion approximations," J. Econometrics **45**, 7–38 (1990).

[70] M. Turelli, "Random environments and stochastic calculus," Theor. Popul. Biol. **12**, 140–178 (1977).

[71] H. Rajakaruna, A. Potapov, and M. Lewis, "Impact of stochasticity in immigration and reintroduction on colonizing and extirpating populations," Theor. Popul. Biol. **85**, 38–48 (2013).

[72] A. W. C. Lau and T. C. Lubensky, "State-dependent diffusion: Thermodynamic consistency and its path integral formulation," Phys. Rev. E **76**, 011123 (2007).

[73] M. Yang and M. Ripoll, "Brownian motion in inhomogeneous suspensions," Phys. Rev. E **87**, 062110 (2013).

[74] P. Lançon, G. Batrouni, L. Lobry, and N. Ostrowsky, "Drift without flux: Brownian walker with a space-dependent diffusion coefficient," Europhys. Lett. **54**, 28 (2001).

[75] Y. Klimontovich, "Ito, Stratonovich and kinetic forms of stochastic equations," Physica A **163**, 515–532 (1990).

[76] P. Hänggi, "Stochastic processes I: Asymptotic behavior and symmetries," Helv. Phys. Acta **51**, 183–201 (1978).

[77] J. Smythe, F. Moss, and P. V. E. McClintock, "Observation of a noise-induced phase transition with an analog simulator," Phys. Rev. Lett. **51**, 1062–1065 (1983).

[78] P. McClintock and F. Moss, "Further experimental evidence pertaining to the applicability of the Ito and Stratonovic stochastic calculi to real physical systems," Phys. Lett. A **107**, 367–370 (1985).

[79] S. Prager, "Interaction of rotational and translational diffusion," J. Chem. Phys. **23**, 2404–2407 (1955).

[80] P. Ilg, "Anisotropic diffusion in nematic liquid crystals and in ferrofluids," Phys. Rev. E **71**, 051407 (2005).

[81] S. S. Stepanov, *Stochastic World*, 1st ed., Mathematical Engineering, Vol. X (Springer, Cham, 2013).

[82] D. Axelrod, D. Koppel, J. Schlessinger, E. Elson, and W. Webb, "Mobility measurement by analysis of fluorescence photobleaching recovery kinetics," Biophys. J. **16**, 1055 – 1069 (1976).

[83] D. Soumpasis, "Theoretical analysis of fluorescence photobleaching recovery experiments," Biophys. J. **41**, 95–97 (1983).

[84] J. Bechhoefer, J.-C. Géminard, L. Bocquet, and P. Oswald, "Experiments on tracer diffusion in thin free-standing liquid-crystal films," Phys. Rev. Lett. **79**, 4922–4925 (1997).

[85] E. D. Siggia, J. Lippincott-Schwartz, and S. Bekiranov, "Diffusion in inhomogeneous media: Theory and simulations applied to whole cell photobleach recovery," Biophys. J. **79**, 1761–1770 (2000).

[86] M. Krutyeva and J. Kärger, "NMR diffusometry with beds of nanoporous host particles: An assessment of mass transfer in compartmented two-phase systems," Langmuir **24**, 10474–10479 (2008).

[87] M. Nilsson, E. Alerstam, R. Wirestam, F. Ståhlberg, S. Brockstedt, and J. Lätt, "Evaluating the accuracy and precision of a two-compartment Kärger model using Monte Carlo simulations," J. Magn. Reson. **206**, 59–67 (2010).

[88] E. L. Hahn, "Spin echoes," Phys. Rev. **80**, 580–594 (1950).

[89] R. Kimmich, *NMR Tomography, Diffusometry, Relaxometry* (Springer, Berlin, 1997).

[90] W. S. Price, *NMR Studies of Translational Motion* (Camebridge University Press, Cambridge, 2009).

[91] J. Kärger and W. Heink, "The propagator representation of molecular transport in microporous crystallites," J. Magn. Reson. **51**, 1–7 (1983).

[92] D. Magde, E. Elson, and W. W. Webb, "Thermodynamic fluctuations in a reacting system-measurement by fluorescence correlation spectroscopy," Phys. Rev. Lett. **29**, 705–708 (1972).

[93] D. Magde, E. L. Elson, and W. W. Webb, "Fluorescence correlation spectroscopy. II. An experimental realization," Biopolymers **13**, 29–61 (1974).

[94] N. Agmon, "The residence probability: Single molecule fluorescence correlation spectroscopy and reversible geminate recombination," Phys. Chem. Chem. Phys. **13**, 16548–16557 (2011).

[95] J. C. Crocker and D. G. Grier, "Methods of digital video microscopy for colloidal studies," J. Colloid Interf. Sc. **179**, 298–310 (1996).

[96] S. Courty, C. Luccardini, Y. Bellaiche, G. Cappello, and M. Dahan, "Tracking individual kinesin motors in living cells using single quantum-dot imaging," Nano Letters **6**, 1491–1495 (2006).

[97] A. Gahlmann and W. E. Moerner, "Exploring bacterial cell biology with single-molecule tracking and super-resolution imaging," Nat. Rev. Micro. **12**, 9–22 (2014).

[98] C. Ribrault, A. Triller, and K. Sekimoto, "Diffusion trajectory of an asymmetric object: Information overlooked by the mean square displacement," Phys. Rev. E **75**, 021112 (2007).

[99] J. Kärger, D. M. Ruthven, and D. N. Theodorou, *Diffusion in Nanoporous Materials* (Wiley-VCH, Weinheim, 2012).

[100] I. Hanasaki and Y. Isono, "Detection of diffusion anisotropy due to particle asymmetry from single-particle tracking of Brownian motion by the large-deviation principle," Phys. Rev. E **85**, 051134 (2012).

[101] M. Bauer, M. Heidernätsch, D. Täuber, C. von Borczyskowski, and G. Radons, "Investigations of heterogeneous diffusion based on the probability density of scaled squared displacements observed from single molecules in ultra-thin liquid films," Diff. Fund. J. **11**, 1–14 (2009).

[102] T. Albers and G. Radons, "Subdiffusive continuous time random walks and weak ergodicity breaking analyzed with the distribution of generalized diffusivities," EPL **102**, 40006 (2013).

[103] S. Krause, P. F. Aramendia, D. Täuber, and C. von Borczyskowski, "Freezing single molecule dynamics on interfaces and in polymers," Phys. Chem. Chem. Phys. **13**, 1754–1761 (2011).

[104] S. Krause, D. Kowerko, R. Börner, C. G. Hübner, and C. von Borczyskowski, "Spectral diffusion of single molecules in a hierarchical energy landscape," Chem. Phys. Chem. **12**, 303–312 (2011).

[105] B. Araoz, A. Carattino, D. Täuber, C. von Borczyskowski, and P. F. Aramendia, "Influence of the glass transition on rotational dynamics of dyes in thin polymer films: Single-molecule and ensemble experiments," J. Phys. Chem. A **in Print** (2014), 10.1021/jp500272y.

[106] M. J. Saxton, "Single-particle tracking: The distribution of diffusion coefficients," Biophys. J. **72**, 1744–1753 (1997).

[107] S. Hess, D. Frenkel, and M. Allen, "On the anisotropy of diffusion in nematic liquid crystals: Test of a modified affine transformation model via molecular dynamics," Molecular Physics **74**, 765–774 (1991).

[108] S. M. Blinder, "Green's function and propagator for the one-dimensional δ-function potential," Phys. Rev. A. **37**, 973–976 (1988).

[109] A. Erdélyi, W. Magnus, F. Oberhettinger, and F. G. Tricomi, *Tables of Integral Transforms*, edited by A. Erdélyi, Vol. 1 (McGraw Hill, New York, 1954).

[110] F. Cooper, A. Khare, and U. Sukhatme, "Supersymmetry and quantum mechanics," Phys. Rep. **251**, 267–385 (1995).

[111] J. C. Cox and S. A. Ross, "The valuation of options for alternative stochastic processes," J. Financ. Econ. **3**, 145–166 (1976).

[112] D. C. Emanuel and J. D. MacBeth, "Further results on the constant elasticity of variance call option pricing model," J. Financ. Quant. Anal. **17**, 533–554 (1982).

[113] A. G. Cherstvy, A. V. Chechkin, and R. Metzler, "Anomalous diffusion and ergodicity breaking in heterogeneous diffusion processes," New J. Phys. **15**, 083039 (2013).

[114] A. G. Cherstvy and R. Metzler, "Population splitting, trapping, and non-ergodicity in heterogeneous diffusion processes," Phys. Chem. Chem. Phys. **15**, 20220–20235 (2013).

[115] D. Revus and M. Yor, *Continuous Martingales and Brownian Motion*, 2nd ed., edited by Springer, Grundlehren der mathematischen Wissenschaften, Vol. 293 (Springer, Berlin, 1954).

[116] P. Szymczak and A. J. C. Ladd, "Boundary conditions for stochastic solutions of the convection-diffusion equation," Phys. Rev. E **68**, 036704 (2003).

[117] S. Marksteiner, K. Ellinger, and P. Zoller, "Anomalous diffusion and Lévy walks in optical lattices," Phys. Rev. A **53**, 3409–3430 (1996).

[118] E. Lutz, "Anomalous diffusion and Tsallis statistics in an optical lattice," Phys. Rev. A **67**, 051402 (2003).

[119] E. Lutz, "Power-law tail distributions and nonergodicity," Phys. Rev. Lett. **93**, 190602 (2004).

[120] P. Douglas, S. Bergamini, and F. Renzoni, "Tunable Tsallis distributions in dissipative optical lattices," Phys. Rev. Lett. **96**, 110601 (2006).

[121] G. S. Manning, "Limiting laws and counterion condensation in polyelectrolyte solutions I. colligative properties," J. Chem. Phys. **51**, 924–933 (1969).

[122] E. Levine, D. Mukamel, and G. M. Schütz, "Long-range attraction between probe particles mediated by a driven fluid," Europhys. Lett. **70**, 565 (2005).

[123] F. Bouchet and T. Dauxois, "Prediction of anomalous diffusion and algebraic relaxations for long-range interacting systems, using classical statistical mechanics," Phys. Rev. E **72**, 045103 (2005).

[124] F. Bouchet and T. Dauxois, "Kinetics of anomalous transport and algebraic correlations in a long-range interacting system," J. Phys. Conf. Ser. **7**, 34 (2005).

[125] P. H. Chavanis and M. Lemou, "Kinetic theory of point vortices in two dimensions: Analytical results and numerical simulations," Europ. Phys. J. B **59**, 217–247 (2007).

[126] A. Hanke and R. Metzler, "Bubble dynamics in DNA," J Phys. A - Math. Gen. **36**, L473 (2003).

[127] A. Bar, Y. Kafri, and D. Mukamel, "Loop dynamics in DNA denaturation," Phys. Rev. Lett. **98**, 038103 (2007).

[128] D. A. Kessler and E. Barkai, "Infinite covariant density for diffusion in logarithmic potentials and optical lattices," Phys. Rev. Lett. **105**, 120602 (2010).

[129] A. Dechant, E. Lutz, E. Barkai, and D. Kessler, "Solution of the fokker-planck equation with a logarithmic potential," J. Stat. Phys. **145**, 1524–1545 (2011).

[130] O. Hirschberg, D. Mukamel, and G. M. Schütz, "Diffusion in a logarithmic potential: Scaling and selection in the approach to equilibrium," J. Stat. Mech. Theor. Exp. **2012**, P02001 (2012).

[131] A. Dechant, E. Lutz, D. A. Kessler, and E. Barkai, "Superaging correlation function and ergodicity breaking for Brownian motion in logarithmic potentials," Phys. Rev. E **85**, 051124 (2012).

[132] A. Göing-Jaeschke and M. Yor, "A survey and some generalizations of Bessel processes," Bernoulli **9**, 313–349 (2003).

[133] W. Feller, "Two singular diffusion problems," Ann. Math. Sec. Ser., **54**, 173–182 (1951).

[134] W. Feller, "Diffusion processes in genetics," in *Proceedings of the Second Berkeley Symposium on Mathematical Statistics and Probability* (University of California Press, Berkeley, Calif., 1951) pp. 227–246.

[135] J. C. Cox, J. Ingersoll, Jonathan E., and S. A. Ross, "A theory of the term structure of interest rates," Econometrica **53**, 385–407 (1985).

[136] M. Abramowitz and I. A. Stegun, eds., *Handbook of Mathematical Functions with Formulas, Graphs, and Mathematical Tables*, 10th ed. (Dover Publications, New York, 1972).

[137] R. Festa and E. d'Agliano, "Diffusion coefficient for a Brownian particle in a periodic field of force: I. large friction limit," Physica A **90**, 229–244 (1978).

[138] D. Weaver, "Effective diffusion coefficient of a Brownian particle in a periodic potential," Physica A **98**, 359–362 (1979).

[139] S. Lifson and J. L. Jackson, "On the self-diffusion of ions in a polyelectrolyte solution," J. Chem. Phys. **36**, 2410–2414 (1962).

[140] V. Fréedericksz and V. Zolina, "Forces causing the orientation of an anisotropic liquid," Trans. Faraday Soc. **29**, 919–930 (1933).

[141] P. G. de Gennes, *The Physics of Liquid Crystals*, 2nd ed., International Series of Monographs on Physics, Vol. 83 (Clarendon Press, Oxford, 1995).

[142] Y. Han, A. M. Alsayed, M. Nobili, J. Zhang, T. C. Lubensky, and A. G. Yodh, "Brownian motion of an ellipsoid," Science **314**, 626–630 (2006).

[143] Y. Han, A. Alsayed, M. Nobili, and A. G. Yodh, "Quasi-two-dimensional diffusion of single ellipsoids: Aspect ratio and confinement effects," Phys. Rev. E **80**, 011403 (2009).

[144] T. Munk, F. Höfling, E. Frey, and T. Franosch, "Effective Perrin theory for the anisotropic diffusion of a strongly hindered rod," Europhys. Lett. **85**, 30003 (2009).

[145] W. Helfrich, "Deformation of cholesteric liquid crystals with low threshold voltage," Appl. Phys. Lett. **17**, 531–532 (1970).

[146] W. Helfrich, "Electrohydrodynamic and dielectric instabilities of cholesteric liquid crystals," J. Chem. Phys. **55**, 839–842 (1971).

[147] N. A. Clark and R. B. Meyer, "Strain-induced instability of monodomain smectic A and cholesteric liquid crystals," Appl. Phys. Lett. **22**, 493–494 (1973).

[148] M. Delaye, R. Ribotta, and G. Durand, "Buckling instability of the layers in a smectic-A liquid crystal," Phys. Lett. A **44**, 139–140 (1973).

List of Figures

List of Acronyms

MSD	mean squared displacement
ODE	ordinary differential equation
PDE	partial differential equation
SDE	stochastic differential equation
lhs	left-hand side
rhs	right-hand side
CEV	constant elasticity of variance
PDF	probability density function
CIR	Cox-Ingersoll-Ross
FCS	fluorescence correlation spectroscopy
FRAP	fluorescence recovery after photobleaching
SPT	single particle tracking
SMT	single molecule tracking
PFG NMR	pulsed field gradient nuclear magnetic resonance
AID	asymptotic invariant density
MD	molecular dynamic

Selbstständigkeitserklärung

Erklärung zur Promotionsordnung § 6 Absatz 2 Nr. 4,5:

Ich erkläre, dass ich die vorliegende Arbeit selbstständig und nur unter der Verwendung der angegebenen Literatur und Hilfsmittel angefertigt habe.

Ich erkläre, nicht bereits früher oder gleichzeitig bei anderen Hochschulen oder an dieser Universität ein Promotionsverfahren beantragt zu haben. Falls diese Erklärung nicht zutrifft, füge ich eine Stellungnahme diesem Antrag bei.

Ich erkläre, obige Angaben wahrheitsgemäß gemacht zu haben und erkenne die Promotionsordnung der Fakultät für Naturwissenschaften der Technischen Universität Chemnitz vom 31. Januar 2011 an.

Chemnitz, den 25. Mai 2015

Heidernätsch, Mario

Curriculum Vitae

General Information

Name	Mario Heidernätsch
Email	Mario.Heidernaetsch@gmx.net
Date of Birth	06/06/1983
Place of Birth	Karl-Marx-Stadt (today: Chemnitz), Germany

Education

since 04/2009	**PhD studies in Physics** at the chair of Complex Systems and Nonlinear Dynamics, Technische Universität Chemnitz
10/2006 - 03/2009	**Study in Computation Science**, Technische Universität Chemnitz, Degree: Master of Science, Grade: 1.4 (very good)
10/2003 - 10/2006	**Study in Computation Science**, Technische Universität Chemnitz, Degree: Bachelor of Science, Grade: 2.3 (good)
08/1994 - 06/2002	**Grammar School**, Gymnasium Einsiedel, Germany Degree: Abitur, Grade: 2.0

Research and Teaching Experience

since 04/2009	**Research associate** at the chair of Complex Systems and Nonlinear Dynamics,Technische Universität Chemnitz, Research Topic: Diffusion in heterogeneous and anisotropic systems, Tutorial: Mechanics, Stochastic Systems, Electrodynamics and Thermodynamics
01/2009 - 02/2009	**Graduate student assistant** at the chair of Complex Systems and Nonlinear Dynamics, Technische Universität Chemnitz, Research Topic: Diffusion in heterogeneous systems
10/2008 - 12/2008	**Graduate student assistant** at the chair of Theoretical Physics - Simulation of New Materials, Technische Universität Chemnitz Tutorial: Mechanics
01/2008 - 09/2008	**Graduate student assistant** at the chair of Complex Systems and Nonlinear Dynamics, Technische Universität Chemnitz, Research Topic: Development of computer program for presentation of physical problems
07/2007 - 12/2007	**Graduate student assistant** at the chair of Optical Spectroscopy and Molecular Physics, Technische Universität Chemnitz, Research Topic: Binding kinetics of nanoaggregates

Publications

Journal Publications

1. S. Krause, M. Hartmann, I. Kahle, M. Neumann, M. Heidernätsch, S. Spange, and C. von Borczyskowski, Optical tracking of single Ag clusters in nanostructured water films, J. Phys. Chem. C **117**(47), 24822–24839 (2013).

2. M. Heidernätsch, M. Bauer, and G. Radons. Characterizing N-dimensional anisotropic Brownian motion by the distribution of diffusivities, J. Chem. Phys. **139**(18), 184105 (2013).

3. T. Albers, M. Bauer, M. Heidernätsch, and G. Radons, Characterization of diffusion processes by the distribution of diffusivities, Diffusion Fundamentals Journal **20**, 24(2) (2013).

4. M. Heidernätsch and G. Radons, Determination of eigenvalues of the diffusion tensor in anisotropic system with spatial orientation change, Diffusion Fundamentals Journal **20**, 90(2) (2013).

5. M. Bauer, M. Heidernätsch, D. Täuber, J. Schuster, C. von Borczyskowski, and G. Radons, Investigations of static and dynamic heterogeneities in ultra-thin liquid films via scaled squared displacements of single molecule diffusion, Diffusion Fundamentals Journal bfseries 11, 70(2) (2009).

6. D. Täuber, J. Schuster, M. Heidernätsch, M. Bauer, G. Radons, and C. von Borczyskowski, Discrimination between static and dynamic heterogeneities in single dye diffusion in ultrathin liquid films, Diffusion Fundamentals Journal **11**, 76(2) (2009).

7. M. Bauer, M. Heidernätsch, D. Täuber, C. von Borczyskowski, and G. Radons, Investigations of heterogeneous diffusion based on the probability density of scaled squared displacements observed from single molecules in ultra-thin liquid films, Diffusion Fundamentals Journal **11**, 104(14) (2009).

8. D. Täuber, M. Heidernätsch, M. Bauer, G. Radons, J. Schuster, and C. von Borczyskowski, Single molecule tracking of the molecular mobility in thinning liquid films on thermally grown SiO2, Diffusion Fundamentals Journal **11**, 107(11) (2009).

9. M. Heidernätsch, M. Bauer, G. Radons and C. von Borczyskowski, An advanced method of tracking temporarily invisible particles in video imaging, Diffusion Fundamentals Journal **11**, 111(2) (2009).

10. É. I. Zen'kevich, T. Blaudeck, M. Heidernätsch, F. Cichos, and C. von Borczyskowski, Effects of electron tunneling and nonresonance quenching of photoluminescence in semiconducting CdSe/ZnS and CdSe nanocrystals by porphyrin molecules in joint complexes, Theo. Exp. Chem. **45**(1), 23–34 (2008).

Proceedings

11. M. Bauer, M. Heidernätsch, D. Täuber, J. Schuster, C. von Borczyskowski, and G. Radons, Investigations of static and dynamic heterogeneities in ultra-thin liquid films via scaled squared displacements of single molecule Diffusion, Diffusion Fundamentals **III**,441-442 (2009), ISBN 978-3-86583-387-7.

12. D. Täuber, J. Schuster, M. Heidernätsch, M. Bauer, G. Radons, and C. von Borczyskowski, Discrimination between static and dynamic heterogeneities in single dye diffusion in ultrathin liquid films, Diffusion Fundamentals **III**, 452-453 (2009), ISBN 978-3-86583-387-7.

13. É. I. Zen'kevich, T. Blaudeck, M. Heidernätsch, and C. von Borczyskowski, Non-FRET emission quenching and electron wave function tunneling in excited nanocomposites "CdSe/ZnS Quantum Dots - Porphyrins", Physics, Chemistry and Application of Nanostructures: Proceedings of the International Conference, Nanomeeting–2009, 144-147 (2009), ISBN 9789814280358

14. É. I. Zen'kevich, T. Blaudeck, F. Cichos, M. Heidernätsch, and C. von Borczyskowski, Electron wave function tunneling in excited nanocomposites based on semiconductor CdSe/ZnS quantum dots and porphyrins, Proc. **VII** International Conference "Laser Physics and Optical Technologies", Minsk, National Academy of Sciences of Belarus, 238-231 (2008), ISBN 9789850809391

Theses

15. M. Heidernätsch, Development of a computer program for simulation and analysis of particle movement in thin liquid films, Master Thesis, Technische Universität Chemnitz, April 2009.

16. M. Heidernätsch, Development of a computer program for interactive failure analysis and improvement of scanning electron microscopy images, Bachelor Thesis, Technische Universität Chemnitz, October 2006.

Scientific Presentations and Posters

17. T. Albers T., M. Bauer, M. Heidernätsch, and G. Radons, Characterization of diffusion processes by the distribution of diffusivities (Poster), Diffusion Fundamentals **V**, Leipzig, Germany, August 2013.

18. M. Heidernätsch and G. Radons, Determination of eigenvalues of the diffusion tensor in anisotropic systems with spatial orientation change (Poster), Diffusion Fundamentals **V**, Leipzig, Germany, August 2013.

19. M. Heidernätsch and G. Radons, Determine principal eigenvalues of the diffusion tensor in anisotropic systems with orientation change in time and space (Talk), DPG Spring Meeting - Section Condensed Matter, Regensburg, Germany, March 2013.

20. M. Heidernätsch and G. Radons, Characterizing anisotropic diffusion via distribution of generalized diffusivities (Poster), DPG Spring Meeting - Section Condensed Matter, Berlin, Germany, March 2012.

21. M. Heidernätsch and G. Radons, A new method to characterize surface texture via observation of single molecules in video microscopy (Poster), DPG Spring Meeting - Section Condensed Matter, Dresden, Germany, March 2011.

22. M. Heidernätsch, M. Bauer, and G. Radons, Application of the maximum entropie method for heterogeneous diffusion systems (Poster), DPG Spring Meeting - Section Condensed Matter, Regensburg, Germany, March 2010.

23. M. Heidernätsch, M. Bauer, D. Täuber, G. Radons, and C. von Borczyskowski, An advanced method of tracking temporarily invisible particles in video imaging (Poster), Diffusion Fundamentals **III**, Athens, Greece, August 2009.

24. D. Täuber, M. Heidernätsch, M. Bauer, G. Radons, J. Schuster, and C. von Borczyskowski, Discrimination between static and dynamic heterogeneities in single dye diffusion in ultrathin liquid films (Poster), Diffusion Fundamentals **III**, Athens, Greece, August 2009.

25. M. Heidernätsch and G. Radons, A new method of tracking feature points in videos (Talk), DPG Spring Meeting - Section Condensed Matter, Dresden, Germany, March 2009.

26. M. Heidernätsch, T. Blaudeck, J. Schuster, and C. von Borczyskowski, Adsorption kinetics of individual dye molecules on semiconductor nanocrystal surfaces (Poster), DPG Spring Meeting - Section Condensed Matter, Berlin, Germany, March 2008.